Tesis doctoral

Departament de Bioquímica i de Biologia Molecular

HER2 hyper-activation through the production of carboxy-terminal fragments

Constitutive HER2 signalling promotes breast cancer metastasis through cellular senescence

Pier Davide Angelini

Emili Itarte
Tutor
Joaquín Arribas
Director

ABBREVIATIONS

Abreviations

aa	amino acid
AIOT	Alternative Initiation Of Translation
ANGPTL4	Angiopoietin-Like 4
AR	Amphiregulin
ARF	Alternative Reading Frame
ASF1	Anti-Silencing Function 1
ASGP2	Ascites Sialoglycoprotein 2 (Muc-4)
ATM	Ataxia Telangiectasia Mutated
ATR	ATM and Rad3 Related
ATRA	All-Trans Retinoic Acid All-Trans Retinoic Acid
BMI1	B-lymphoma Mo-MLV Insertion 1
BTC	Betacellulin
C/EBPβ	CCAAT/Enhancer Binding Protein β
CBL	Casitas B-lineage Lymphoma
CDC25	cell division cycle 25
CDK4	Cyclin Dependent Kinases 4
CDK6	Cyclin Dependent Kinases 6
CDKI	Cyclin-Dependent Kinase Inhibitor
cDNA	complementary Deoxyribonucleic Acid
CHK1	Check Point Kinase 1
CHK2	Check Point Kinase 2
CIP/KIP	CDK Interacting Protein/Kinase Inhibitor Protein
CSF-1	Colony Stimulating Factor 1
CTFs	Carboxyl-Terminal Fragments
CYR61 or CCN1	Cysteine Rich 61
DD	DNA Damage
DDR	DNA Damage Response
DDR	DNA Damage checkpoint Response
dEGFR or DER	drosophila-EGFR
DNA	Deoxyribonucleic Acid
DNA-SCARS	DNA Segments with Chromatin Alterations Reinforcing Senescence
Dox	Doxocyclin
DSBs	DNA Double Strand Breaks
EGF	Epidermal Growth Factor
EGFR	Epidermal Growth Factor Receptor
ELK1	ETS like gene 1
EMT	Epithelial-to-Mesenchymal Transition
EMT	Epithelial-to-Mesenchymal Transition
EPGN	Epigen/Epithelial Mitogen
EPR	Epiregulin

ER	Estrogen Receptor
ErbB family	erythroblastic leukemia viral oncogene homolog
ETS	E26 transformation-specific
FKHRL1	Forkhead-related transcription factor 1
FLuc	Firefly Luciferase
FOS	FBJ Murine Osteosarcoma Viral Oncogene Homolog
GRB2 and 7	Growth factor Receptor-Bound protein 2 and 7
H2AX	Histone-2AX
H3K9me3	tri-methylation of histone H3 on Lysine 9
HB-EGF	Heparin-Binding EGF
HDACs	Histone Deacetylases
HDMT	Histone Demethylase
HE	hematoxilin-eosin
HER2	human EGFR related-2
HER2-FL	Human EGFR related 2- Full Length
HIRA	Histone cell cycle Regulation defective homologue A
HMGA2	High Mobility Group A2
HMT	Histone Methytransferase
HomRec	Homologous Recombination
HP1	Heterochromatin Protein 1
HP1γ	Heterochromatin Protein 1
HSCs	Hepatic Stellate Cells
IF	immunofluorescence
IGFBP	Insulin-Like Growth Factor Binding Protein
IHC	immunohistochemistry
IL11	Interleukin 11
IL6	Interleukin 6
IMR90	immortalized diploid lung fibroblasts
INK4	INhibitors of CDK4
JMJD3	Jumonji Domain containing 3
JNK	c-Jun N-terminal kinase
JUN	V-Jun Avian Sarcoma Virus 17 Oncogene Homolog
KD	Knock-Down
KO	knock-out
LAMP2	Lysosomal-Associated Membrane Protein 2
LAP	Lapatinib
Mab	Monoclonal antibody
MAPK	Mitogen Activated Protein Kinases
MAPKAPK3	mitogen-activated protein kinase-activated protein kinase 3
MCF10A	Michigan Cancer Foundation 10A breast cancer cell line
MCF7	Michigan Cancer Foundation 7 breast cancer cell line
MCP-1	Monocyte Chemo-attractant Protein 1
MDA-MB-231	cbreast cancer cell line derived from metastatic site (pleural effusion)
MDM2	HDM2 [the human homolog of Mouse Double Minute 2
MEFs	Mouse Embryonic Fibroblasts
MEFs	Mouse Embryonic Fibroblasts

MET	approved gene symbol for hepatocyte growth factor receptor
MINK1	Misshapen-like Kinase 1
MLL1	HMT Myeloid/Lymphoid Or Mixed-Lineage Leukemia 1
MMP1	Matrix Metalloproteases 1
MMP1	Matrix metalloproteinase-1
mTORC1	mammalian target of rapamycin complex 1
Muc-4	Mucin-4
MYC	Avian Myelocytomatosis Viral Oncogene Homolog
NBN or NBS1	Nibrin
NFκB	Nuclear Factor κB
NGF	Nerve Growth Factor
NKs	Natural Killer Cells
OIS	Oncogene-Induced Senescence
p53BP1	p53-Binding Protein 1
p95HER2	constitutively active HER2 carboxyterminal fragment
PAI-1	Plasminogen Activator Inhibitor-1
PcG	Polycomb Group
PI3K-PKB-mTOR	Phosphoinositide-3-Kinase - Protein Kinase B -mammalian Target of Rapamicin
PICS	PTEN-loss Induced Cellular Senescence
PLCγ	Phospholipase C gamma
PRCs	PcG proteins form Polycomb Repressive Complexes
proT-SASP	protumorigenic-Senescence Associated Secretory Phenotype
PSG9	Pregnancy Specific beta-1-Glycoprotein 9
PTB	Phospho-Tyrosine Binding
PTEN	Phosphatase and Tensin homolog
RAS	Rat Sarcoma
Rb	Retinoblastoma protein
RepS	Replicative Senescence
RING	Really Interesting New Gene
RIP	Regulated Intramebrane Proteolysis
RNAi	RNA-interference
ROS	Reactive Oxygen Species
RTKs	Tyrosine Kinase Receptors
SA-β-Gal	Senescence-Associated β-Galactosidase
SAHF	Senescence-Associated Heterocromatin Foci
SASP	Senescence-Associated Secretory Phenotype
SH2	Src Homology like 2
SHC	Src Homology 2 domain Containing transforming
SKP2	S-phase Kinase-associated Protein 2
SMS	Senescence Messaging Secretome
SOS	Son Of Sevenless
SP1	Specificity Protein 1
SRC	Sarcoma
STATs	Signal Transducers and Activators of Transcription
SV40-LTAg	Simian Virus 40 Large T-Antigen
SWI/SNF	SWItch/Sucrose Non-Fermentable

TFs	Transcription Factors
TGF-alpha7TGF-α	Transforming Growth Factor-α
TGFβ	Transforming Growth Factor-β
TIF	Telomere dysfunction–Induced Foci
TKB	N-terminal Tyrosine Kinase Binding
TKI	Tyrosine Kinase Inhibitor
TrxG	Trithorax Group
UPR	Unfolded Protein Response
β-Gal	β-D-Galactosidase
γ-H2AX	H2AX the phosphorylated form

INDEX

Index

INTRODUCTION

Chapter 1

Introduction

1.1 The Epidermal Growth Factor Receptor Family

1.1.1 Evolution and Function

Eukaryotic cells constantly receive and integrate a continuous flow of information coming from the extracellular medium. Evolution has endowed cells with multiple mechanisms of ever increasing complexity to cope with the complex mixture of messages coming from the extracellular matrix, as well as from neighbouring cells. The Tyrosine Kinase Receptors (RTKs) of the Epidermal Growth Factor Receptor (EGFR or HER) family are among the best-characterized components of these mechanisms. Mammalian EGFR and related receptors evolved from a simple system composed of one receptor and one ligand, present in the most primitive metazonas such as *Caenorhabditis Elegans*. Arthropods, such as *Drosophila Melanogaster*, have one receptor and four different ligands [1, 2]. Mammals have a more complex system of four different receptors and more than ten ligands [3 and references therein]. In humans, the EGFR family, also known as ErbB (name derived from the homolog Erythroblastic Leukemia viral oncogene) family, comprises in addition to EGFR itself (also called ErbB1/HER1) the closely related receptors ErbB2/HER2/Neu, ErbB3/HER3 and ErbB4/HER4 (Fig. 1).

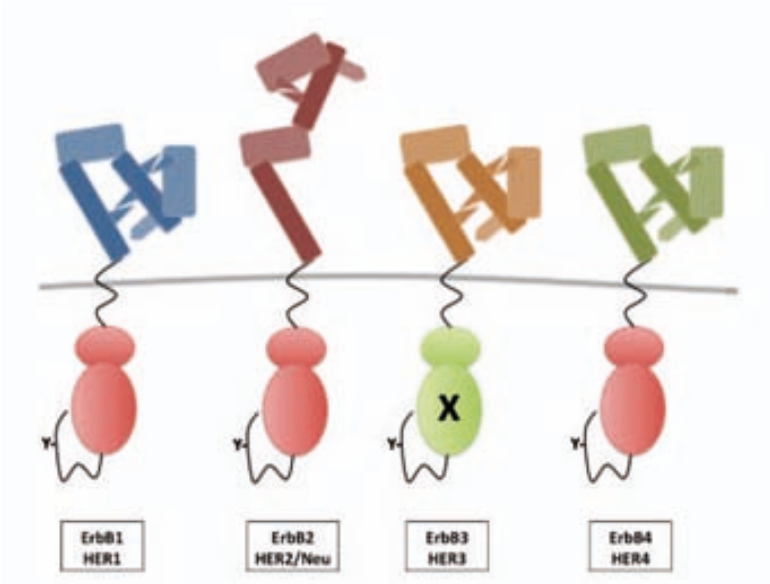

Figure 1: Schematic representation of the four members belonging to the EGFR (or ErbB) family of human receptors.

This dissertation does not aim to detail the function of each one of them. Briefly, in normal physiological conditions, all of the four receptors exert fundamental functions during the embryonic development: knock-out (KO) mice of any of them show embryonic or early postnatal lethality. The study of the phenotype of these pups and embryos indicated the functions of each receptor. HER1 is implicated in the respiratory, follicular, epidermic and gastrointestinal epithelia development [4 and references therein -70, 71-]. HER2 and HER4 have overlapping functions in neuromuscular junctions as well as cardiac development [4 and references therein -72, 74-]. HER3 participates in the neuronal crest formation by helping the maturation of Schwann cells precursors [4 and references therein -73-]. The impossibility to obtain constitutive KO animals for any of the receptors imposed the generation of conditional KOs mice, which uncovered the function of the receptors during adulthood. HER1 is fundamental in lactation and pubertal mammary duct development [6, 7]. HER2 regulates lobulo-alveolar differentiation and lactation [8]. It exerts specific functions in the physiology of the heart [9] and in muscle regeneration [9b] during adulthood.

1.1.2 EGFR Discovery

Back in 1952, Rita Levi-Montalcini discovered a secreted factor produced by mouse tumor cells that was able to induce neurite growth in chicken embryos [4 and references therein -1-]. It was the first growth factor ever discovered, the Nerve Growth Factor (NGF). After having contributed to the isolation and purification of the NGF in 1957 [4 and references therein -2, 3-], Stanley Cohen isolated another growth factor from the murine submaxillary gland, in 1962 [4 and references therein -4-]. This secreted protein was named Epidermal Growth Factor (EGF) because of its ability to induce proliferation of epithelial cells [4 and references therein -5-]. One specific receptor binding this molecule was found in 1975 on the surface of fibroblasts using ^{125}I-labelled EGF [4 and references therein -6-]. A bit later, in 1978, Carpenter and colleagues decided to use the epidermoid squamous carcinoma cells A431 to purify and to clone the DNA sequence encoding this EGF receptor. This choice was critical and it was made because crude membrane preparations obtained from these were known to possess an extraordinary high concentration of EGF binding units.. In the 1980s the homology between EGFR and the v-erbB (avian erythroblastosis virus) viral oncogene became clear. Hunter and colleagues showed that the receptor possessed tyrosine kinase activity, which was increased by EGF stimulation [4 and references therein -9, 13, 14-]. EGFR became the prototypical Human Tyrosine Kinase Receptor. Subsequent studies investigated the physiological role of endogenous EGFR, already overviewed at the end of the paragraph 1.1.1. Due to the impact of their initial discovery of NGF and EGF, Levi-Montalcini and Cohen were awarded the Nobel Prize in Physiology or Medicine in 1986 (Fig. 2).

Figure 2: Rita Levi-Montalcini (left) and Stanley Cohen (right) photographed in their respective laboratories in the same year in which they received the Nobel Prize.

1.1.3 HER2 Discovery

The tyrosine kinase receptor originally called Neu (p185) was discovered in 1981 as a tumor antigen found in carcinogen-induced rat brain cancers [10], and it was soon found to be related to EGFR [11]. During the same year, the human sequence coding for a potential cell surface tyrosine kinase receptor was cloned and characterized. The gene, located on chromosome 17q21.1, shared high homology with the human EGFR and was named Human EGFR-Related 2 (HER2) [12]. In 1986, Akiyama and colleagues used the nucleotide sequence to extrapolate the expected carboxyl terminus of the HER2 protein and generated a 14 residues synthetic peptide. They raised antibodies against it and then used them to immunoprecipitate the 185kDa HER2 protein [13]. Subsequent studies characterized the physiological functions of endogenously expressed HER2, already overviewed at the end of the paragraph 1.1.1. In non-physiological contexts, when ectopically expressed in various cell types, HER2 possesses potent transforming activity. Overexpression of the receptor makes mouse fibroblasts tumorigenic [14, 15, 16] and it increases invasiveness and tumorigenicity of breast cancer cell lines [17]. Upon HER2 expression, human mammary epithelial cells acquire proliferative advantage and transformed characteristics that resemble early stages of epithelial cell transformation in vivo [18, 19]. Expression of the human HER2 cDNA in transgenic mice induces metastatic mammary tumors with long-latency [20]. These tumors show frequent genetic alterations of the HER2 transgene. In accordance with previous results [21, 22, 23], recent work from our group [24] confirmed that such alterations include point mutations, deletions and insertions mostly located in the cDNA region corresponding to the juxtamembrane region of the receptor. These alterations have in common that they all lead to an imbalance in the number of cysteine residues. As a result, these mutant HER2 forms gain the ability to form dimers maintained by intermolecular disulfide bonds. The pattern of HER2 expression in naturally occurring human breast cancer will be described in the further on in paragraph 1.1.7.

1.1.4 ErbB Receptors Activation and Signalling

The signalling from ErbB receptors can be generally stratified into three different layers: the “input”, the “signal-processing” and the “output” (Fig. 6). The “input layer” comprises all the ligands and the receptor dimers. ErbB receptors consist of four main functional domains: an intracellular C-terminal regulatory domain, an intracellular tyrosine kinase domain, a transmembrane domain and an extracellular domain. The extracellular ligand-binding domain of each receptor is composed of two homologous Large (L) domains, and two Cysteine-Rich (CR) domains. From the N-terminus the order of the four domains is L1-CR1-L2-CR2. Alternative published nomenclatures are L1-S1-L2-S2, and I-II-III-IV [25 and references there in] (Fig. 3). The latter will be used in this dissertation for simplicity.

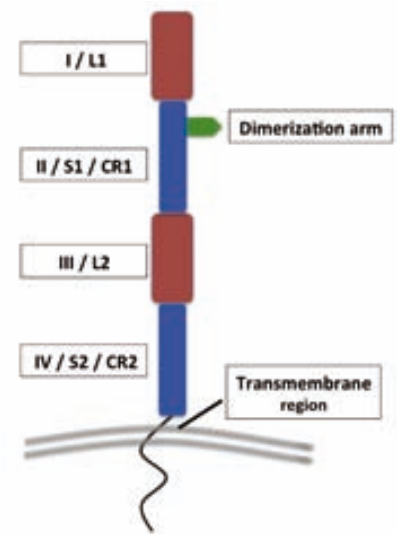

F**igure 3. ErbB receptors extracellular region:** Main structural features characterizing the extracellular region of a prototypical ErbB receptor, from the N-terminus the order of the four domains is L1-CR1-L2-CR2. Alternative published nomenclatures are L1-S1-L2-S2, and I-II-III-IV.

All ErbB receptors, with the exception of HER2, have affinity for specific soluble ligands. All the ligands have in common an EGF-like domain. Among the known ligands EGF, Amphiregulin (AR), Epigen/Epithelial Mitogen (EPGN) and the Transforming Growth Factor-α (TGF-α) specifically bind to ErbB1; Betacellulin (BTC), Heparin-Binding EGF (HB-EGF) and Epiregulin (EPR) bind to both ErbB1 and ErbB4; Neuregulins 1 and 2 bind to ErbB3 and ErbB4 and Neuregulins 3 and 4 bind to ErbB4 [3 and references therein -8-] (Table 1). In general, ErbB ligands act over short distances as autocrine or paracrine growth factors [25].

	ErbB1 HER1	ErbB2 HER2	ErbB3 HER3	ErbB4 HER4
EGF	+	-	-	-
TGF-α	+	-	-	-
HB-EGF	+	-	-	+
AR	+	-	-	-
BTC	+	-	-	+
EPGN	+	-	-	-
EPR	+	-	-	+
NRG1	-	-	+	+
NRG2	-	-	+	+
NRG3	-	-	-	+
NRG4	-	-	-	+

Table 1. Ligand-receptor specificity for the four human ErbB receptors: Epidermal Growth Factor EGF, Amphiregulin (AR), Epigen/Epithelial Mitogen (EPGN) and the Transforming Growth Factor-α (TGF-α) specifically bind to ErbB1; Betacellulin (BTC), Heparin-Binding EGF (HB-EGF) and Epiregulin (EPR) bind to both ErbB1 and ErbB4; Neuregulins 1 and 2 bind to ErbB3 and ErbB4 and Neuregulins 3 and 4 bind to ErbB4

When inactive, each of the four human receptors presents auto-inhibitory interactions between domains I and II. These interactions prevent dimerization and are conserved, as they can be found in the inactive *drosophila*-EGFR (dEGFR or DER), [26]. Evolution endowed all human receptors, again with the exception of HER2, with additional auto-inhibitory intra-molecular interactions between the domains II and IV. Such interactions confer to the three receptors the characteristic tethered, or “close”, conformation, in which dimerization is further inhibited [25, 26]. Upon binding, the ligand promotes the interaction between the domains I and III of the receptor and induces an outward rotation (142º) of the extracellular region [3 and refrences therein -11-]. The ligand-induced conformational change disrupts all types of auto-inhibitory interactions [25, 26]. This now fully extended conformation predisposes the receptor for dimerization by exposing the dimerization arm (Fig. 4). Since it lacks the interactions between domains II and IV, HER2 is never tethered and constitutively adopts a non-tethered (or “open”) conformation. For this reason, early structural studies suggested that HER2 would be constitutively active [27, 28]. However, HER2 does not have a greater tendency than unligated EGFR to homodimerize [29]. Recent studies suggest that HER2 retains forms of less evolved intrinsic regulation.

Indeed HER2, exactly like its ancestor dEGFR, is constitutively “open” and at the same time presents the auto-inhibitory interactions between domains I and II (Fig. 5B) [26]. Even being constitutively non-tethered like HER2, *drosophila*-EGFR is not constitutively active. On the contrary, dimerization and activation of dEGFR are tightly regulated and only occur upon binding of its ligand, when all auto-inhibitory interactions are broken (Fig. 5A) [33, 26]. Differently from the other human receptors, no soluble ligand is known for HER2. Intriguingly, dEGFR ligands are not active as soluble proteins, as they require membrane-association to induce proper activation of the receptor [30]. Similarly, Muc4 (ASGP2), one EGF-like domain-containing and membrane-bound protein, directly interacts with and activates HER2 [31 and references therein]. So the existence of other factors able to act as membrane-associated ligands for HER2 cannot be excluded. Along the same line, a regulatory role of the trans/juxta membrane region of the receptor, has been proposed (Fig. 5B) [21, 22, 23]. Nonetheless, HER2 unique structure makes it the preferred heterodimerization partner for other ErbB family members when they are bound to their ligands [4 and references therein -96, 97-].

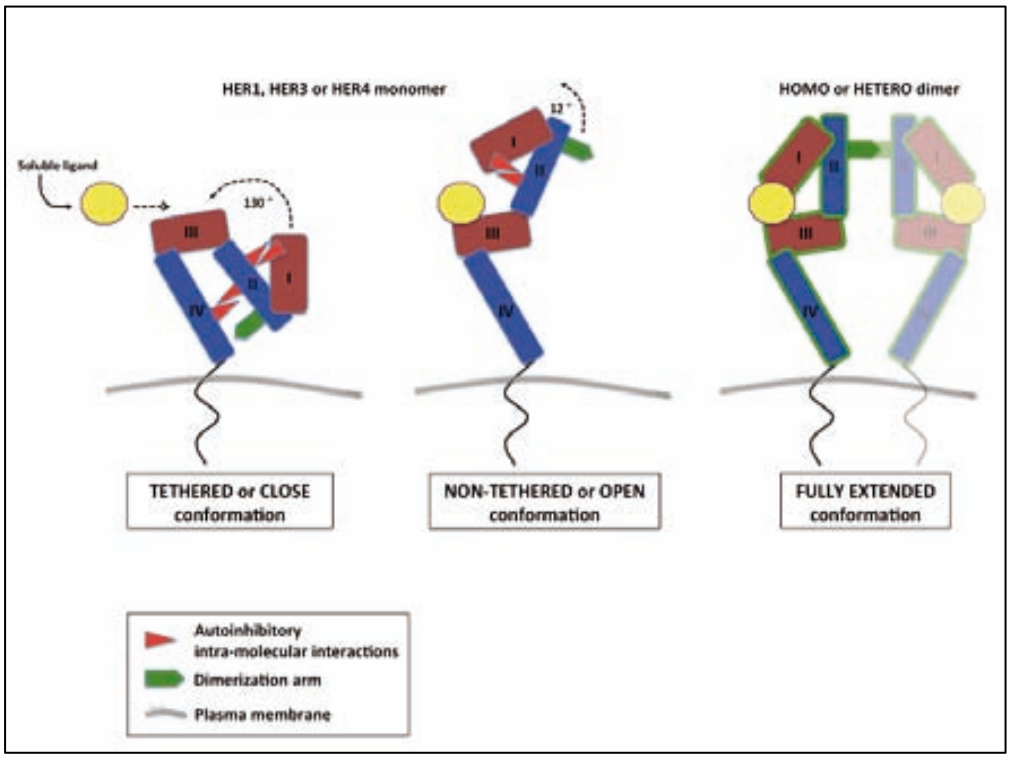

Figure 4. Dimerization process upon binding of a soluble ligand. In the case of HER1, HER3 or HER4, binding of the ligand (yellow) promotes the interaction between the domains I and III of the receptor and induces an outward rotation (142º). The ligand-induced conformational change disrupts all types of auto-inhibitory interactions (red). This now fully extended conformation predisposes the receptor for dimerization by exposing the dimerization arm (green).

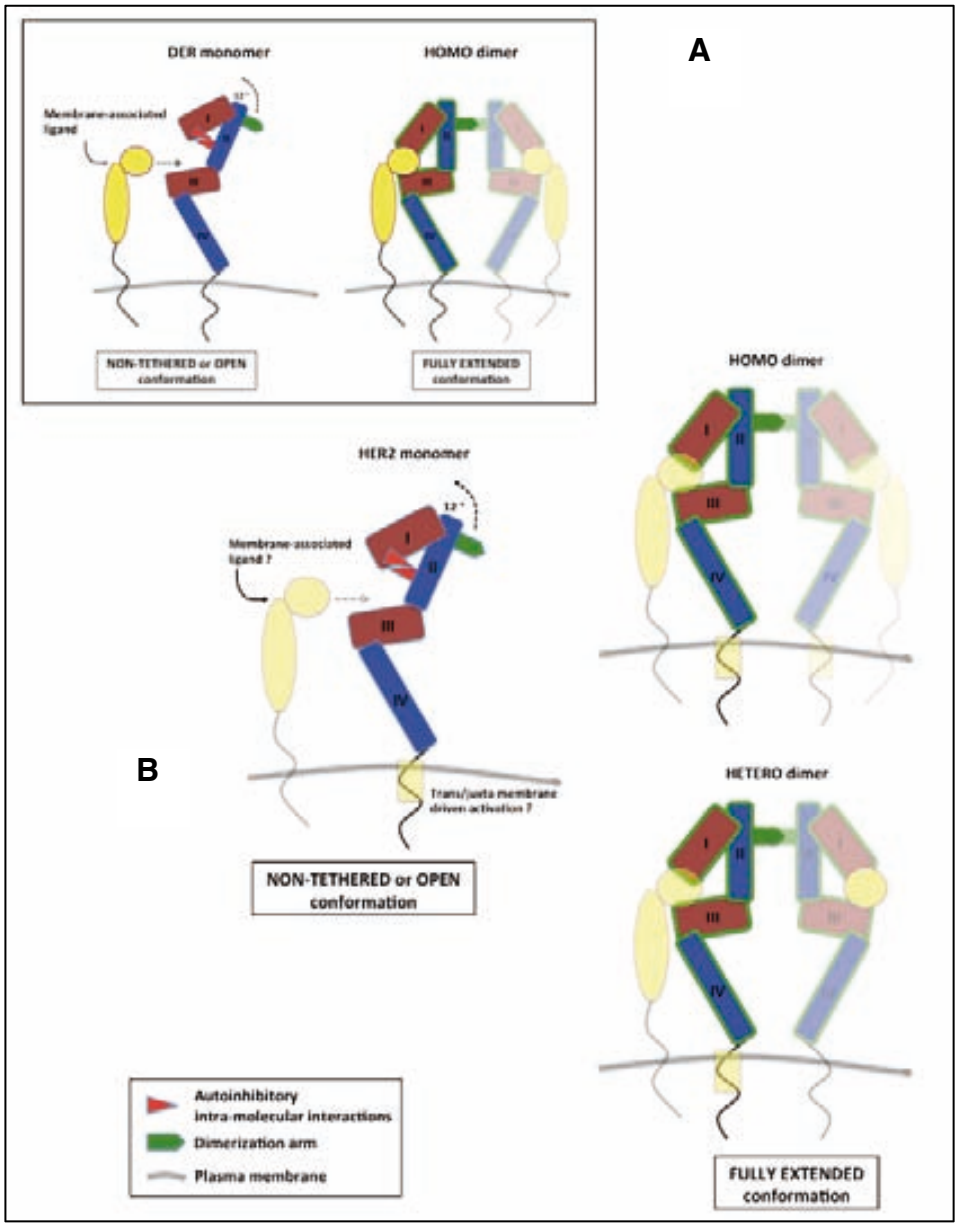

Figure 5. Proposed dimerization process for HER2: A. Dimerization and activation of DER are tightly regulated and only occur upon binding of its ligand, when all auto-inhibitory interactions (red) are broken. DER ligands require membrane-association to induce activation of the receptor. **B.** The existence of factors able to act as membrane-associated ligands for HER2 cannot be excluded. Neither it can a regulatory role of the trans/juxta membrane region of the receptor. HER2 is the preferred heterodimerization partner for other ErbB family members when they are bound to their ligands.

Thus, the binding of a soluble ligand to EGFR, HER3 or HER4 induces a conformational change in their extracellular region that exposes the dimerization arm (see Fig. 4). The latter allows the interaction with the exposed dimerization arms of another activated receptor [25 and reference therein].

Overall, the levels of expression of ligands and receptors dictate the identity of dimers formed. Invariably, dimerization brings in close proximity the intracellular tyrosine kinase domains. These domains are composed of a smaller N-lobe containing the alpha-C helix and a slightly bigger C-lobe, as well as by the carboxy-terminal regulatory tail [25]. When in close proximity the interaction between the C-lobe of the kinase domain of one receptor and the N-lobe of the kinase domain of another activates the latter, allowing intermolecular phosphorylation of intracellular tyrosine residues (Fig. 6) and subsequent downstream signalling [25, see also the next paragraph]. The only exception is represented by HER3 homodimers, due to the impaired tyrosine kinase activity of this member of the family (Fig. 1). Homo-dimerization of HER4 or HER1, as well as their respective hetero-dimerization with HER3, leads to relatively weak signalling. HER2 predominantly acts as a signal amplifier [3 and references therein]. Indeed, heterodimers containing HER2 exhibit prolonged activation of downstream signalling pathways [25 and reference therein].

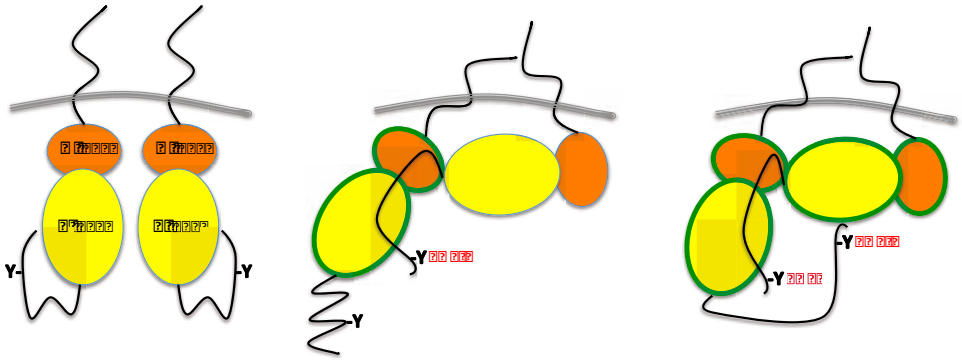

Figure 6. Intermolecular phosphorylation of the intracellular kinase domain: Dimerization brings in close proximity the intracellular tyrosine kinase domains. These domains are composed of a smaller N-lobe containing the alpha-C helix and a slightly bigger C-lobe, as well as by the carboxy-terminal regulatory tail. When in close proximity the interaction between the C-lobe of the kinase domain of one receptor and the N-lobe of the kinase domain of another activates the latter, allowing intermolecular phosphorylation of intracellular tyrosine residues and subsequent downstream signalling.

The "signal-processing layer" comprises adaptor molecules and enzymes, the signalling cascade and the transcription factors ultimately activated. As already described in the previous section, upon dimerization, the tyrosine kinase domains within the intracellular part of the receptor interact, become activated and trans-phosphorylate. Phosphorylated tyrosine residues are docking sites that recruit a variety of intracellular adaptor and enzyme molecules [3 and references therein]. The three protein domains able to bind to receptor phosphotyrosines are the SH2 (Src Homology like 2), the PTB (Phospho-Tyrosine Binding) and the TKB (N-terminal Tyrosine Kinase Binding).. Some adaptors, like Src Homology 2 domain Containing transforming (SHC), possess both SH2 and PTB domains. Others, like Growth factor Receptor-Bound protein 2 and 7 (GRB2 and 7), only have SH2 domains. Once bound to the receptor, they recruit additional effector proteins such as the guanine nucleotide exchange factor Son Of Sevenless (SOS) typically involved in Rat Sarcoma (RAS) activation [32]. Among the enzymes some, like the Phospholipase C gamma (PLCγ), use SH2 domains. Others, like the E3 ubiquitin ligase Casitas B-lineage Lymphoma (CBL), carry TKB domains. These types of interaction trigger a complex downstream signaling cascade regulated at multiple levels. The main signaling pathways activated downstream of HER receptors are the RAS-driven Mitogen Activated Protein Kinases (MAPK) pathway, the Phosphoinositide-3-Kinase - Protein Kinase B -mammalian Target of Rapamicin (PI3K-PKB-mTOR) pathway, the c-Jun N-terminal kinase (JNK) pathway, the Sarcoma (SRC) pathway and the Signal Transducers and Activators of Transcription (STATs) pathway. [3 and references therein]. The signalling cascade ends regulating the activity of several Transcription Factors (TFs) including the proto-oncogenes JUN, FOS and MYC, zinc-finger-containing TFs like SP1 and EGR1, as well as ETS family members such as ELK1 or forkhead TFs like FKHRL1. After this extraordinary complex signal processing the final output can range from proliferation and migration to differentiation and apoptosis [3].

1.1.5 ErbB Receptors Deregulation

Several mechanisms can lead to the deregulation of ErbB receptors signalling, which characterizes various types of hyperproliferative diseases including psoriasis [34], cardiac hypertrophy and various cancers [4 and references therein -64, 65, 66-]. To start with, overproduction of ligands both from the tumor stroma or from the cancer cells themselves can cause abnormal transactivation of the receptors. The increased ligand production can be due to direct transcriptional activation or to the activity of matrix metalloproteinases involved in the cleavage of the mature membrane-bound precursors. Eventually, the release of the soluble active form of the ligand contributes to instauration of autocrine positive feedback [4]. Probably the best characterized example is represented by the abnormally high production of TGF-alpha by carcinoma cells of the liver, oesophagus, ovary, lungs, colon and pancreas. In early androgen-dependent prostate cancers, stromal cells provide paracrine TGF-alpha. In more advanced androgen-independent diseases, tumor cells produce the ligand in an autocrine fashion. Mammary adenocarcinomas can overexpress NRG1 [3 and references therein -108, 51, 52, 109-]. At the receptor level, EGFR, HER2 and HER3 are overexpressed or overactivated in a subset of solid tumors of different origin, both individually or concomitantly. This generally indicates more aggressive disease and predicts worse outcome for the patients. Overexpression is frequently caused by gene amplification [3 and references therein -53, 55 -] and less frequently by impaired receptor internalization [4 and references therein -86, 87, 88-]. Overactivation results in increased catalytic activity and it occurs due to mutations or to expression of either splicing or translation variants [4 and references therein -84, 85-].

1.1.6 EGFR and cancer

EGFR overexpression in breast cancer is an indicator of recurrence in operable cases and bad prognosis in the advanced disease. It is overexpressed as well in non-small-cell lung cancers, prostate and bladder carcinomas where it has prognostic value. Cases of overexpression are reported also in head and neck as well as kidney carcinomas. In addition, The frequent EGFR overexpression in brain tumors correlates with grade and poor survival. Notably, 40% of gliomas present

amplification of the EGFR gene [3 and references therein -110, 111, 35-]. The EGFR gene is found mutated or rearranged in breast, ovary and lung carcinoma as well as in gliomas [3 and references therein -53, 54-]. Clinically relevant EGFR mutations are found within its kinase domain and make the receptor more susceptible to ligand-induced activation [35 and references therein -18, 19, 67-]. Lung cancer patients carrying gain-of-function somatic mutations tend to respond to specific EGFR-targeting drugs. In some cases the appearance of additional mutations is associated with acquired treatment resistance [35 and references therein -18, 20, 66, 73-]. The most frequent rearrangement, often observed in gliomas, gives rise to the constitutively active EGFRvIII. This variant of EGFR is generated by an in-frame genomic deletion of 801 base pairs in its coding region, between exons 2 and 7, corresponding to aa 6 to 273 of the protein. This deletion in the extracellular ligand-binding domain produces a truncated receptor that is constitutively active and promotes cellular transformation in vitro [3 and references therein -35, 53, 54-]

1.1.7 HER2 and cancer

HER2 is overexpressed in 15-30% of breast and ovarian cancers, which combined account for one-third of all cancers and approximately one-quarter of cancer related deaths in woman [36]. Overexpression of HER2 correlates with chemo-resistance and poor prognosis. In breast adenocarcinomas it also correlates with tumor size, tumor spreading to lymph nodes, higher percentage of cells in the S-phase, aneuploidy and loss of expression of steroid hormone receptors [37]. HER2-positive tumors are generally less differentiated and have a particularly high tendency to metastatize to lung and brain [37b, 38]. Overexpression is frequently associated with gene amplification, with tumors carrying up to 25-50 copies of the HER2 gene (Fig. 7). This translates in expression of up to 2 million receptor molecules at the tumor-cell surface, a protein level 40-100 fold higher than the one found in normal cells [39, 40, 41]. HER2 gene amplification tends to be an early event and is maintained during progression to invasive disease, nodal metastasis and distant metastasis [42, 43, 44, 45]. Large-scale gene-expression analysis clearly shows that HER2 amplification defines a specific breast cancer subtype [46, 47]. HER2 increased expression and association with worse disease is also seen in subsets of gastric, esophageal and endometrial cancers [48, 49, 50] and more rarely in lung, bladder and the

oropharyngeal tumors [51, 52, 53]. Compared to EGFR, HER2 mutations in human tumors are quite uncommon. Historically important for its wide scientific use as a prototypical activated HER2-mutant is the rat-derived NeuT variant. NeuT is the name assigned to the HER2-V664E mutant originally isolated from chemically induced rat tumors [56]. This mutation, located in the transmembrane region of the receptor, promotes receptor dimerization and, therefore, tyrosine kinase activity [57]. Several mouse transgenic models have confirmed the causal role of this oncogene in tumorigenesis [58, 59]. Despite generally not found in spontaneous human tumors, mutations homologous to the one present in NeuT have been introduced in the human HER2 for the sake of study (mentioned in 31, 60). Only few months ago, at the Vall d' Hebron Hospital, the first-in-men HER2-V659E mutant has been identified. It was found in a recent lung tumor of a 29-year-old patient carrying a germline p53 mutation (Li-Fraumeni Syndrome) [60]. Cases of HER2 tyrosine kinase mutation have been reported in lung cancer [54, 61] and a very recent multicenter study showed that mutated HER2 is a driver in 2% of lung adenocarcinomas. Like with EGFR, these mutations are clinically relevant and HER2-targeted therapy is promising in these cases [62]. Another recent report identifies a panel of seven somatic activating mutations in the tyrosine kinase domain of HER2 in 13 gene-amplication negative breast cancer patients [54]. One deletion-mutant homologous to the previously described EGFRvIII is been reported in few lung and breast adenocarcinomas [54]. Despite these observations, the fact that human cancers are generally characterized by overexpression of the wild-type HER2 [55] indicates the existence of non-mutational mechanisms of activation. Along this line, work from different groups described the existence of a splicing variant of HER2, the ΔHER2. This alternative transcript lacks 48 bp of the 16th coding-exon producing a 16 aa deletion in the juxtamembrane region. This generates a cysteine-imbalanced receptor reminiscent of the mutant HER2 forms found in murine transgenic tumors (see the end of paragraph 1.1.4). ΔHER2 forms disulphide-bridged homodimers and is therefore constitutively active [63]. Previous in vitro studies suggested that ΔHER2 confers resistance to Herceptin® (also called Trastuzumab), a therapeutic Monoclonal antibody (Mab) targeting the extracellular domain of HER2 [64, 67]. More recent xenograft experiments do not confirm this evidence [65]. This splicing variant represents approximately 2-9% of HER2 mRNA in human breast carcinomas. It correlates with worse prognosis as well as with the presence of lymph node metastases [63, 66]. Previous work from our group demonstrated that other HER2

variants are produced by alternative initiation of translation from downstream AUG codons in the wilde-type HER2 mRNA [68]. We were then able to prove that this process represents a different mechanism of non-mutational HER2 activation. Indeed, translation starting at methionine 611 of the HER2 transcript generates a truncated form of the receptor, which is cysteine-unbalanced. The resulting HER2 variant, p95HER2, forms disulphide-bonded homodimers, which are constitutively active [24]. The fact that ΔHER2 and p95HER2 are expressed in breast cancers [64, 70] contributes to explain the low frequency of HER2 activating mutations in such tumors. The experimental section of this dissertation will report results obtained expressing p95HER2 in various breast epithelial cell lines. This work is incremental with respect to previous publications from our group concerning this HER2 variant. For this reason, the next paragraph will be dedicated to the characterization of p95HER2 carried out in our laboratory, to which I contributed.

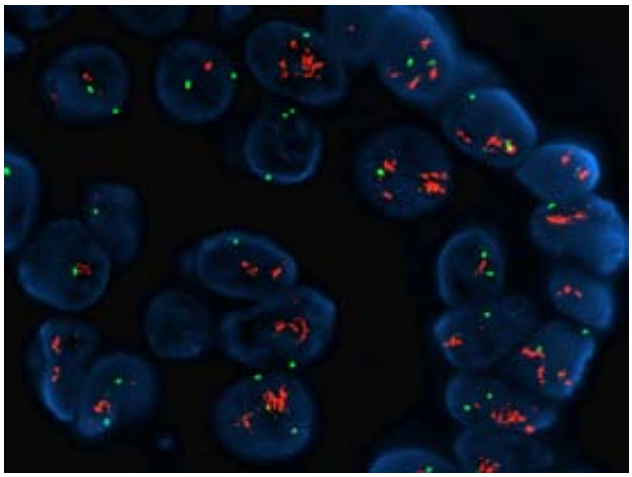

Figure 7. Example of HER2 Fluorescence In Situ Hibridization (FISH): Paraffin section FISH is performed on paraffin embedded breast tissues from patients. It detects Her2 gene (red) copy number gain compared with a control probe that in this case is alpha satellite 17 (green). The ratio between the two signals is used to extrapolate the degree of gene amplification. This information is relevant with respect to the therapeutic options for a given tumor [image taken from East of Scotland Regional Genetics Service webpage].

1.1.8 p95HER2 characterization

Breast cancers positive for both full length HER2 and HER2 Carboxyl-Terminal Fragments (CTFs), compared with the ones expressing predominantly HER2-FL, have higher tendency to metastasize at limph nodes [71]. Indeed, early reports showed that patients carrying these tumors have worse prognosis [72]. In these studies, tumors that were considered positive for HER2-CTFs presented expression of a heterogeneous mixture of different fragments. Initially, all these fragments were assumed to arise from proteolytic cleavage of the HER2-FL. In 2006, the first evidence for alternative initiation of translation from downstream methionines in the wilde-type HER2 mRNA was published [68]. This allowed the prediction of four possible HER2-CTFs and the generation of constructs to ectopically express them. The 611-CTF and the 687-CTF recapitulated the two products of alternative initiation of translation at methionines 611 and 687 of the HER2 mRNA [68] (Fig. 8). The 648-CTF and the 676-CTF reproduced the two possible HER2 fragments arising from proteolytic cleavage [73]. The HER2 CTFs encompassing the transmembrane domain, 611- and 648-, were efficiently transported to the plasma membrane. The two remaining CTFs, 687- and 676-, were soluble. We proceeded to the comprehensive analysis of the four fragments and found that soluble HER2-CTFs were inactive. The membrane-bound product of ectodomain shedding, HER2-648-CTF showed activity comparable to that of the full-length receptor. The membrane-bound product of alternative initiation of translation, HER2-611-CTF (since then called p95HER2) proved to be a constitutively active truncated receptor able to signal as a HER2 disulphide-bonded homodimer [24]. Indeed, we found that p95HER2 expression readily transformed immortalized Mouse Embryonic Fibroblasts (MEFs), which become able to form subcutaneous tumours dependent on p95HER2 expression (see paragraph 3.2 of the results section). These cells represented a suitable model to test the efficacy of different drugs in the treatment of p95HER2 positive tumor-xenografts. Indeed, in collaboration with the Neal Rosen's lab (at the Memorial Sloan-Kettering Cancer Center of New York -USA-) we showed that subcutaneous tumors formed by MEFs expressing p95HER2 are sensitive to HSP90 inhibitors [74]. Soon after, we showed that these tumors respond to the EGFR/HER2 dual Tyrosine Kinase Inhibitor (TKI) Lapatinib [75]. Expression of p95HER2 in human breast cancer cells strongly activates various signal transduction pathways. This activation induces the transcriptional up-regulation of genes associated with tumour

malignancy and poor prognosis in cancer patients such as MET, MMP1 and ANGPTL4 [24] and it increases their motility [69]. The effect of sustained expression of p95HER2 in the same cells will be the subject of the experimental work presented in this thesis. Importantly, others and we also demonstrated that p95HER2 is expressed in about 30% of HER2 positive breast cancers [76, 70]. Initial studies showed that p95HER2-positive patients may exhibit a worse response to Herceptin®, the therapeutic Mab directed against the extracellular region of the full-length receptor. A subsequent clinical study did not confirm this evidence (ref: GeparQuattro) and the eventual correlation with resistance to the treatment is currently being addressed in a new clinical trial (ref: NeoAltto). However, expression of the HER2 fragment confers distinctive biological and clinical features to the tumors. In particular, compared to tumors exclusively positive for full-length HER2, they do not express the Estrogen Receptor (ER) and have higher tendency to metastasize correlating with poorer prognosis [70].

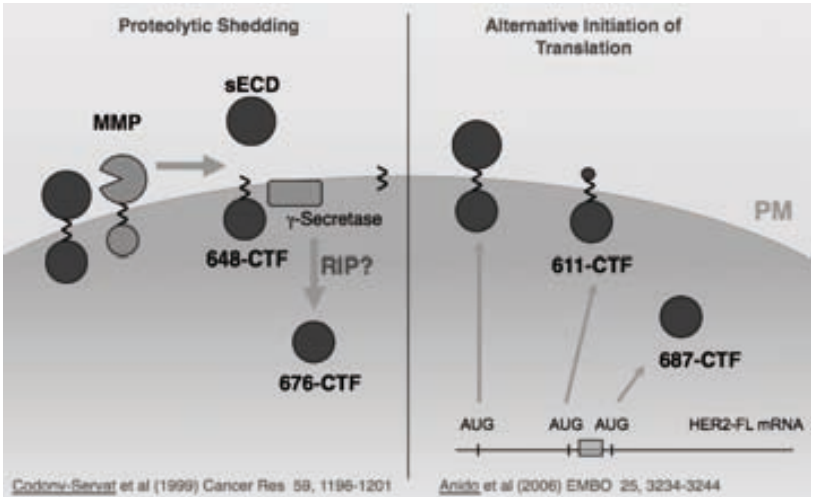

Figure 8. Scheme representing the four possible HER2 CTFs: The 611-CTF (p95HER2 in the rest of this dissertation) and the 687-CTF recapitulated the two products of alternative initiation of translation at methionines 611 and 687 of the HER2 mRNA. The 648-CTF and the 676-CTF reproduced the two possible HER2 fragments arising from proteolytic cleavage. The HER2 CTFs encompassing the transmembrane domain, 611- and 648-, are efficiently transported to the plasma membrane. The two remaining CTFs, 687- and 676-, are soluble.

1.1.9 HER3 and cancer

Compared to EGFR and HER2, the characterization of the role of HER3 in human tumors and its potential relevance is still in its early age. The available information is limited but promising. A recent retrospective study summarizes the evidence for HER3 overexpression in head and neck, breast, colorectal, gastric, ovarian and cervical carcinomas. Overall the receptor is overexpressed in around the 40% of cases and associates with worse prognosis, especially when co-expressed with HER2 [77]. A recent report shows recurrent oncogenic HER3 somatic mutations in colon and gastric cancers [78]. Finally, a novel V855A somatic mutation located in the exon 21 of the HER3 tyrosine kinase domain has been recently identified in one case of Non Small Cell Lung Cancer. The mutation confers gain-of-function to HER3 and correlates with sensitivity to the TKI Afatinib [79]. Non-mutational mechanisms of activation have not been reported for HER3.

1.1.10 HER4 and cancer

Even less information on the role of HER4 in cancer is available. Some studies from the late 1990s suggested that reduced HER4 expression in breast and prostate cancers would correlate with relatively differentiated tumor histology [80]. Another work found co-expression of HER4 and HER2 in more than half of the 70 pediatric medulloblastomas analyzed. Co-expression appeared to be a non-favorable prognostic factor [81]. Finally in 2006, a Korean research group screened 595 cancer samples from breast, lung, colon and stomach. Beside other cancer-relevant mutant proteins, they looked for HER4 somatic mutations in its tyrosine kinase domain. 1-3% of cases in all tumor types showed mutant HER4 as the only detectable genetic abnormality. The authors interpreted that the mutation in HER4 could be the one driving the tumor in these subgroups [82]. Of note, a non-canonical form of signalling has been described in the case of HER4. This receptor undergoes Regulated Intramebrane Proteolysis (RIP). A double sequential poteolytic cleavage releases an intracellular soluble HER4 fragment [83, 84]. The latter translocate to the nucleus and act as a transcriptional regulator [85, 86]. Mab-mediated inhibition of HER4 shedding, the first step of RIP, inhibits the growth of breast cancer cells tumor xenograft. Though, even if 20% of breast cancer patients show evidence of elevated HER4 shedding, the relevance of RIP in these cases remains unclear [87].

1.2 Cellular Senescence

1.2.1 Overview

Back in 1961, Leonard Hayflick and Paul S. Moorhead first used the term ‘‘cellular senescence’’ to describe the spontaneous and irreversible proliferation arrest of primary human fibroblasts growing in vitro [88]. In 1965, Hayflick showed that these cells were able to grow in culture for approximately 55 population doublings and then exhausted their proliferative potential [89]. Thereafter, the number of in vitro divisions allowed for non-immortalized cells before they stop dividing was given the name of “Hayflick limit” and the arrest defined as Replicative Senescence (RepS from now on). With time, it became clear that several types of cells undergo senescence in response to a variety of stressful conditions. The molecular events associated with the induction of RepS, as well as other forms of non-spontaneous cellular senescence, have been in part discovered. Active investigation is currently ongoing to elucidate additional aspects of this complex cellular process. Without the pretention of being fully comprehensive, the next paragraphs will summarize the best-characterized aspects of cellular senescence.

1.2.2 Symptoms of the “cellular senescence syndrome”

Cellular senescence can be considered as a syndrome defined by several phenotypes. Among them, the most characteristic is a largely irreversible arrest in cell proliferation. At present, no physiological stimuli has been shown to induce senescent cells to re-enter the cell cycle. Only genetic manipulations, like the inactivation of certain tumor suppressor genes, can cause senescent cells to resume cell division [90]. Even assuming that still unknown physiological conditions may favor the overcoming of senescence, its associated proliferation arrest is undoubtedly stringent. Senescent cells show persistent activation of the DNA Damage checkpoint Response (DDR) as shown by the appearance of the characteristic nuclear DDR-foci [104, 105, 106] (see also paragraph 1.2.4). The main tumor suppressor pathways p53/p21 and p16INK4A/pRb, indeed, contribute to establishment and maintenance of the senescent state [119, 120, 121] (see also paragraph 1.2.5). Accordingly, senescence can act as a tumor barrier by limiting the expansion of damaged cells [98,104]. Cellular senescence is also characterized by the presence of

heterochromatin. In some human senescent cells this results in the formation of Senescence-Associated Heterocromatin Foci (SAHF). These foci are defined by specific mofdifications like the tri-methylation of histone H3 on Lysine 9 (H3K9me3), and the presence of factors such as the Heterochromatin Protein 1 (HP1γ) and the High Mobility Group A2 (HMGA2) [121a, 121b]. The p16INK4A/pRb pathway, together with Anti-Silencing Function 1 (ASF1) and Histone cell cycle Regulation defective homologue A (HIRA) proteins participate in SAHF generation [133, 134]. These heterochromatic regions enforce cellular senescence by suppressing the transcription of genes involved in proliferation [121a]. In addition to stop dividing, senescent cells carry enlarged or multiple nuclei and present widespread changes in gene expression [121a, 122]. These alterations are associated with mayor changes in cell morphology, which become enlarged up to 8-fold in volume [123]. When adherent, hypertrophic senescent cells look flattened and highly vacuolated. Two cellular processes frequently taking place simultaneously to senescence are believed to account for this extensive vacuolization: a cellular stress response associated with the endoplasmic reticulum known as Unfolded Protein Response (UPR) [112] and autophagy [113, 114]. The latter, in fact, represents an important aspect of senescence and several autophagic markers are increased in arrested cells [114]. Recently, local activation of autophagy coupled to mTOR-dependent protein translation within a spatially confined perinuclear subcellular region has been described during senescence [115]. Consistently, senescent cells show an expanded lysosomal compartment [111]. This translates in an increase in the amount of the lysosomal enzyme β-D-Galactosidase (β-Gal), encoded by the GLB1 gene [116], whose activity in normal cells is optimal at pH4. β-Gal high expression contributes to explain why senescent cells are characterized by its easily detectable enzymatic activity at suboptimal pH6 [117]. Indeed, this so-called Senescence-Associated β-Galactosidase (SA-β-Gal) activity is the original and still most used markers for the detection of senescent cells both in vitro and in vivo [91]. In the same line, another lysosomal enzyme, the α-L-fucosidase, has been recently reported as an alternative senescence marker [118]. All the components recovered after autophagic degradation from the lysosomes are then utilized as building blocks for production of new proteins. While some of the factors synthesized de novo probably contribute to the profound remodeling of the senescent cell, some others are secreted [115]. Another characteristic feature of cells that have entered senescence is, in fact, the active secretion of numerous pro-inflammatory cytokines, chemokines, growth factors

and proteases [92]. All these components can exert powerful autocrine and paracrine activities whose effect is variable according to the specific cellualr context. Such property has been referred to as the Senescence-Associated Secretory Phenotype (SASP) [124], or the Senescence Messaging Secretome (SMS) [125]. For simplicity only the term SASP will be used from now on in this dissertation. Due to the complexity of the subject and to its implication in the experimental work that will be presented, one of the next paragraphs will be dedicated to a more detailed description of the SASP.

1.2.3 Events inducing cellular senescence

In the early 1970s, Alexey M. Olovnikov and James D. Watson independently defined the so-called “end replication problem” [107, 108]. This basically consists in the fact that DNA polymerase fails to completely replicate the chromosomal extremes. Such failure implies that repeated rounds of cell division and DNA replication produce a progressive erosion of the telomeric regions at the end of the chromosomes. Indeed, already in 1990, RepS was shown to be linked with a progressive telomere shortening [92 and references therein -61-]. However, senescence can occur prematurely in response to several alternative triggers, the most of which produces some kind of DNA perturbation. Reactive Oxygen Species (ROS) associated with oxidative stress, genotoxic chemical compounds as well as physical genetic damage induced by ionizing radiation are typical examples. The resulting DDR activation is causally linked to the induction of the proliferative arrest (see next paragraph). Cellular senescence can also be induced by excessive mitogenic stimuli [93]. When this is the case the phenotype is normally referred to as Oncogene-Induced Senescence (OIS). Upon overexpression, the hyperactive RAS mutant HRASG12V, for example, is able to induce senescence in normal [94] as well as in transformed cells [95]. Similarly, the oncogenic version of several other components of the MAPK pathway has the same ability [96, 97, 98]. The same is true for activated forms of growth factor receptors such as HER2, when overexpressed [99]. Senescence is also induced upon loss of negative regulators of signaling like the Phosphatase and Tensin homolog (PTEN). This specific type of senescence was observed in prostate tumor cells and is normally referred to as PTEN-loss Induced Cellular Senescence (PICS) [100]. Chronic stimulation by cytokines such as interferon-β [101], as well as other cases of unrestrained mitogenic signals [93, 102, 103] can produce a

senescent growth arrest. For a more comprehensive list of senescence-inducing stimuli see table 2.

1.2.4 DDR activation during cellular senescence

During their lifetime, eukaryotic cells have to deal with genetic damage, whose severity can range from low to cytotoxic levels, on a constant basis. Such DNA Damage (DD) is produced by endogenous stress (like reactive oxygen species or inaccurate DNA replication) as well as by exogenous insults (like UV light, genotoxic stress or DD-inducing drugs). Waves of transient DD Response (DDR) activation allow reparation of these genetic lesions. Specific checkpoints during cell cycle progression, through DDR, induce a temporary arrest and dictate if the cell can survive [92]. Whatever the origin, immediately after DNA Double Strand Breaks (DSBs) formation, Ataxia Telangiectasia Mutated (ATM) and a related enzyme ATM and Rad3 Related (ATR) are recruited at the damage site and activated. Here these two serine/threonine kinases phosphorylate Histone-2AX (H2AX, the phosphorylated form is refered to as γ-H2AX) as well as other several substrates. Among these there are DNA repair proteins like the p53-Binding Protein 1 (53BP1) and Nibrin (NBN or NBS1) as well as checkpoint proteins like Check Point Kinase 1 and 2 (CHK1 and CHK2). All of them accumulate at the DSBs site where γ-H2AX acts as a scaffold protein. This assembly contributes to a positive feedback-loop that amplifies and stabilizes H2AX γ-phosphorylation, which shows a typical focal increase. In fact, the presence of nuclear foci positive for γ-H2AX (and also for 53BP1) is widely accepted as a reliable marker of DDR activation [129]. After recruitment at these DDR-foci, CHK1 and CHK2 continue the signalling cascade regulating the activity of many factors including two cell-cycle master regulators. On one side, they phosphorylate and mediate the degradation of the proto-oncogene Cell Division Cycle 25 (CDC25) whose function is fundamental for cell cycle progression [128]. On the other, they phosphorylate, stabilize and activate the tumor suppressor p53 whose transcriptional targets, such as p21, are then induced [119]. If the damage is fixed, the DDR-foci disappear and the associated signaling ceases, allowing the cells to re-start the cell cylce. If the DNA cannot be repaired, the DDR-foci become persistent and cells are not allowed to re-enter the cell cycle. According to the severity of the irreparable damage, cells can choose between at least two different “final solutions” in order to exit the cell cycle. When the persistent DDR signaling is intense, implying that the

DNA is highly compromised, an apoptotic response in engaged [126]. Alternatively, if the persistent DDR signaling is adequately low, cells adopt a state of permanent cell-cycle arrest, i.e. senescence [92]. Indeed, the typical DDR associated to DD-induced senescence follows a biphasic activation pattern [127]. The first wave of activation is rapid and intense, occurring within minutes to one hour after the induction of the DD [126]. Fumagalli and collegues, using BJ human fibroblasts exposed to γ-irradiation, showed that in this phase the vast majority of cells present very high number of DDR-foci per cell (>100) [110]. This initial phase is attenuated within few days [126], time during which the number of DDR-foci per cell is substantially reduced (4-fold). In the second phase, starting from two weeks after the induction of DD up to several months, the number of DDR-foci per cell decreases by 10-fold [110]. This stable limited number of DDR-foci translates in persistent low levels of p53 activation and p21 induction [127 and references therein -42, 43, 75-]. Both the same and another research group independently demonstrate that DD randomly occurring at telomeres cannot be repaired [110, 132]. Consistently in the mentioned study, despite the marked decrease in number of DDR-foci per cell, the high percentage of cells presenting such foci after irradiation is maintained in time [110]. This discovery explains why low DDR activation is maintained for such long periods and poses telomeres at the cross-road between DD-induced premature senescence and RepS. In the latter, indeed, when telomeres reach a critical minimal length, their protective structure get disrupted. This disruption triggers the formation of DDR-foci, specifically termed Telomere dysfunction–Induced Foci (TIF), and the associated signaling persists along with the establishment of the growth arrest [109]. However, it should be remarked that while DDR-foci are a reliable marker of DDR activation [129] , they are an indirect marker of senescence [104, 105, 106]. When detected, they don't necessarily imply the actual presence of DNA breaks [129]. Consistently, ATR exogenous activation is able to induce senescent cells showing nuclear γ-H2AX foci in the absence of detectable DNA damage [130]. Persistent DDR-foci also characterize OIS. The continuous proliferative stimuli causes unscheduled attempts of DNA replication characterized by inappropriate multiple replicon firing and altered replication forks progression. This DNA hyper replication stress generates DSBs, which results in the formation of non-telomeric DDR-foci named DNA Segments with Chromatin Alterations Reinforcing Senescence (DNA-SCARS) [137]. These DNA regions fuel a persistent ATR-dependent low DDR signaling somewhat similar to the one previously described in non-oncogenic types of senescence [105]. Specifically, in

cases of OIS, SAHF formation plays a critical role in the modulation of the DDR intensity. Indeed, induction of heterochromatin relaxation augments DDR signalling and produces a switch from oncogenic senescence to apoptosis [133]. Undoubtedly, DDR activation is a mechanistically relevant feature shared by the mayor part of senescent cells independently from the initial trigger. However, as usual in biology, exceptions to the apparent general rule exist. The hyper-activation of the stress-responsive p38MAPK pathway, for example, is capable of inducing senescence in the absence of DDR activation [138].

1.2.5 Tumor suppressors implicated in cellular senescence

The Cyclin-Dependent Kinase Inhibitor (CDKI) family known as INhibitors of CDK4 (INK4) plays a central role in cell cycle regulation controlling the G1-S phase transition. The family includes the four proteins p16/INK4a, p15/INK4b, p18/INK4c and p19/INK4d, which specifically associate with and inhibit the Cyclin Dependent Kinases 4 and 6 (CDK4 and CDK6). The inactivation of these two CDKs, both dependent on D-type cyclins, delays or impedes DNA synthesis for replication. p18/INK4c and p19/INK4d are induced in some terminally differentiated cells but generally not in senescence [139 and references therein]. However, recent studies implicating p19/INK4d in the response to specific kind of DD suggest its participation in senescence induction in certain circumstances [140, 141]. The genes encoding p16/INK4a and p15/INK4b are adjacent (located on chromosome 9p21 in humans) and are both induced in senescent cells [142, 143]. The INK4a coding-region shares the same gene-locus with another region coding for a second protein. The two genes are partially overlapped and have in common one whole exon, which exhibits an Alternative Reading Frame (ARF). From this genomic peculiarity, the second gene-product has been given the name of p14/ARF (the human homologue of murine p19/ARF). This protein is structurally and functionally unrelated to CDKIs of the INK4 family like p16, but is still involved in the inhibition of cell cycle progression [139 and references therein] (see below). The Ink4a/ARF locus is induced in response to diverse senescence-inducing stresses [92] and is a late event occurring in response to DD [142, 143] (see previous paragraph). Among the mechanisms that can drive its expression during senescence, a crucial one involves proteins of the Polycomb Group (PcG) and Trithorax Group (TrxG) [157 and reference therein, 158]. In

proliferating cells, PcG proteins form Polycomb Repressive Complexes (PRCs), which bind to the promoter of p16 and ARF and directly inhibit their transcription. The Histone Methyl-Transferase (HMT) Enhancer of Zeste Homolog 2 (EZH2) adds three methyl-groups to lysine 27 of the Histone H3 and generates H3K27Me3, a typical mark of transcriptional repression. The RING (Really Interesting New Gene) finger protein B-lymphoma Mo-MLV Insertion 1 (BMI1) indirectly mediates the monoubiquitination of lysine 119 of the Histone H2A, another typical repressive mark. During senescence, the expression levels of both these two key PRC components decrease [157 and reference therein]. At the same time the Histone Demethylase (HDMT) Jumonji Domain containing 3 (JMJD3) removes the H3K27Me3 mark, mediating transcriptional de-repression of the locus. Subsequently, the HMT Myeloid/Lymphoid Or Mixed-Lineage Leukemia 1 (MLL1) newly methylates histone H3 on lysine 4. This generates the activation mark H3K4Me3 and leads to transcription of the INK4a/ARF locus [157 and reference therein]. Expression of p16 and ARF is also observed upon activation of the stress-induced p38-MAPK pathway. Upstream of p38 are, among others effectors, the ERK1/2-activated MAPKK3 kinases and the ROS-activated Misshapen-like Kinase 1 (MINK1) [157 and reference therein]. The mechanism by which activated p38-MAPK induces INK4a/ARF is not fully established. Activation of its downstream target MAPKAPK3, which is able to phosphorylate the PcG complex inducing its dissociation from the DNA, may explain at least in part the observed correlation [157 and reference therein]. The specific function of p14/ARF is to interact with and inhibit the ubiquitin ligase E3-type enzyme HDM2 [the human homolog of Mouse Double Minute 2 (MDM2)], which normally targets p53 for degradation. This provides a second input stimulating p53 transcriptional activation in response to DD, which adds on the first acute and specific activation induced by the DDR signalling (see previous paragraph). Another mechanism for senescence-associated p53 activation is been described during spontaneous RepS. In response to telomeres shortening the relative levels of two distinct p53 isoforms regulate its activity. The simultaneous progressive increase in p53β and decrease in Δ133p53 results in transcriptional activation and growth arrest. Perturbation of the levels of these two p53-isoforms allows cells to keep dividing beyond the minimal telomeres length normally tolerated [145b]. Whatever the mechanism contributing to its stabilization, once active, p53 mediates the transcriptional up-regulation of genes involved in cell-cycle arrest, DNA repair and apoptosis. Among them, Plasminogen Activator Inhibitor-1 (PAI-1) is critical in the

induction of replicative senescence in both primary mouse embryo fibroblasts and primary human BJ fibroblasts. p53-dependent up-regulation of PAI-1 leads to down-regulation of PI3K-PKB- GSK3β signaling, nuclear exclusion of cyclin D1 and proliferation arrest [161]. Another p53 target very important in senescence is p21, which belongs to a second group of CDKIs known as the CDK Interacting Protein/Kinase Inhibitor Protein (CIP/KIP) family. The latter includes, in addition to p21/WAF1/CIP1, p27/KIP1 and p57/KIP2. Besides performing other functions that will not be detailed in this dissertation, these proteins associate with and inhibit all CDKs that depend on A- and E-type cyclins. The three of them prevent cell cycle progression and their expression can be associated with premature cellular senescence [146, 147, 148. 149]. Among all mentioned CDKIs, from both the INK4 and the CIP/KIP families, p21 and p16, and p19/ARF are the most widely involved in senescence initiation and maintenance across cell types. However, according to the specific cellular context, functional implications of the others CDKIs in the senescent phenotype have been described. P. P. Pandolfi and colleagues, for example, have recently found that cells can be predisposed to OIS by loss or inhibition of S-phase Kinase-associated Protein 2 (SKP2). This protein is an E3-ubiquitin ligase responsible for the degradation of both p21 and p27. Consistently, this novel senescence pathway does not depend on p53 but strictly depends on the induction of the two CKIs [commented in 150]. p27 up-regulation has been shown to be particularly relevant also in senescent prostate cancer cells [147]. On the other hand, p15 induction has an important role in the induction of senescence in hepatocellular carcinoma cells [151] and, more generally, in TGFβ-induced senescence [152]. Beside other individual specific functions that will not be detailed in this dissertation, all CDKIs finally converge on one indirect common effect. They inhibit the cyclin-dependent phosphorilation of the Retinoblastoma protein (Rb), keeping it hypo-phosphorylated and thus active. The Rb-family of transcriptional repressors includes Rb itself, RbL1/p107 and RbL2/p130. All of them are regulated during the cell cycle, exert similar effects and can compensate each other activity in certain conditions. However, some specific differences among these three proteins (that will not be detailed in this dissertation) exist at the level of both function and expression [155]. Regarding cellular senescence, the most relevant member of the family is undoubtedly Rb [168]. The latter is a potent tumor suppressor that avoids cell-cycle progression in various ways. On one side, it physically binds and inhibits the transcriptional activation domain of various members of the E2F family, whose

activity is required for the expression of genes fundamental for DNA replication and mitosis [153, 154]. At the same time, Rb acts as a transcriptional repressor, which recruits several cofactors involved in chromatin remodeling [155]. These epigenetic effectors include Histone Deacetylases (HDACs) as well as factors of the PcG (see above) or components of the SWItch/Sucrose Non-Fermentable (SWI/SNF) chromatin-remodeling complex [155]. When recruited to the promoter of target genes, these factors contribute to a closed chromatin state and thus to transcriptional repression. Specifically during senescence, Rb can mediate repression of E2F-regulated promoters interacting with the Histone Methytransferase (HMT) SUV39 [156]. The latter methylates histone H3 allowing the recruitment of Heterochromatin Protein 1 (HP1), which promotes heterochromatin condensation [152]. Finally, the evidence of Rb direct association to DNA in close proximity to replication origins suggests a regulating function in DNA replication [155]. Many studies have been conducted in the attempt to investigate the relative contributions of both the p53 and the Rb arms of the tumor suppressor pathway activated during senescence. Inactivation of p53 and Rb was often achieved expressing viral onco-proteins like the Simian Virus 40 Large T-Antigen (SV40-LTAg) or the Human Papillomavirus Early Antigens 6 and 7 (E6 and E7) [159]. Expression of dominant-negative isoforms [90, 160] or nuclear microinjection of anti-p53 antibodies [162] have aslo been exploited. In alternative, RNA-interference (RNAi) [163, 164], germline Homologous Recombination (HomRec) in mouse models [165, 166] or somatic HomRec in human cells [164, 167] have been applied to interfere with the expression and function of p53, p21, p16 and Rb. Overall the evidences obtained in these studies draw a complex scenario with some differences between mouse and human cells that will not be described in details here. Briefly, inactivation of p53 alone prevents senescence in Mouse Embryonic Fibroblasts (MEFs) [169]. Nonetheless, these cells undergo senescence normally in the absence of p21 expression [170]. This underlies p53 ability to induce senescence through other effectors such as, for example, the above-mentioned PAI-1 [161]. Inactivation of Rb alone has no effect, but concomitant ablation of Rb, p107 and p130 is able to avoid the senescent arrest [165, 166]. When MEFs are already senescent, inactivation of either p53 or Rb allows them to resume proliferation [169, 166]. In human IMR90 (immortalized diploid lung fibroblasts), simultaneous inactivation of both p53 and Rb is needed for senescence suppression [171]. Individual inactivation in the same cells only delays the permanent cell cycle arrest [172]. In primary lung fibroblasts, in contrast, inactivation of either p53 or Rb

prevents senescence [164]. Differently from MEFs, in human diploid fibroblasts inactivation of p21 is sufficient to avoid senescence [173]. When cells have already entered replicative senescence, inactivation of p53 allows some, but not all, human fibroblasts strain to restart dividing [90, 172].

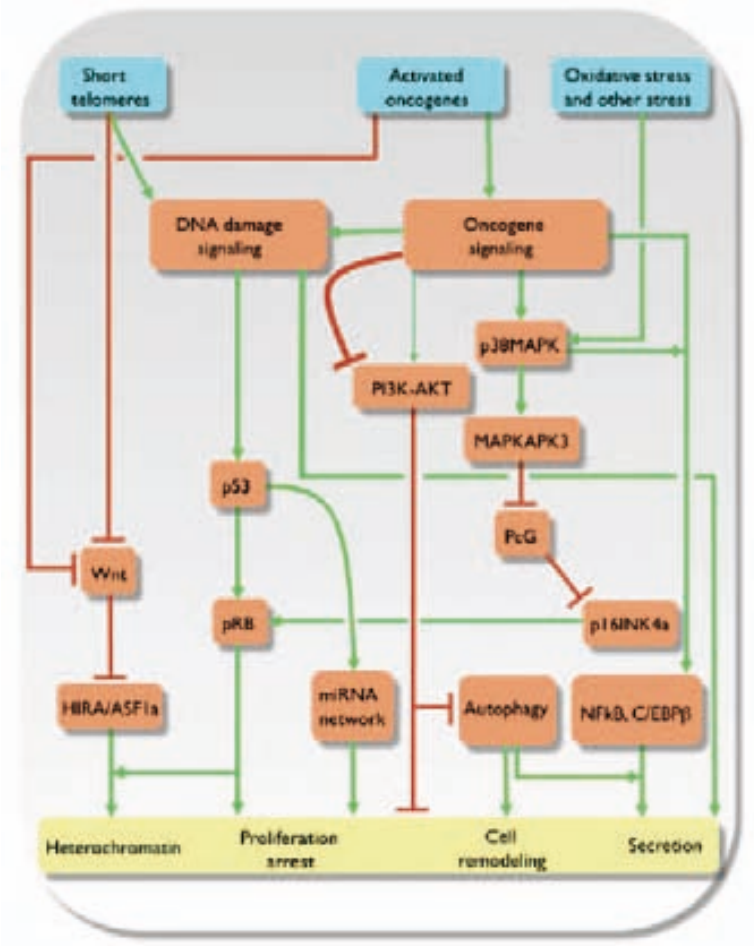

Figure 9. Schematic resume of the different routes to senescence: This complex scheme tries to summarize the most of the pathways mentioned along this introductive section on cellular senescence. The p53-dependent miRNA is being omitted as the contribution of this pathway to senescence is awaiting for confirmation in a wider spectrum of cellular contexts. The senescence secretome (bottom right of this scheme) is the subject of the next paragraph [scheme taken from ref. 156].

1.2.6 The Senescence Associated Secretory Phenotype (SASP)

A final important feature of cells induced to senescence by many different stimuli is the Senescence Associated Secretory Phenotype (SASP). Mechanistically, production of the senescence-associated secretome tends to be accompanied by activation of a sustained DDR. According to the inducing event, different SASPs develop relatively slowly after the senescent growth arrest [124, 137]. DDR components like ATM and CHK2 appear to be important to establish and sustain the SASP [unpublished data from Judit Campisi's lab mentioned in 137]. On the other hand, inactivation of p53, central player in DDR, strongly amplifies the SASP of some senescent cells [137]. A contribution of this SASP-amplifying effect in resuming the proliferation of senescent fibroblasts upon p53 inactivation [90] (see the end of the paragraph 1.2.5) has been suggested [137]. As breafly described in the paragraph 1.2.2, autophagy can contribute to SASP production in senescent cells. In particular, during OIS, protein translation dependent on the activity of the PI3K-PKB-mTOR pathway specifically contributes to the production of some secreted factors [115]. Consistent with DDR requirement for SASP, ectopic overexpression of p21 or p16INK4a causes a senescent-like growth arrest devoid of secretion [174]. However, also in this case at least one exception has been reported. As mentioned at the end of paragraph 1.2.4, p38-MAPK activation can induce senescence in the absence of DDR activation [138]. Nevertheless, p38 is also found to induce a SASP, which is produced through activation of the transcription factor Nuclear Factor κB (NFκB) [138]. The latter, similarly to the transcription factor CCAAT/Enhancer Binding Protein β (C/EBPβ) [179], positively regulates the transcription of various SASP components [177, 180]. This is the case in different types of senescence irrespectively from DDR being activated or not. Overall, the composition of the SASP presents certain variability across cell types and senescent-inducing stimuli [124, 175-181]. However, in general, senescent cells secrete a plethora of pro-inflammatory cytokines, growth factors, chemokines and proteases, which act in both autocrine and paracrine fashion. In the attempt to summarize and simplify a complex scenario, the multiple effects exerted by the senescence sectretome can be grouped into three main functions. The first is an autocrine function that reinforces the senescent phenotype. Different factors have been reported to participate in this autocrine loop. Examples are the already mentioned PAI-1 [161] in RepS (see paragraph 1.2.5), IL-6, IL-8 [179, 180] and IGFBP proteins [181] in OIS. The second is a paracrine immune-modulating

function that mediates the clearance of senescent cells. Various SASP factors are indeed able to attract different cellular components of the immune system. Examples are IL-6 [182], Monocyte Chemo-attractant Protein 1 (MCP-1) and Colony Stimulating Factor 1 (CSF-1) [183, 184]. The third is a paracrine function of the senescence-secretome on non-senescent surrounding cells. With respect to actively secreting senescent cells, target cells within a given tissue may belong either to the same or to a different compartment (e.g. epithelial or stromal). According to the different experimental settings, the study of different cell types and tissues have led to all kind of evidence. IL-1α and various ligands of the TGF-β family, for example, have been implicated in paracrine transmission of senescence. This was observed in both fibroblasts and mammary epithelial cells of human origin undergoing OIS [185]. To the opposite extreme, IL-6 and IL-8 have been shown to stimulate hyper-proliferation and Epithelial-to-Mesenchymal Transition (EMT) of non-senescent premalignant epithelial cells [124]. In this case the cytokines were produced by human fibroblasts and epithelial prostate cells undergoing senescence upon various stimuli. As a final example, PAI-1, while being an autocrine mediator of RepS [161], is also causally linked to tumor progression and metastasis [186]. Underlying the complexity of this senescence-associated phenotype, many secreted factors, participate in more than one function of the SASP. As one of many possible examples, the secretion of IL-6 and PAI-1 by a cluster of senescent epithelial cells might well be pro- as well as anti-tumorigenic. Various physiological processes, in different tissues, rely on the induction of senescence and its associated secretion in a specific subset of cells. One example is represented by the role of senescence during normal development. Very recent work from two different groups revealed that senescence spontaneously occurs at multiple locations in mammalian embryos. Embryonic cells are likely induced to senescence by pERK-dependent paracrine signaling coming from the underlying stroma. Senescent cells promote, through their secretion, both tissue remodeling [188] and embryonic patterning [189], at specific developmental stages. Subsequently, macrophages infiltrate and mediate the clearance of senescent embryonic cells [189]. In both studies, the genetic impairment of senescence results in various non-lethal embryonic abnormalities. Another example is offered by the role of senescence during tissue regeneration in adults. Toxins induce acute liver damage accompanied by local and transient inflammation, which stimulates Hepatic Stellate Cells (HSCs) to generate new tissue. Soon after activation, these cells enter senescence and start secreting proteases, specially MMP1 and 3, which limit fibrosis

and promote tissue remodeling. Here, inhibition of senescence causes prominent fibrosis, indicating its requirement to achieve full tissue restoration. Finally, senescent HSCs attract Natural Killer Cells (NKs) and get cleared the innate immune system [190]. Similarly, resident fibroblasts are activated after skin wound. Subsequently, mobilization of proteins associated to the extracellular matrix, like Cysteine Rich 61 (CYR61 or CCN1), induces activated fibroblasts to senesce. Also in this context, the resulting SASP mediates complete wound-healing and subsequent immune-clearance of the senescent fibroblasts [191]. These examples refer to tissues with normal regeneration capacity (i.e. stem cell function) and characterized by reasonably good preexisting homeostatic conditions (i.e. relatively young and/or healthy and with normal stem cell function). When such conditions are perturbed, a subset of cells becomes senescent in response to specific environmental stimuli. Arrested cells, through their SASP, establish a fine interplay with surrounding non-senescent cells as well as with cellular components of the immune system. When the components participating in this complex tapestry are well functioning and adequately coordinated, senescence can exert its beneficial effects and help restoring the original conditions. Of course, this is not always the case and many different sources of deregulation can compromise either tissue homeostasis or immune functions. Moreover, mechanisms through which senescent cells can avoid immune-recognition have been proposed [192, 193]. In situations like obesity, alcoholism or chronic hepatitis, for example, the liver is exposed to sustained inflammation. This kind of permanent injury highly increases the frequency of senescent cells whose presence cannot be compensated by immune-clearance. Differently from what previously described in acute liver damage, in these cases the SASP is deleterious. It contributes to chronic inflammation and to the loss of normal tissue-architecture favoring cirrhosis and eventually liver cancer [194 and unpublished results from Scott Lowe's lab mentioned in its website]. Comparing tissues from young and old mice, age-associated increase in the percentage of senescent cells is observed in liver, skin, lung, and spleen [195]. Consistently, expression of the senescence-associated Ink4a/ARF locus exponentially increases with age in mice and humans [196, 197, 198]. Aging is characterized by the accumulation of DNA damage that might progressively alter tissue homeostasis at different levels [132, 195, 199]. In addition, age-related immunological disorders have been reported [200, 201, 202]. Thus, both increased generation-rate and decreased immune-clearance of senescent cells are likely to occur in old tissues. Accumulation

of senescent cells correlates with a variety of late-life dysfunctions, including cognitive impairment [203, 204], cardiovascular disease [205, 206] and osteoarthritis [207, 208]. In all these cases the SASP is likely to contribute to the disease. However, only some of the studies have specifically looked at secreted factors and suggested their involvement [205, 206, 207, 208]. In another study, oxidative stress generated by mitochondrial dysfunction produces the early appearance of senescent cells in the skin. These cells persist and correlate with age-phenotypes of the skin such as epidermis reduction and increase of the stratum corneum [209]. In contrast with their positive contribution during wound-healing, in this case senescent cells in the skin are likely detrimental. Here again, a causal contribution of the SASP is suggested [127, 210], but no experiments are shown to prove it [209]. In summary, it seems reasonable to speculate that appearance and clearance of senescent cells within a given tissue at the appropriate time allows the positive effects of the SASP. On the contrary, sustained presence of senescent cells within the same tissues is associated with various disorders, including the development of cancer. The senescence secretome is predicted to contribute to these negative effects.

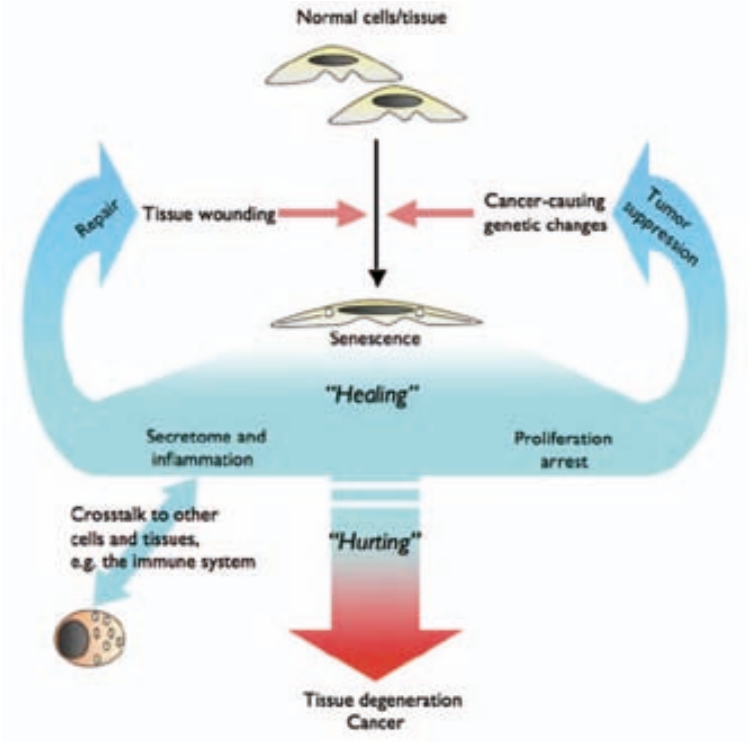

Figure 10. Schematic resume of the contradictory effects of the SASP: The SASP mediates complete wound-healing and subsequent immune-clearance. Arrested cells, through their SASP, establish a fine interplay with surrounding non-senescent cells as well as with cellular components of the immune system. When the components participating in this complex tapestry are well functioning and adequately coordinated, senescence can exert its beneficial effects and help restoring the original conditions. Of course, this is not always the case and many different sources of deregulation can compromise either tissue homeostasis or immune functions. Sustained presence of senescent cells and their SASP can be associated with various disorders, including the development of cancer [scheme taken from ref. 156].

Table 1

Oncogenes and tumor-suppressor genes triggering senescence.

Action	Gene	Pathway — Function	Reference
In vivo			
Inactivation	*PTEN* (TSG)	Downregulates PI3K/Akt/mTOR signaling	[28••]
	VHL (TSG)	Targets HIF for degradation	[29]
	Hsp72	Promotes PI3K/Akt (p53-dependent) and ERK (p53-independent) signaling	[51]
	c-Myc	Ras signaling effector — transcription and chromatin remodeling factor	[120,121]
	Rb (TSG)	Regulates E2F activity	[33]
Activation	*TGFβ*	Promotes Smad signaling	[71]
	H-ras^{V12}	Ras signaling	[25]
	K-ras^{G12V}	Ras signaling	[116]
	N-ras^{G12D}	Ras signaling	[15••]
	BRAF^{E600}	Promotes Ras signaling	[17,117]
	c-Myc^{a,c}	Effector of Ras signaling — transcription and chromatin remodeling factor	[93•]^{a}, [71]^{c}
	β-Catenin	Promotes Wnt signaling	[103]
	Akt	PI3K/Akt signaling	[119]
	Rheb	Promotes PI3K/Akt/mTOR signaling	[118]
	E2F3	Promotes G1 to S phase — transcription factor	[114]
Restoration	*p53* (TSG)	Effector of various signaling pathways — transcription factor	[89••,90••]
In vitro			
Inactivation	*Rac1*	Modulates Rho signaling	[104]
	NF1 (TSG)	Downregulates Ras signaling	[66•]
	PTEN (TSG)	Downregulates PI3K/Akt/mTOR signaling	[28••]
	VHL (TSG)	Targets HIF for degradation	[29]
Activation	*TGFβ*	Promotes Smad signaling	[108]
	INFβ	Promotes STAT signaling — activates p53	[126]
	CXCR2 (IL8RB)	Angiogenic CXC chemokine receptor	[37•]
	Rac1	Modulates Rho signaling	[105]
	Smurf2	Upregulation by telomere attrition; promotes p53/pRb senescence	[110]
	Runx1, Runx2, Runx3	Transcription and chromatin remodeling factors	[24]
	PTEN (TSG)	Downregulates PI3K/Akt/mTOR signaling	[66•]
	Sprouty 2	Downregulates Ras signaling	[66•]
	EGFR	Promotes Ras signaling	[104]
	H-ras^{V12}	Ras signaling	[23]
	N-ras	Ras signaling	[15••]
	Raf	Ras signaling	[106]
	BRAF^{E600}	Promotes Ras signaling	[16••]
	Mos	Promotes Ras signaling	[34••]
	MEK	Promotes Ras signaling	[23,107]
	c-Myc^{a,b}	Ras signaling effector — transcription and chromatin remodeling factor	[115]^{b}, [93]^{a}
	IGFBP3, IGFBP5	Modulates IGF1 signaling pathway	[111,112]
	IGFBP7	Modulates IGF signaling; downregulates Ras signaling	[67]
	p38α-D176A, p38γ-D179A	Promotes p38MAPK signaling	[62]
	STAT5	Promotes JAK–STAT signaling	[43]
	Cyclin E	Activated cyclin-dependent kinase-2: promotes G1 to S phase	[34••]
	E2F1	Transcription factor: promotes G1 to S phase:	[43,45]
	E2F3	Transcription factor: promotes G1 to S phase:	[114]
	Cdc6	Replication licensing factor: promotes S phase progression	[34••]
	Cdt1	Replication licensing factor: promotes S phase progression	[44]
	p16^{INK4A} (TSG)	Cyclin-dependent kinase inhibitor: inhibits G1 progression	[23,106]
	PML	Ras signaling effector; induces p53	[113]
	p53^{VP16} (TSG)	Effector of various signaling pathways–transcription factor	[102]
	PAI-1	p53 effector	[109]
	DEC1	p53 effector	[122]

Abbreviation and notes. Genes and the proteins encoding: TSG: tumor-suppressor gene; *PTEN*: phosphatase and Tensin homolog; *VHL*: von Hippel-Lindau; *HIF*: hypoxia inducible factor; *Hsp72*: heat shock protein-72; *Rb*: retinoblastoma protein; *NF1*: neurofibromin 1, *TGFβ*: transforming growth factor *β*; *STAT5*: signal transducer and activator of transcription 5; *IGF1*: insulin growth factor 1; *IGFBP3, 5, 7*: insulin growth factor binding protein-3,5,7; *EGFR*: epidermal growth factor receptor; *PML*: promyelocytic leukemia protein; *PAI-1*: plasminogen activator inhibitor-1; *DEC1*: differentiated embryo-chondrocyte expressed gene 1; *H-Ras^{V12}* and *BRAF^{E600}* represent constitutively active forms of *H-Ras* and *BRAF*, respectively. *p53^{VP16}*: a mutant form of p53 leading to a transcriptionally active form with the DNA binding domain intact, but deficient for the amino-terminal domain. DDR: DNA damage response pathway.

[a] *c-Myc*: activation of *c-Myc* induces senescence both *in vivo* and *in vitro* in a *Cdk2*$^{-/-}$ setting.

[b] *c-Myc*: upregulation of *c-Myc* induces senescence in the absence of Werner syndrome RecQ helicase protein.

[c] *c-Myc*: upregulation of *c-Myc* promotes senescence in transgenic mice in Suv39h1-depedent manner.

Table 1. Schematic resume of the contradictory effects of the SASP: To our knowledge this is probably the most comprehensive list of senescence inducing stimuli published with respect to OIS, taken from the following review: Oncogene-induced senescence: the bright and dark side of the response. Vassilis G Gorgoulis1 and Thanos D Halazonetis. Current Opinion in Cell Biology 2010, 22:816–827

OBJECTIVES

Chapter 2

Objectives

1. **p95HER2**

   Breast cancers positive for both full length HER2 and HER2 Carboxyl-Terminal Fragments (CTFs), compared with the ones expressing predominantly FL-HER2, have higher tendency to metastasize at limph nodes [71] Indeed, early reports showed that patients carrying these tumors have worse prognosis [72]. Among all possible HER2-CTFs we found that p95HER2, originating by alternative initiation of translation, had a remarkable ability to activate several down-stream pathways more potently than its full-length counterpart. This prompted us to go further in the biochemical characterization of the fragment. We ectopically express p95HER2 in various cell lines, including HEK293, MEFs, MCF7, MCF10A T47D, MDA-MB-453 cells.

2. **In vitro biochemical characterization of p95HER2 constitutive activation**

   We proceed to targeted mutation of specific residues within the small extracellular domain of p95HER2 to individuate potentially important structural features. Expression of tagged versions of the HER2 fragment and other biochemical procedures were applied to understand its “signalling behavior” This work was conducted mainly in HEK293 and MCF7 cells.

3. **In vivo characterization of p95HER2 oncogenic activity**

   MEFs stable clones inducible for p95HER2 expression were generated to test the oncogenic activity of the HER2 fragment. These cells were then used to perform subcutaneous injection in immuno-deficient mice and test the transforming capability of p95HER2.

4. **In vitro characterization of p95HER2 biological function**

   Both inducible and constitutive stable clones were generated in various breast cancer cell lines including MCF7, MCF10A T47D, MDA-MB-453 to figure out the effect of p95HER2 expression in this cell type. The fragment tendency to induce premature senescence in breast epithelial cells pushed us to further study this phenotype. Work for this aim was mainly conducted on MCF7.

5. **In vitro characterization of p95HER2-induced secretory response**

   Particular attention was then dedicated to the characterization of the secretory response induced by p95HER2 activity in senescent breast epithelial cells. In particular the study would focus on the impact of the kinase activity of the HER2 fragment on senescent cell secretion. Some degree of characterization of the molecular events eventually mediating p95HER2 pro-secretory activity was also aimed. This work was mainly conducted on MCF7 and MCF10A cells.

6. **In vivo characterization of p95HER2-induced secretory response**

   The work subsequently evolved to address if the p95HER2-dependent secretion could be detected and thus have an impact in vivo. To this aim MCF7 cells were used to generate subcutaneous xenograft tumors that were then characterized by immunostaining. Evidences for secretion in vivo were also pursued.

7. **Functional relevance of p95HER2-expressing senescent cells in vivo**

   The final objective consisted in assessing the functional relevance of senescent MCF7 cells expressing p95HER2 in vivo. To this scope both subcutaneous and orthotopic xenograft tumors were generated. In addition another cell line, MDA-MB-231, was used as reporter and in vivo imaging techniques were applied.

RESULTS

Chapter 3

Results

Introductive note to the experimental section:

As mentioned in the paragraph 1.1.8 of the introduction, p95HER2 is a naturally occurring product of AIOT at a downstream AUG codon in the wild-type HER2 mRNA [68]. This alternative start codon corresponds to the methionine 611 of the HER2-FL protein. Accordingly, the construct used to express p95HER2 was generated. The resulting truncated receptor located at the plasma membrane [24]. p95HER2 has a small extracellular domain containing five cysteine residues and one N-glycosylated asparagine [24] (see also schematic in Fig. 1C). Figures 1 and 2 of this experimental section represent a re-adaptation of results that we previously published [24, 74, 75]. Figures 7, 8 and 10 represent very recent unpublished results. All the remaining figures are a re-adaptation of results that we published this year [211].

3.1 p95HER2 is a constitutively active variant of HER2

In MCF7 cells, during the first 24h after induction of its expression, p95HER2 induced acute activation of all the pathways analyzed while HER2-FL produced little or no activation (Fig. 1A). In the following 36h, the level of activation upon HER2-FL expression tended to gradually increase without reaching a plateau. On the contrary, the level of active pathway components decreased (p-Erk1/2, p-Akt, and p-Jnk) or plateaued (p-Src) in the case of p95HER2 (Fig. 1A). Transiently transfected Hemagglutinin- (HA-) and FLAG-tagged versions of p95HER2 co-immunoprecipitated showing that p95HER2 homodimerizes (Fig. 1B). Western blot (WB from now on) analysis in the absence of β-Mercaptoethanol revealed high molecular weight signal for p95HER2 but not HER2-FL (Fig. 1D). Mutation to alanine of the five cysteines in the extracellular domain of p95HER2 abrogated its oligomerization (Fig. 1C and D). The expression of these p95HER2 oligomers correlated with ERK1/2 phosphorilation (Fig. 1D). In summary, these data shows that intermolecular disulphide bonds covalently stabilize p95HER2 dimers resulting in the constitutive activation of the fragment.

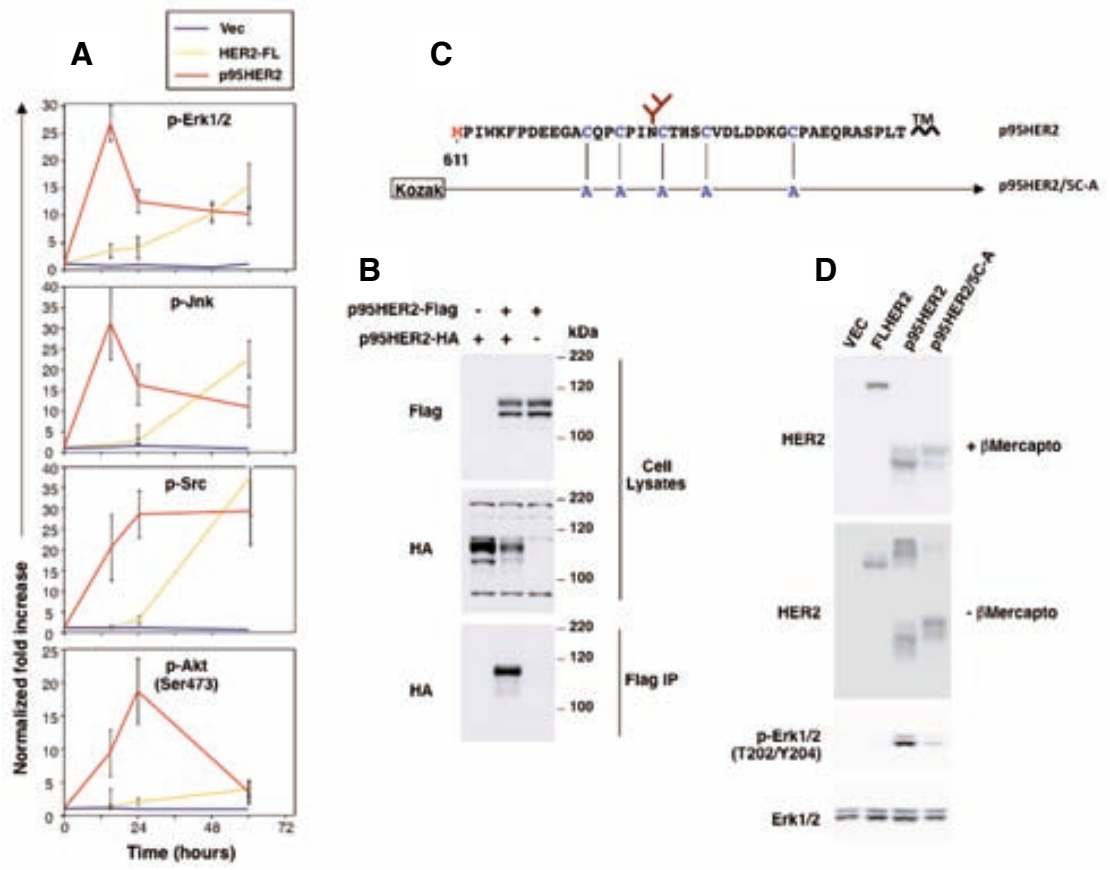

Figure 1. Characterization of p95HER2: **A.** Western blot of the indicated phosphoproteins upon expression of the indicated constructs and in the three independent experiments. Signals at different time points were quantified and averages are presented. **B.** Co-immunoprecipitation of Flag- and HA-tagged p95HER2. MCF7 transient clones expressing p95HER2 with or without a carboxy-terminal FLAG-tag (p95HER2-Flag - + +) for 20 hours were transiently transfected with a plasmid expressing an HA tagged version of p95HER2 or with an empty vector (p95HER2-HA + + -). 2% of the cell lysate was analyzed by Western blot with an anti- FLAG or -HA antibody, the rest was used for immunoprecipitation with an anti-FLAG antibody. The immunoprecipitates were analyzed by Western blot with an anti-HA antibody. **C.** Schematic showing the primary sequence of the small extracellular region of p95HER2 with methionine 611 in red, the five cysteines present in the region marked in blue, the glycosylated asparagine (causing the characteristic double band in WB [24]) and the transmembrane domain (TM). The schematic below shows the different cysteine substitutions inserted in the cDNA of p95HER2/5C-A. **D.** HEK293T cells were transiently transfected with the empty vector (-), the vector containing the cDNA of HER2-FL, p95HER2 or p95HER2 with five cysteines substituted by alanines (5C-A). After 48h, the cells were lysed, fractionated by SDS-PAGE in the presence or absence of beta-mercaptoethanol, and analyzed by Western blot (note the signal at high molecular weight under non-reducing conditions). Blots showing activation of ERK1/2 in the different conditions is shown below.

3.2 p95HER2 is an oncogene

The induction of p95HER2 expression increased the proliferation and changed the morphology of Mouse Embryonic Fibroblasts (MEFs) (data not shown). When injected subcutaneously in nude mice, p95HER2-expressing MEFs, but not wild-type cells (data not shown), generated fast growing xenograft tumors (Fig. 2A). p95HER2 activity can be blocked treating cells with the dual EGFR/HER2 Tyrosine Kinase Inhibitor (TKI) Lapatinib (LAP from now on) [24]. Indeed, MEFs xenograts showed a

clear response to the treatment with this small molecule TKI (Fig. 2A). Immunohistochemical analysis of the tumors proved a reduction in ERK1/2 activation upon treatment (Fig. 2B). For additional control, a separate group of animals carrying already big tumors was supplied with Doxyciclin (Dox from now on) in the drinking water. The tumors completely regressed in few days and WB analysis confirmed the inhibition of p95HER2 expression by Dox (Fig. 2C and D). These results show that p95HER2 is an oncogene able to transform MEFs cells and make them tumorigenic. The resulting tumors are dependent on expression and activity of the HER2 constitutively active fragment.

Note: Further details on the initial characterization of p95HER2 can be found in the paragraph 1.1.8 of the introduction of this dissertation and in the relative references [24, 69, 70, 74 and 75].

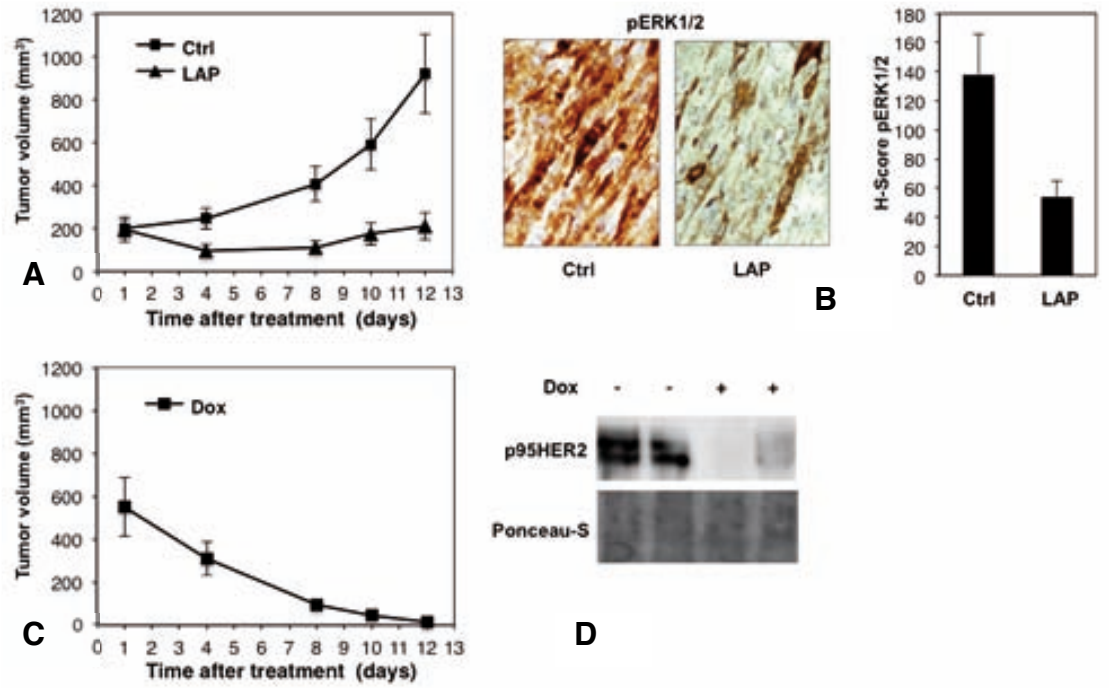

Figure 2. Tumor xenografts formed by MEFs expressing p95HER2: A. Established xenografts (five mice per group) derived from MEFs expressing 611-CTF were randomized to receive either placebo (Ctrl) or treatment with 150 mg/kg oral lapatinib daily. $P < 0.01$ Ctrl versus LAP. **B.** representative p-ERK1/2 staining in p95HER2 MEFs tumors receiving either placebo (Ctrl) or LAP. Tumors were collected at the end of the experiment shown in A, quantification of the histochemical staining (H score) was obtained by scoring two slides each from five different tumors from both placebo and lapatinib-treated animals. Columns, mean; bars, SEM. $P < 0.01$ Ctrl versus LAP.**C.** six mice bearing MEFs 611-CTF xenografts with a volume of ≥500 mm3 received 1 g/l doxycycline in the drinking water. Complete tumor shrinkage was achieved in 11 days. 611-CTF. **D.** Lysates from two control tumors in A and 2 tumors in C were analyzed by WB and p95HER2 expression in the absence (-Doxy) or presence (+Doxy; 96 h) of doxycycline is shown.

3.3 Effect of p95HER2 expression in different breast epithelial cell lines

Lentiviral delivery and stable expression of p95HER2 in MCF10A, a non-transformed immortalized mammary epithelial cell line obtained from fibrocystic breast tissue, produced an increase in the rate of cell proliferation (Fig. 3A). In contrast, stable expression of the HER2 fragment, through the same system, in the breast cancer cell line MDA-MB-453 resulted in a marked proliferation arrest and increased levels of the Senescence-Associated-β-Galactosidase activity (SA-β-Gal activity) (Fig. 3B). These same 2 phenotypes, normally associated with OIS, were also observed when p95HER2 was expressed using an inducible system in other two breast cancer cell lines, T47D and MCF7 (Fig. 3C and D).

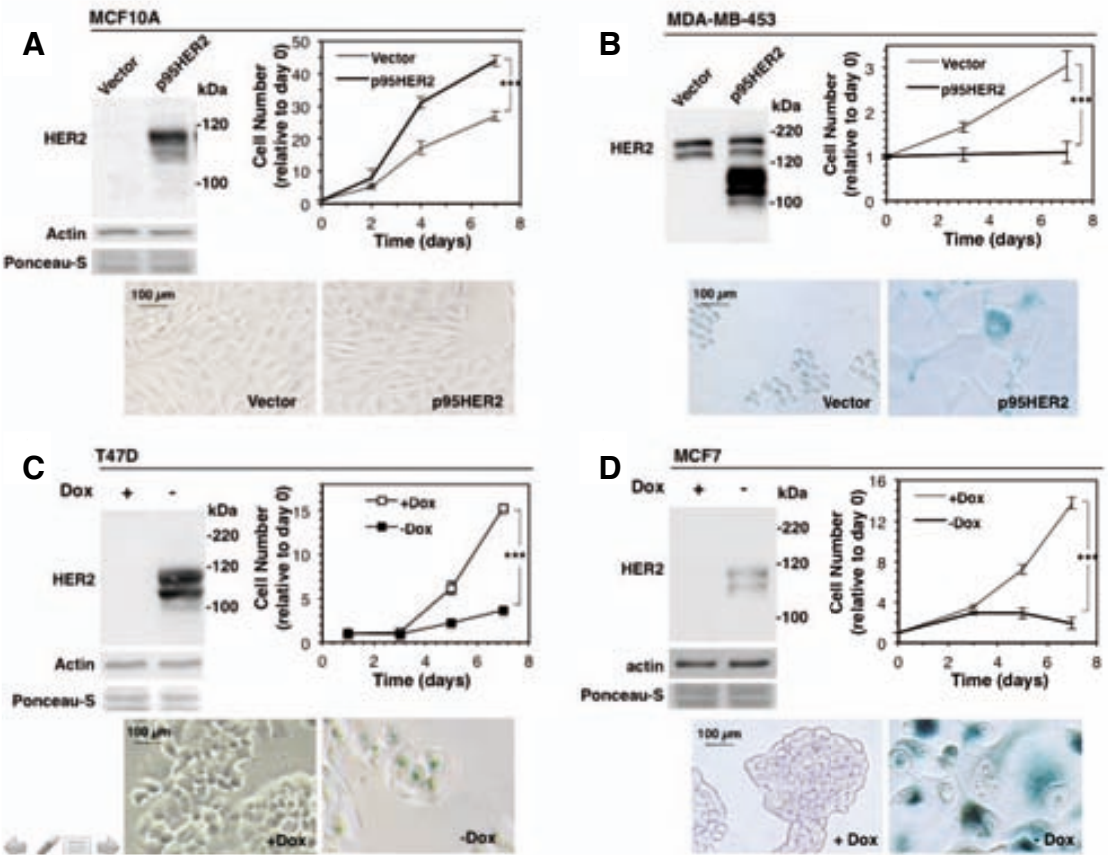

Figure 3. p95HER2 expression in different breast epithelial cell lines: A and B. MCF10A and MDA-MB-453 cells stably transduced with lentiviruses carrying either an empty vector or the same vector encoding p95HER2 and selected in the presence of puromicin during one week. **C and D.** Stable inducible clones were obtained from both MCF7 and T47D cells as indicated in the section dedicated to materials and methods. Soon after selection (for A and B) or one week after Dox removal (for C and D), cells were harvested and the cell lysates were analyzed by WB with antibodies against HER2 (upper left panels). At the same time (for A and B) or one day after Dox removal, plates were seeded to assess proliferation by cell counting at the indicated time points. P values were obtained by two-tailed Student's t test, ***P< 0.001 (upper right panels). The same cells seeded for the proliferation assay were fixed and stained for β-galactosidase activity in a separate dish after one week in culture (lower panels). In all cases p95HER2-expressing cells are compared side by side with non-expressing counter parts.

3.4 p95HER2-induced senescence (OIS)

MCF7 cells were chosen for further characterization of the senescence induced by sustained expression of p95HER2. Pulses of p95HER2 expression were obtained by removal and subsequent re-addition of Dox from the culture medium (see Experimental Procedure). p95HER2 expression during 12 or 24 hours had, respectively, negligible or inhibiting effects on cell proliferation (Fig. 4A). p95HER2 expression during 48 hours was sufficient to induce a complete and irreversible arrest comparable to the one observed in cells kept in the absence of Dox (Fig. 4A). Analysis of the arrested cells by confocal microscopy showed enlarged nuclei with focal accumulation of γ-H2AX and 53BP1 (see paragraph 1.2.4 of the introduction). Quantification and representative images of these DDR-foci are presented (Fig. 4B). WB analysis showed that arrested p95HER2-expressing cells also presented activation of Rb and p53 as well as up-regulation of the CDKI p21 (Fig. 4C). Treatment with the DNA-damaging agent doxorubicin, known to promote senescence in MCF7 cells [212], was used as control and gave comparable results (Fig. 4C). Despite not dividing, senescent cells are known to remain metabolically active [193, 213]. Compared to dividing control cells, after less than three days of p95HER2 expression, arrested MCF7 were characterized by significantly higher dehydrogenase activity (Fig. 4D). Pulse and chase experiments at three and seven days after seeding indicated that senescent cells had also a higher rate of protein biosynthesis (Fig. 4E). Accordingly, at seven days of p95HER2 expression MCF7 cells exhibited a 4-fold increase in diameter with respect to dividing control cells (Sup. Fig. 1). The experiments described in the last two paragraphs show that sustained expression of p95HER2 mediated the proliferative arrest of 3 out of 4 breast epithelial cell lines tested. The arrest is accompanied by increased Senescence-Associated-β-Galactosidase activity (see paragraph 1.2.2 of the introduction) in all cell lines. Further characterization of arrested MCF7 identifies various hallmarks of Oncogene Induced Senescence (OIS). We concluded that p95HER2 oncogenic activity in breast cancer cells preferentially induces premature senescence.

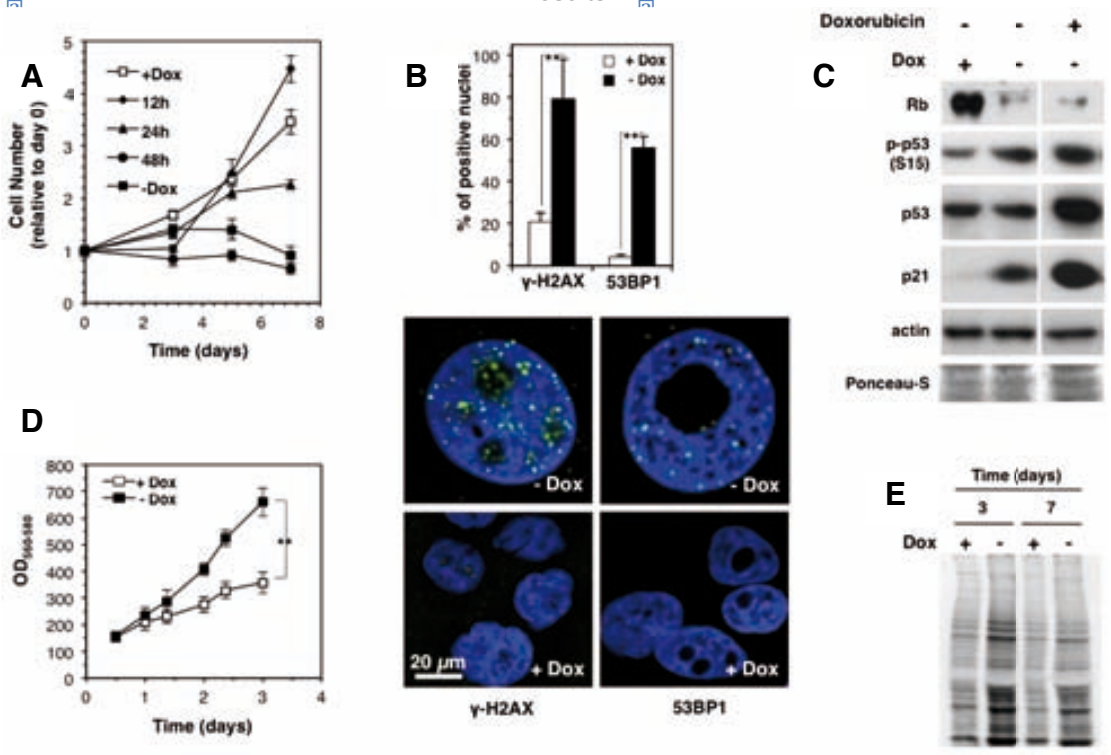

Figure 4. Characterization of MCF7 cells expressing p95HER2: A. Stable inducible MCF7 clones were induced for p95HER2 expression by doxycycline removal, seeded and kept in the absence of doxycyclin during 12, 24, or 48 hours, respectively. Then, doxycycline was added back and the cells seeded to assess proliferation in comparison with MCF7 cells in the absence or presence of Dox, as in Fig. 3D (upper right panel). Cell count at the indicated time points is presented. **B.** Washed MCF7_tet-off_p95HER2 cells seeded in presence or absence of Dox were in culture during one week and fixed. Immunofluorescence was performed using the indicated antibodies and the number of positive nuclei was quantified. The bars represent the averages of three independent experiments where four separate fields containing at least 5 nuclei were counted in each condition. P values were obtained by 2-tailed Student t test, $P < 0.01$. At the bottom representative nuclei are shown. **C**. Cells treated as in B (prior to fixation) were lysed and the cell lysates analyzed by WB with the indicated antibodies. MCF7 cells treated with 0.5 mmol/L of doxorubicin during 48h were loaded in parallel as control. **D.** Cells treated as in Fig. 3D (upper right panel) were seeded in 96-wells plates and WST1 assay was performed. Data are representedas means ± SD of three independent experiments. P values were obtained by two-tailed Student's t test, **P<0.01. **E.** MCF7 Tet-off / p95HER2 cells were cultured with or without doxycycline for 3 or 7 days. Then, cells were pulsed with 35S-translabel for one hour and lysed. Clarified cell lysates were normalized according to the number of cells and analyzed by SDS-PAGE and fluorography.

3.5 p95HER2-induced senescent cells express a pro-tumorigenic SASP

The SASP is considered a phenotypic hallmark of senescence, especially when accompanied by an active DDR (see paragraph 1.2.6 of the introduction). In spite of the previous results (see Fig 4B), p95HER2-expressing senescent MCF7 cells were expected to express a SASP. Expression of HER2-FL in breast cancer cells is known to induce secretion of several factors [214]. MCF7 cells entered OIS in response to HER2 constitutive activation (i.e. p95HER2 expression) while they kept proliferating upon HER2-FL expression (Supp. Fig. 2). We compared the transcriptomes induced by the two forms of the receptor to find out components mainly up-regulated in

p95HER2-induced senescence. p95HER2 modified the expression level of 1,631 genes (1.9 **>** log2FC **>** 0.9) among which 944 were similarly controlled by HER2-FL. Among the rest, more acutely regulated by the HER2 fragment, 367 genes were down- and 320 up-modulated (Fig. 5A, see also note at the end of the paragraph). In this last group, roughly 20% of the genes codifies for transmembrane or secreted proteins potentially secreted. Label-free proteomics analysis of the conditioned media identified 361 proteins more abundantly secreted by senescent MCF7 cells (log2FC **>** 0.9) in comparison with control cells (Supp. Table 2 [extract], see also note at the end of the paragraph). 55 of these proteins were actually encoded by the up-regulated genes (Fig. 5B and Table 1). These data confirm the existence and define the composition of a specific pro-tumorigenic SASP (proT-SASP) during p95HER2-induced senescence. By comparison, the transcriptomic and the proteomic results indicate that part of the secreted components (around 15%) is transcriptionally regulated. This also implies that many of the secreted factors are induced at post-transcriptional level.

Note: Both the Sup. Table 1, with the list of genes represented in Fig. 5A and their respective Lo2FC and the complete Sup. Table 2, from which an extract is presented in the end of this section, can be found in the Excel file supplied with the electronic version of this thesis or downloadable on-line in [211]).

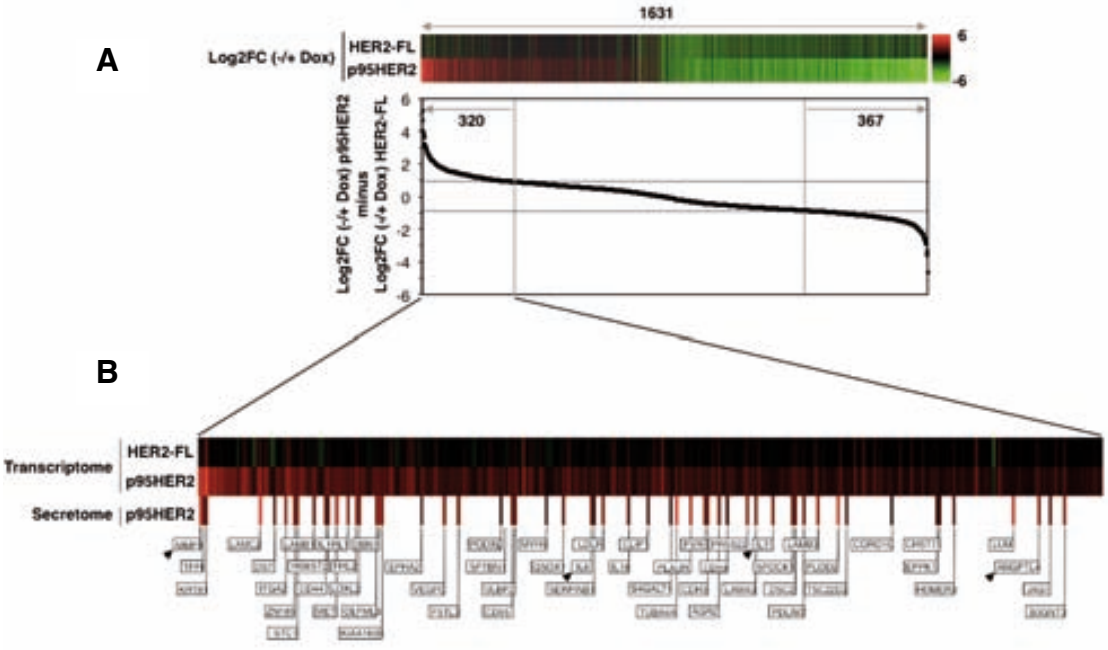

Figure 5 and Table 1. p95HER2-induced senescence secretome: A. The transcriptomes of MCF7 Tet-off cells after 60h of p95HER2 or HER2-FL were compared. 1,631 genes regulated by p95HER2 (i.e., genes encoding transcripts with log2FC > 0.9 or <_0.9 upon expression of the fragment in

comparison with vector control) are represented in the upper line of the heatmap. The lower line of the heatmap represents the regulation of the same 1,631 genes in cells expressing HER2-FL. The graph underneath the heatmap was obtained by ordering the genes according to the difference in the degree of regulation that each transcript shows upon expression of p95HER2 and HER2-FL, respectively [i.e. log2FC (-/+Dox) p95HER2 minus log2FC (+/- Dox) HER2-FL]. The resulting graph showed a core of 944 genes comparably regulated by both HER2 variants and two tails of genes more intensely up- or down-regulated by p95HER2. **B.** Enlarged heatmap of the 320 genes transcriptionally up-regulated by p95HER2 but not (or to a much lesser extent) by HER2-FL (upper lines). Heatmap of the 55 gene products that were also found in the proteomic analysis conducted comparing the secretomes of MCF7 Tet-off/p9HER2 cells treated with and without doxycycline (see Supplementary Table S2[extract]). Arrows mark genes chosen for the validation of the analysis (lower line and boxes). For more clarity the same 55 genes are shown in the table below.

Gene ID	Transcriptome			Secretome
	Log2FC HER2-FL	Log2FC p95HER2	Log2FC p95HER2 minus Log2FC HER2-FL	Log2FC p95HER2 (protein)
MMP1	0.96	5.60	4.64	5.82
TFPI	1.17	5.21	4.04	2.26
KRT81	3.02	6.93	3.91	2.74
LAMC2	1.75	4.25	2.49	6.46
DST	-0.94	1.32	2.26	2.09
ITGA2	1.28	3.53	2.25	3.82
ZNF185	0.74	2.95	2.21	2.55
STC1	0.10	2.27	2.18	2.80
LAMB1	1.04	3.15	2.11	2.77
CD44	0.71	2.72	2.01	2.41
HS6ST2	1.05	3.07	2.01	2.44
MET	0.45	2.38	1.93	6.34
IL1RL1	0.05	1.94	1.88	3.46
FHL2	1.38	3.23	1.85	3.73
LOXL2	0.15	2.00	1.85	3.27
DBN1	0.57	2.35	1.78	2.74
OLFML3	0.63	2.40	1.78	3.91
KIAA1609	0.27	2.05	1.77	3.13
EPHA2	1.12	2.76	1.65	1.74
VEGFC	-0.13	1.45	1.58	4.39
FSTL3	0.22	1.75	1.54	2.95
PODXL	-0.22	1.29	1.51	1.25
CD55	0.29	1.77	1.48	3.07
ULBP2	1.17	2.65	1.48	2.83
MYH9	-0.49	0.93	1.42	5.51
QSOX1	0.96	2.35	1.39	2.29
IL6	0.48	1.84	1.36	2.78
SERPINB1	0.03	1.40	1.36	1.42
LDLR	0.11	1.46	1.35	2.77
IL18	1.48	2.80	1.32	2.12
CLIP1	-0.30	0.99	1.29	1.60
B4GALT1	-0.18	1.07	1.25	1.41
TUBA4A	1.37	2.61	1.24	7.02
PLAUR	0.74	1.96	1.22	5.05
CDH3	0.43	1.62	1.20	3.04
PVR	0.18	1.38	1.20	3.02
AGR2	1.45	2.64	1.19	1.71
CD59	0.76	1.94	1.18	1.37
PRSS22	1.17	2.33	1.17	4.07
LAMA3	-0.05	1.12	1.16	2.27
IL11	-0.15	0.97	1.12	3.13
DSC2	0.92	2.02	1.10	2.86
SPOCK1	1.02	2.12	1.10	1.87
PDLIM7	0.99	2.07	1.09	2.89
LAMB3	0.52	1.60	1.08	2.94
PLOD2	0.46	1.52	1.06	5.92
TSC22D2	0.04	1.09	1.05	1.53
CORO1C	0.32	1.33	1.01	0.92
CHST11	0.67	1.65	0.98	1.69
EPPK1	0.00	0.99	0.98	2.01
HOMER3	1.09	2.05	0.97	2.12
LUM	0.12	1.06	0.94	2.17
ANGPTL4	0.93	1.86	0.93	3.60
JAG1	0.45	1.37	0.92	1.96
B3GNT3	1.40	2.32	0.91	3.84

3.6 p95HER2 signalling is required for proT-SASP production during OIS

MCF7 cells treated with LAP (see above in paragraph 3.2) at the same time of p95HER2 induction by Dox withdrawal proliferate normally (Fig. 6B, see also schematic in Fig. 6A). Conversely, p95HER2-expressing MCF7 cells treated with LAP when already senescent did not resume proliferation (Fig. 6B) and remained SA-β-Gal positive (Fig. 6C). WB analysis proved that the treatment was effective in these conditions (Sup. Fig. 3). Understanding how senescent cells modulate their secretion is relevant because of the contradictory cell-non-autonomous effects exerted by the SASP (see paragraph 1.2.6 of the introduction). For this reason, we addressed the question of weather p95HER2-inhibition, despite not rescuing MCF7 cells from senescence, could still modulate their SASP. To test this hypothesis, the transcriptionally regulated and well-characterized protumorigenic factors Angiopoietin-Like 4 (ANGPTL4), Matrix Metalloproteases 1 (MMP1), Interleukin 6 and 11 (IL6 and IL11) were chosen (see Fig. 5B and Table 1). Their levels were measured in culture media conditioned by cells expressing either FL- or p95HER2, upon LAP treatment. In agreement with the gene expression analysis, the four factors were secreted by p95HER2-induced senescent cells and not by cells expressing HER2-FL (Fig. 6D). Despite being not able to avoid SA-β-Gal activity or to restore cell proliferation (see Fig 6B and C), the inhibition of p95HER2 kinase activity impaired the secretion of all factors analyzed (Fig. 6D). These results show that continuous p95HER2 activity is required for the production of the proT-SASP but not for the maintenance of the senescent state.

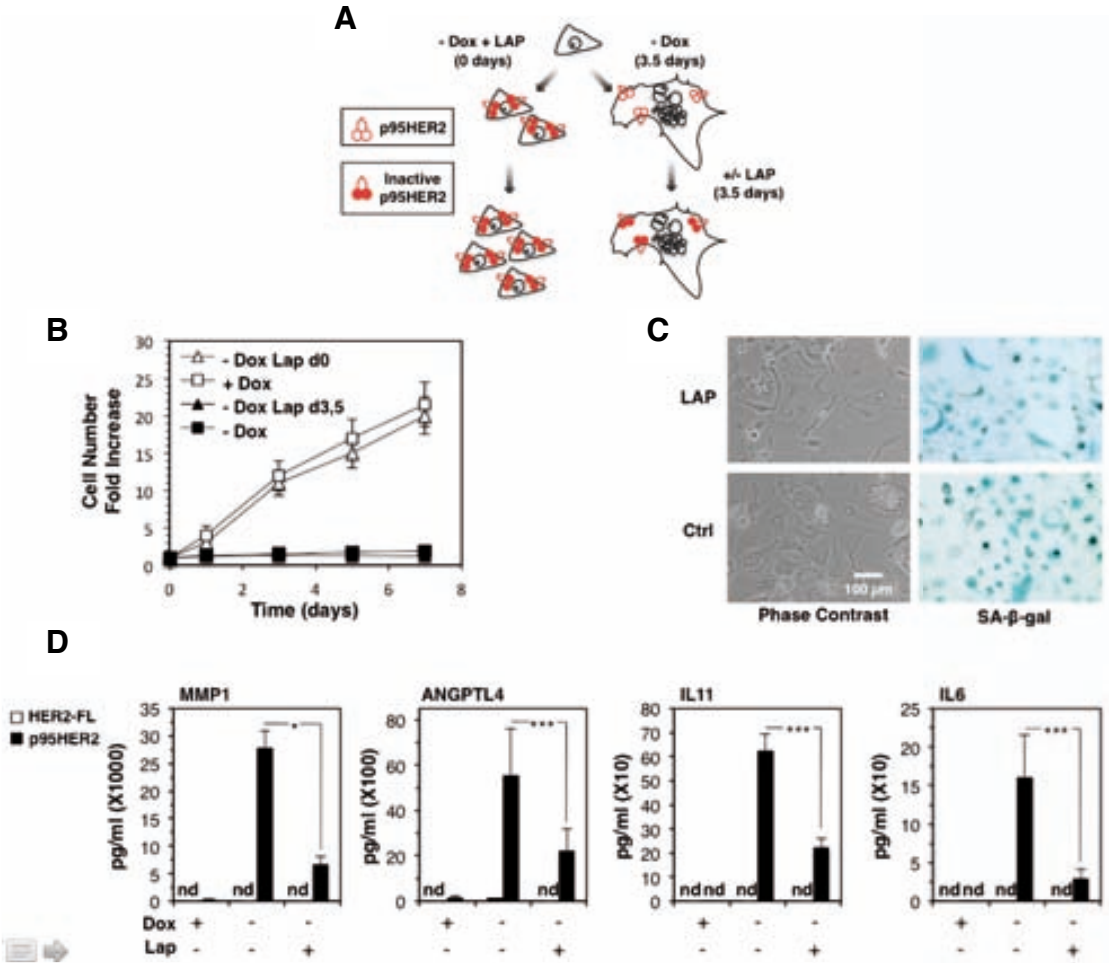

Figure 6. proT-SASP dependency on p95HER2 activity during OIS: A. Schematic showing the procedure used. MCF7 Tet-Off / p95HER2 cells were cultured without doxycycline during 7 days. Lapatinib was added to culture media either at seeding of the cells or at day 3.5 after seeding. **B.** Cells treated as reported in A were counted at the indicated time points. Each point of the curve represents the means ± SD of counting in three independent culture plates. **C.** Non proliferating cells from B, treated or not with LAP, were fixed and immediately stained for SA-β-Gal. Representative phase contrast microscopy images of both unstained and stained cells, are shown. **D.** Repeating the procedure in A, MCF7_tet-off_p95HER2 and MCF7_tet-off_HER2-FL were grown during one week in presence or absence of Dox and treated or not with Lap during the last 3,5 days. Histograms represent the concentration of the indicated factors in the conditioned media as obtained by ELISA. P values were obtained by 2-tailed Student t test. * $P < 0.05$; *** $P < 0.001$; nd stands for not detectable.

3.7 NFkB activity is involved in the generation of the p95HER2-induced SASP

NFkB transcriptional activity underlies the production of many proinflammatory cytokines found in the SASP of cells made senescent by various stimuli [138, 177, 180]. We wanted to assess weather this was the case also for the secretome induced by p95HER2. MCF7 cells with stable Knock-Down (KD) of the NFkB subunit p65 and inducible for p95HER2 expression were generated. KD of p65 did not alter the ability

of p95HER2 to induce senescence in MCF7 cells (Fig. 7A and B). However, it significantly reduced the secretion of both IL6 and IL8 (Fig. 7C), despite effective but not complete knockdown p65KD (Fig. 7D). This preliminary result clearly implicates NFkB activity in the generation of at least part of the p95HER2 SASP.

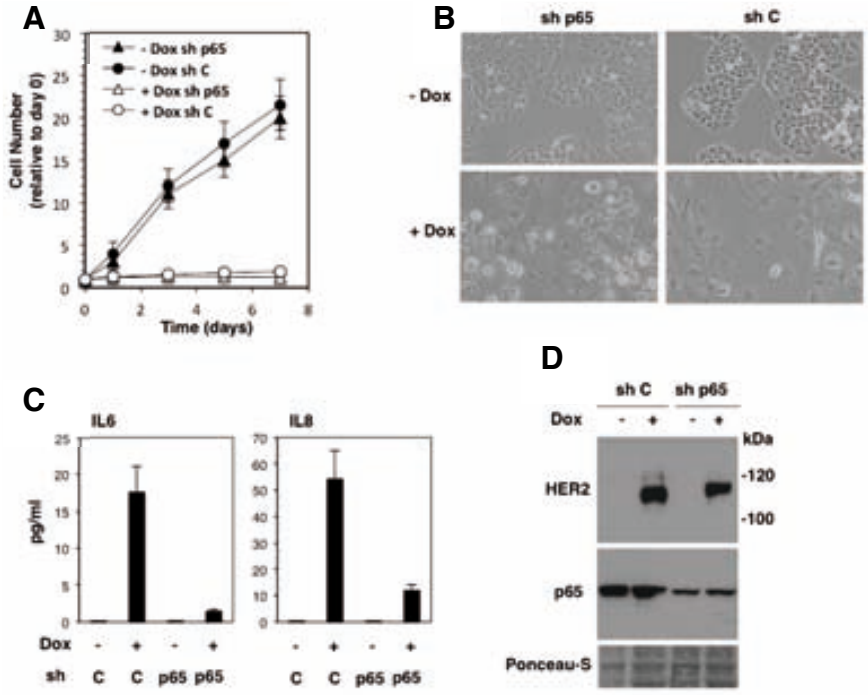

Figure 7. Effect of NFkB KD on the production of the p95HER2-induced SASP: A. Stable clones carrying a constitutive p65 (NFkB sub-unit) Knock-Down (KD) and inducible for p95HER2 expression were obtained from MCF7 (see the section dedicated to materials and methods for details). Control (sh C) and p65KD (sh p65) MCF7_tet-on_p95HER2 cells were grown in presence or absence of Dox and were counted at the indicated time. **B.** No major morphological differences were observed between control and p65KD cells treated as in A at one week after seeding. Representative phase contrast microscopy images of cells either proliferating or induced to senescence are shown. **C.** Control (sh C) and p65KD (sh p65) MCF7_tet-on_p95HER2 cells were grown in presence or absence of Dox during one week. Histograms represent the concentration of the indicated factors in the conditioned media as obtained by ELISA. **D.** Cells treated like in C were lysed and the cell lysates analyzed by WB with the indicated antibodies.

3.8 The PI3K-mTor axis mediates the p95HER2-induced SASP production

Recent work, conducted on fibroblasts induced to senescence by HRAS-G12V, identified another mechanism contributing to the SASP. It consists in a local intracellular coupling of autophagy with mTOR-dependent protein translation [115] (see paragraph 1.2.2 of the introduction). The coupling of these two processes can be monitored by confocal microscopy. In particular, a characteristic perinuclear co-

localization of mTORC1 and LAMP2 proteins can be observed. Analysis by immunofluorescence of senescent MCF7 cells expressing p95HER2 revealed the presence of such co-localization (Fig. 8A). At the same time, AKT and mTOR inhibition (Fig. 8B) resulted in partial reduction of the secretion of all factors analyzed (Fig. 8C). These data suggest that the above-mentioned mechanism contributes to the generation of the p95HER2 secretome through the PI3K-mTOR axis.

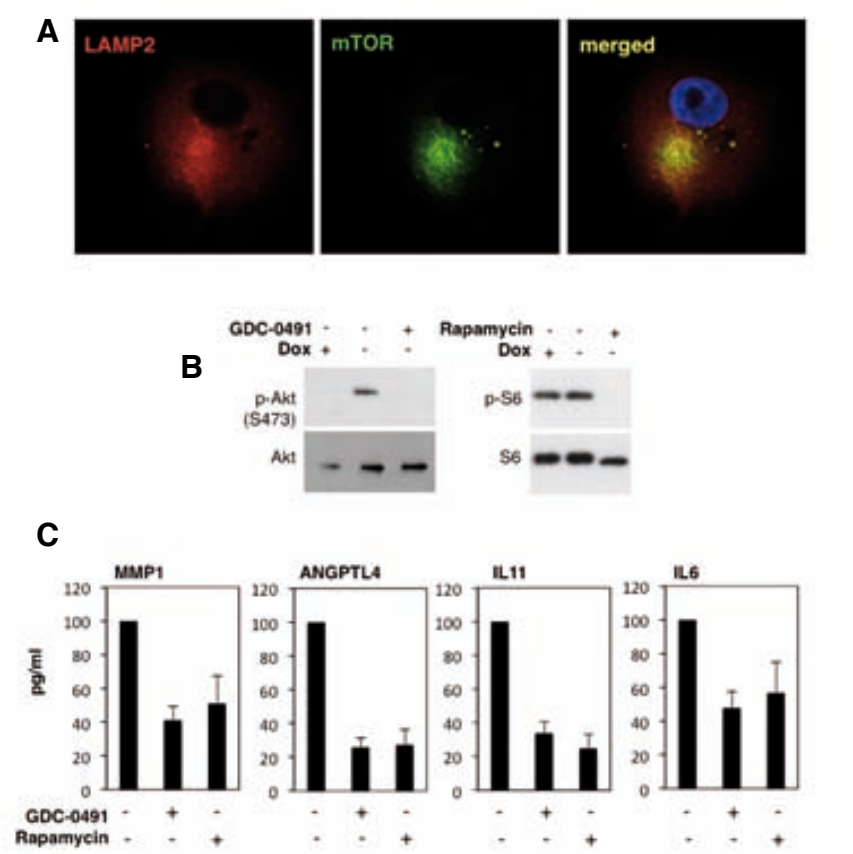

Figure 8. Effect of PI3K-mTOR inhibition the production of the p95HER2-induced SASP: A. Washed MCF7_tet-off_p95HER2 cells seeded in presence or absence of Dox were kept in culture during one week and fixed. Double immunofluorescence was performed using the indicated antibodies. Representative confocal microscopy images are shown **B.** Washed MCF7_tet-off_p95HER2 cells seeded in absence of Dox were treated with a relatively specific PI3K inhibitor (GDC-00491) or with the mTOR inhibitor (Rapamycin). After 48h cells were lysed and the cell lysates analyzed by WB with the indicated antibobies to check the effectivity of the treatment. **C.** MCF7_tet-off_p95HER2 were kept during one week in absence of Dox and treated or not with the indicated inhibitors during the last 3,5 days. Histograms represent the concentration of the indicated factors in the conditioned media as obtained by ELISA.

3.9 p95HER2 activates the proT-SASP also in already senescent cells

We decided to generate prematurely senescent MCF7 cells by different means including γ-irradiation, a CDK4/6 inhibitor (PD0332991), doxorubicin and All-Trans Retinoic Acid (ATRA). All treatments produced a proliferative arrest accompanied by features of senescence including flattened and enlarged morphology and SA-β-Gal positivity (Fig. 9A). MMP1 and IL6, included in the factors selected to validate the p95HER2-associated senescence secretome, are considered prominent SASP components. According to various reports [add ref.], cells induced to senescence by a variety of stimuli [add ref.] secrete, among others, these two proteins. However, we were unable to detect secretion of most of the factors with the exception of IL11 that was found at measurable levels upon doxorubicin treatment (Sup. Fig 4A). We focused on irradiated MCF7 cells as a prototype of DNA-damage induced senescence as opposed to OIS. To our surprise, label-free proteomic analysis of the secretome produced by senescent MCF7 cells at one week after exposure to 10Gy of γ-irradiation revealed secretion of low amount of few proteins (data not shown). Among the few secreted components, one of the most abundant was the Pregnancy Specific beta-1-Glycoprotein 9 (PSG9) and we validated the proteomic result performing WB on concentrated media conditioned by irradiated senescent MCF7 cells (Sup. Fig. 4B). Compared to other types of senescence, MCF7 cells undergoing OIS secreted considerably higher amounts of all factors analyzed, including PSG9 (Sup. Fig 4A and B). We aimed to figure out if this potent p95HER2-driven secretory response during OIS was related with the initial proliferative state of the cells. To address this point we first irradiate MCF7 cells, give them one week to become fully senescent and successively induce p95HER2 expression (See schematic in Fig. 9B). As previously observed, MCF7 cells made senescent by irradiation secreted undetectable levels of the four factors (Fig. 9C). However, p95HER2 expression resulted in a secretion pattern comparable to the one presented in Fig. 6D (Fig. 9C). In this case, LAP efficiently blocked secretion of all factors with the exception of ANGPTL4 (Fig. 9C). This result shows that p95HER2 is able to activate the pro-tumorigenic SASP also in already senescent MCF7 cells.

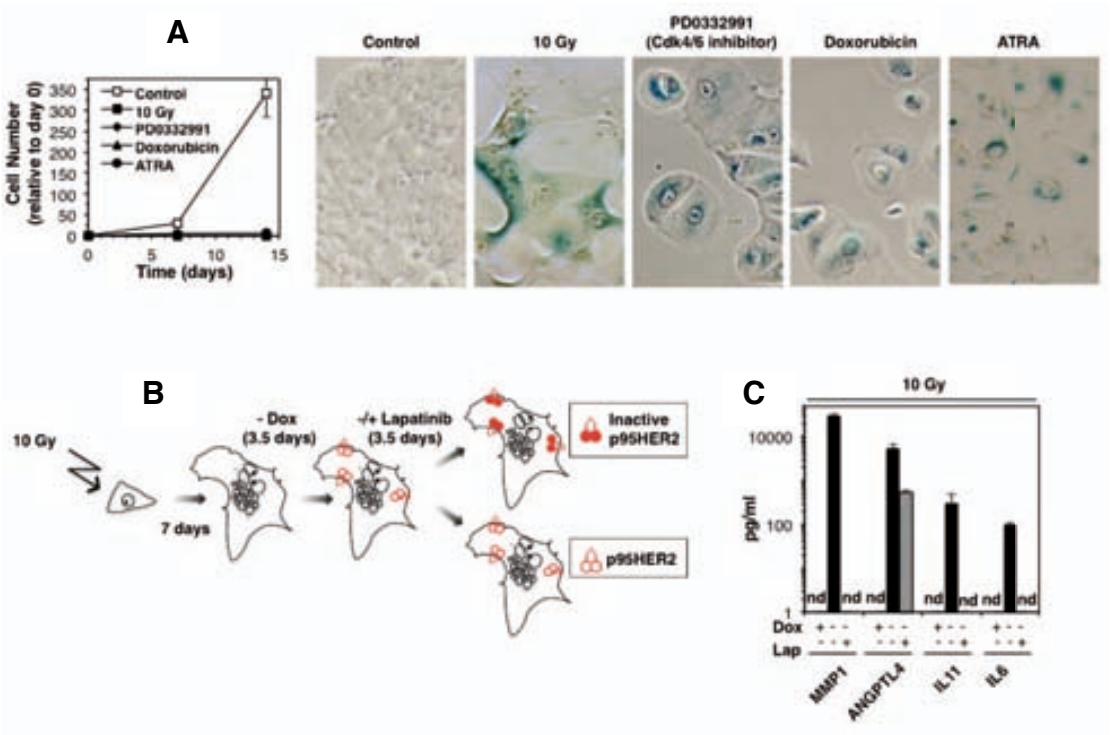

Figure 9. Activation of the SASP by p95HER2 in already senescent cells: A. MCF7_tet-off_p95HER2 grown in the presence of doxycyclin were irradiated with a dose of 10 Gy, treated with the CDK 4/6 inhibitor PD0332991, with Doxorubicin of with ATRA. After treatment cells were seeded and then counted at the indicated time points to confirm the proliferative arrest. After one week all cells were fixed and stained for SA-β-galactosidase activity. Representativephase phase contrast microscopy images are shown. **B.** Schematic showing the procedure used to obtain the result in C. **C.** Already senescent irradiated MCF7_tet-off_p95HER2 cells were grown during one week in presence or absence of Dox and treated or not with Lap during the last 3,5 days. Histograms represent the concentration of the indicated factors in the conditioned media as obtained by ELISA. P values were obtained by 2-tailed Student t test. * $P < 0.05$; *** $P < 0.001$; nd stands for not detectable.

3.10 The p95HER2-driven secretory response is specific of senescent cells

Among the cell lines tested, MCF10A were the only one not entering senescence in response to p95HER2 expression (see Fig. 3A). At this point we aimed to better discriminate the SASP-modulating function of the HER2 fragment from its pro-senescent effect. To this scope, we administered 10 Gy of γ-irradiation to MCF10A cells expressing or not p95HER2. As assessed by proliferation (Fig. 8A) and SA-β-Gal activity (Fig. 8), both cell lines readily become senescent. We then analyzed the media conditioned by control and irradiated cells, treated or not with LAP. While p95HER2 expression in proliferating MCF10A cells resulted in a modest pro-secretory effect, the activity of the fragment in senescent MCF10A produced a

remarkable boost in the secretion of MMP1, ANGPTL4 and IL6 (Fig. 8C). These data demonstrate that the senescence-inducing and the SASP-modulating functions promoted upon constitutive HER2 activation are independent from each other. Furthermore, the potent p95HER2-driven secretory response appears to be specific of senescent cells, as it is not observed in proliferating MCF10A

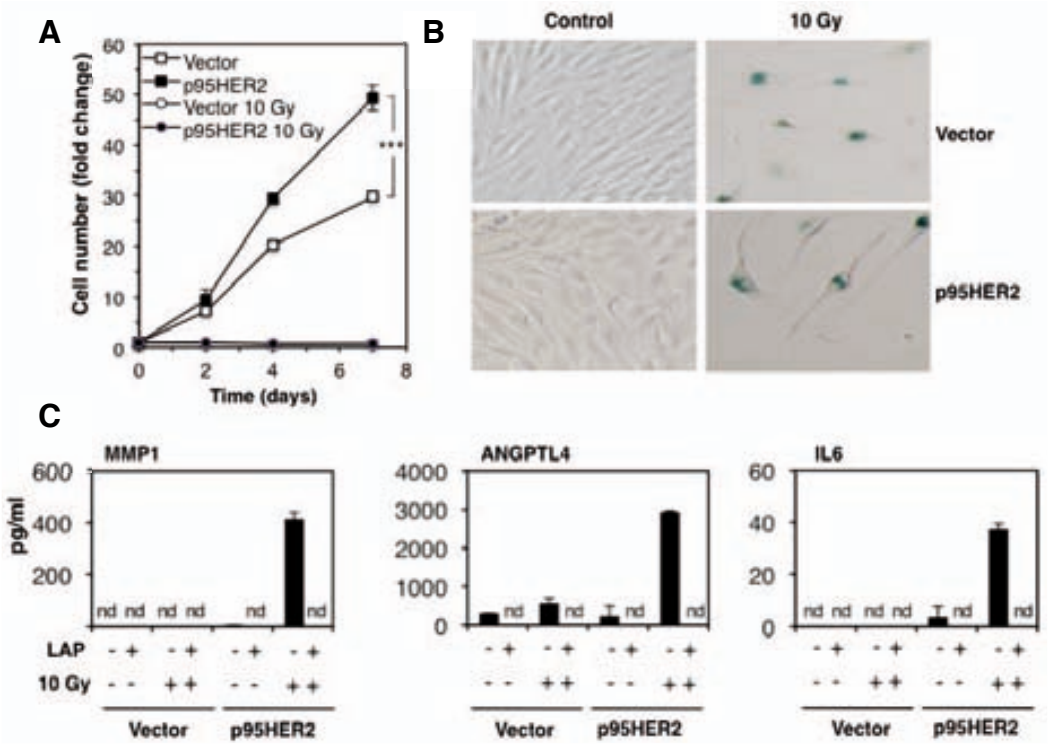

Figure 10. Secretory response driven by p95HER2 in senescent, but not proliferating, MCF10A cells . A. Control and irradiated MCF10A expressing either an empty vector or p95HER2 (see Fig. 3A) were grown during one week and proliferation was assessed by cell count at the indicated times. **B.** Cells as in A were fixed and stained for SA-β-galactosidase activity. Representative phase phase contrast microscopy images are shown. **C.** MCF7 Tet-off/p95HER2 treated Control and irradiated MCF10A expressing either an empty vector or p95HER2 were grown during one week and treated or not with Lap during the last 3,5 days. Histograms represent the concentration of the indicated factors in the conditioned media as obtained by ELISA.

3.11 The p95HER2-driven proT-SASP is produced also in vivo

p95HER2-expressing MCF7 cells were viable in culture for at least four weeks and during this time they remained senescent (Sup. Fig. 5A and B). Culture media were conditioned by senescent MCF7 cells and collected at each week after p95HER2 induction during one month. The analysis of the levels of IL6, IL11, MMP1 and ANGPTL4 indicated active secretion to the extracellular medium during the whole period (Sup. Fig. 5C). Since p95HER2-expressing senescent cells secreted pro-tumorigenic factors with constantly high efficiency for such a long period, we decided to test them in vivo. MCF7 Tet-Off p95HER2 cells were injected into nude mice and allowed to form a subcutaneous tumor. Once the tumors had reached about 150 mm3, doxycyclin was removed from the drinking water of the animals to allow the expression of the oncogene (Fig. 11A). Every seven days, during six weeks after Dox removal, the xenograft tumors were excised. They were then analyzed by immunohistochemistry (IHC) and immunofluorescence (IF) for comparison with control tumors. At two weeks after Dox removal, less tumor cells expressed the cell proliferation marker Ki67, while more showed nuclear p21 expression (Fig. 11B, 14 days). After three additional weeks, these changes had become more dramatic and the hematoxilin-eosin (HE) staining showed a clear hypertrophic cellular morphology. At the same time, IF revealed the presence of γ-H2AX-positive nuclear foci (Fig. 11B, 35 days, see also quantification in Sup. Fig 6). At 5 weeks after Dox withdrawal, increased SA-β-Gal activity was observed in the tumors expressing p95HER2. When these xenografts were put back in culture, as soon as attached to the plastic, the derived cells presented the typical senescent morphology (Fig. 11C). Consistently, tumors in the absence of Dox showed an initial increase in volume and then tended to stabilize (Fig. 11A and Sup. Fig. 6). The experiment was repeated and three animals from each group were sacrificed and exsanguinated at the indicated times to analyze the plasma levels of ANGPTL4 and IL11. Both factors were detected in the plasma of mice carrying senescent tumors at significantly higher levels than in the plasma of animals with proliferating tumors (Fig. 11D). These results show that also in vivo, when forming a xenograft tumor, MCF7 cells can be induced by p95HER2 expression to enter OIS. Moreover, the HER2 fragment sustains the efficient production of the proT-SASP during long periods of time, both in vitro and in vivo.

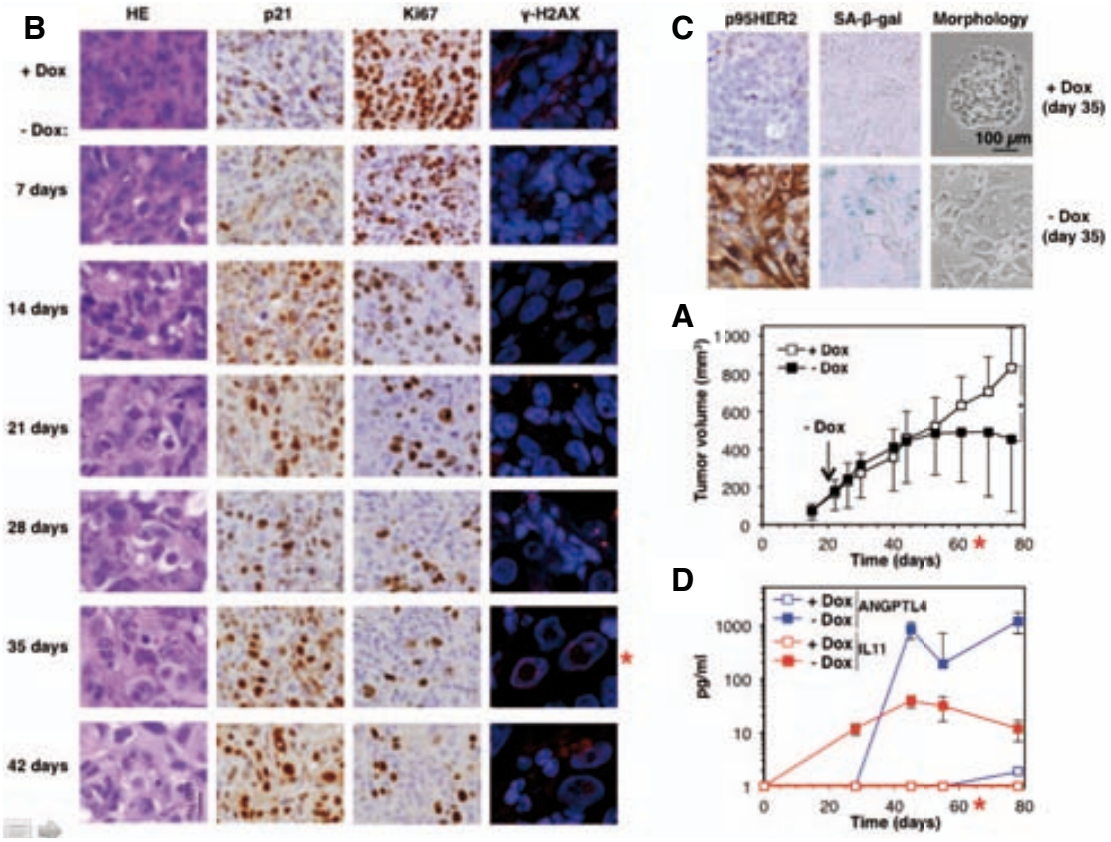

Figure 11. p95HER2-induced senescence and proT-SASP in vivo: A. a total of $3x10^6$ MCF7 Tet-off/p95HER2 cells were injected subcutaneously into the flank of nude mice. Doxycycline was administered in the drinking water until tumors reached about 150mm3, then mice were randomized and doxycycline was withdrawn from the drinking water of half of the mice (**n**.12 in each group). The points represent average tumor volume at each time point_SD. P values were obtained by 2-tailed Student t test, * $P < 0.05$. **B.** Xenografts from mice treated as in A were surgically removed at the indicated times, fixed and paraffin-embedded. Hematoxylin eosin (HE) staining or immunostaining with the indicated antibodies were performed in serial slices from the paraffin-embedded tumors. Representative fields are shown. **C.** Xenografts from mice treated as in A were surgically removed at day 35 and then either minced or formalin fixed. Minced tumors were seeded and cultured in media with or without doxycycline overnight. Representative phase contrast microscopy images are shown (right). Fixed tumors were either paraffin-embedded or immediately stained for SA-β-galactosidase activity. Representative phase contrast microscopy images are shown (center). Slices from the paraffin-embedded tumors were immunostained with a monoclonal antibody against HER2. Representative bright field microscopy images are shown (left). **D.** Concentration of the indicated factors in the sera of mice, treated as in A and exsanguinated at the indicated time points, was determined by ELISA. The points represent the averages of determinations from 3 mice +/- SD.

3.12 p95HER2 senescent cells favor metastasis cell non-autonomously

The previous results opened the possibility of a cell-non-autonomous pro-tumorigenic effect mediated by the p95HER2-induced SASP, in vivo. Poor prognosis and survival of breast cancer patients are frequently associated with progression to metastatic disease [36]. The presence, both spontaneous and therapy-induced, of senescent cancer cells has been reported in breast tumors [216, 217]. In spite of these evidences, we decided to experimentally address the potential cell-non-autonomous pro-metastatic effect of senescent cells, within a primary tumor. MDA-MB-231 breast cancer cells engineered to stably express the Firefly Luciferase (Luc) were chosen as reporter. These cells have been previously used to study the metastatic process in different experimental settings [218]. Since the pro-tumorigenic factors secreted from p95HER2-expressing senescent cells within the primary tumor reached the blood stream (see Fig. 11D), they could favor malignant progression of circulating tumor cells. To test this hypothesis we subcutaneously inject MCF7_tet-off_p95HER2 in the flank of nude mice. When the cells had formed a tumor of about 150 mm3, p95HER2 expression was induced in half of the animals. After additional two weeks, mice from both groups were injected intracardially with MDA-MB-231_Luc cells (see schematic in Fig. 12A). All animals in both groups developed metastases, but quantification of the total light emitted by the reporter cells revealed higher metastatic growth in mice carrying senescent primary tumors (Fig. 12B). The in vivo imaging analysis indicated comparable latency periods prior to the appearance of the first metastases in the two experimental conditions (data not shown). Thus, the observed difference most likely reflects an increased growth of reporter cells after colonization of the target organs. Since doxycyclin has been reported to inhibit some metalloproteases [219, 220] we had to rule out a direct effect of Dox removal on the reporter cells. To this aim, two groups of mice, receiving or not Dox in the drinking water, were injected intracardially with MDA-MB-231_Luc cells (see schematic in Fig. 12C). Again, all animals developed metastasis, but in this case no significant differences in the metastatic growth were observed (Fig. 12D). These results indicate that senescent cells within the tumors favor the growth of circulating tumor cells after metastatic colonization. It can be presumed that the systemic distribution of some SASP components is mediating this effect.

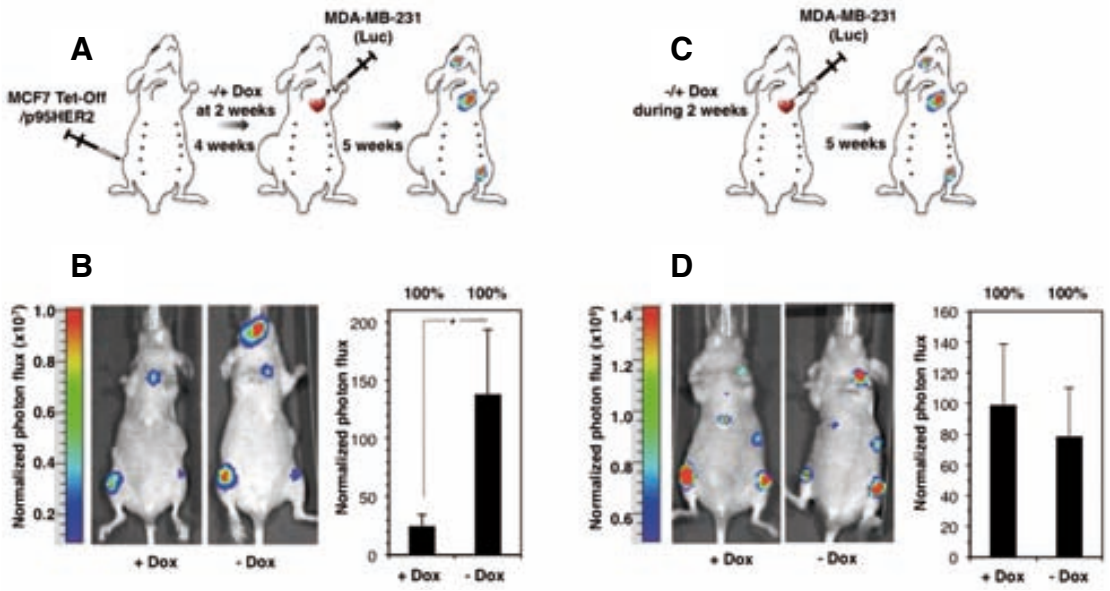

Figure 12. Prometastatic effect of p95HER2-induced senescent cells on circulating tumor cells: A. schematic showing the protocol used. Briefly, 3 x10^6 MCF7 Tet-off/p95HER2 cells were injected subcutaneously into the flank of nude mice. Doxycycline was administered in the drinking water until tumors reached about 150 mm3. Then, mice were randomized and doxycycline was withdrawn from the drinking water of half of the mice (n. 5 in each group). Two weeks after removal of doxycycline from one of the groups, 2.5x10^5 MDA-MB-231/Luc were injected intracardially in all mice and, after 5 weeks, animals undergone weekly in vivo imaging. **B.** Representative luminescence images at 6 weeks after intracardiac injection are shown (left). Histograms representing the metastatic growth measured as total photon flux emission per group at the same time point. Values are mean +/- SD. P values were determined by Student t test, * $P < 0.05$ (right). The percentages above the plots represent how many animals per group developed metastasis. **C and D.** To rule out unspecific effects to to the experimental settings, the exact same procedure as in A and B was conducted on control animals not carrying any subcutaneous tumors (n. 4 in each group).

We then moved on to assess the local cell-non-autonomous pro-metastatic effect of senescent cells on surrounding non-senescent cells within the same tumor. To do so, MCF7 Tet-off p95HER2 together with MDA-MB-231_Luc cells were co-injected in the mammary fat pad of nude mice. When the orthotopic tumors had grown to an approximate size of 200mm3, p95HER2 expression was induced in half of the injected animals. Primary tumors were surgically removed at a maximum approximate size of 700mm3 (Fig. 13B, see schematic in Fig. 13A). Measurement of the volume of the primary tumors showed a negligible difference between the two different experimental conditions (Fig. 13B). The light emitted by the primary tumors was analyzed soon prior to their surgical excision and indicated that MDA-MB-231_Luc cells had grown slightly more in the absence of Dox (Fig. 13C). As expected, dispersed clusters of p95HER2-expressing MCF7 cells were detectable in the tumors grown in the absence of doxycycline (Fig. 13D). These last two evidences might reflect a local effect due to the proximity of senescent MCF7 cells and non-senescent reporter cells within the primary tumor. In the weeks after surgery, the metastatic growth was monitored by in vivo imaging analysis. p95HER2-expressing

senescent MCF7 cells significantly favored both the metastatic spread and the metastatic growth of the reporter MDA-MB-231 Fluc cells (Fig. 13E). These data suggest that the presence of a compartment enriched in senescent cells within the primary tumor can prime surrounding non-senescent breast cancer cells for metastasis.

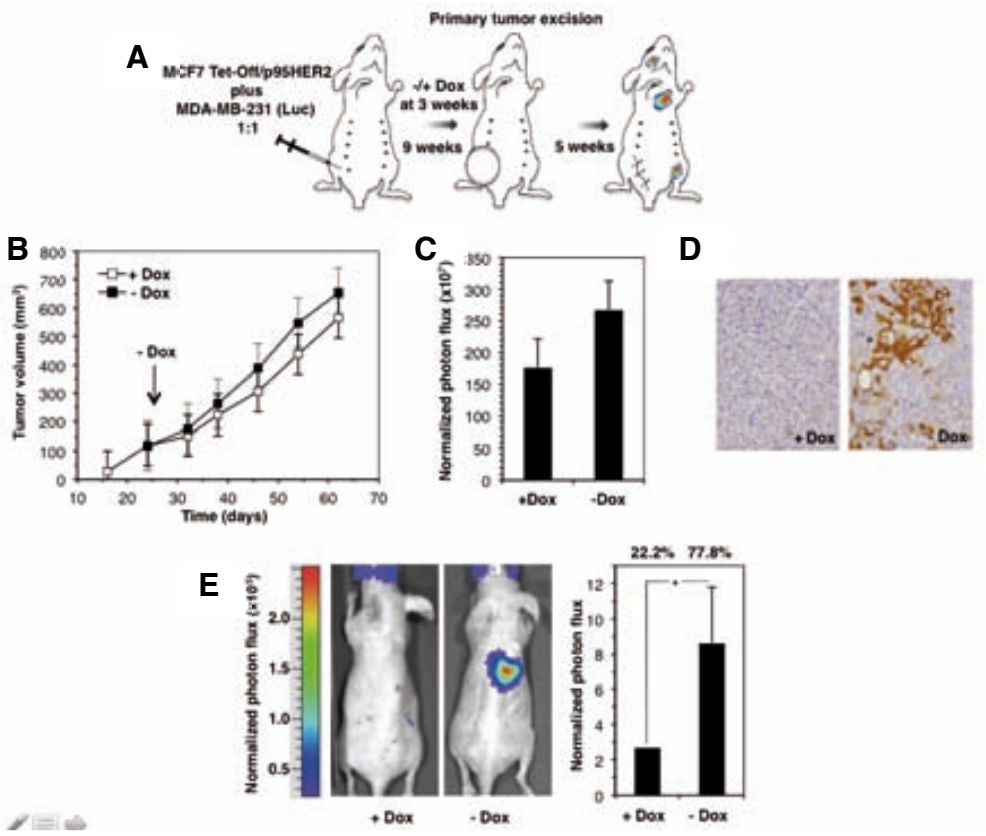

Figure 13. Prometastatic effect of p95HER2-induced senescent cells on neighbor tumor cells: A. schematic showing the protocol used. Briefly, $1.5x10^6$ MCF7_tet-off_p95HER2 mixed with $1.5x10^6$ MDA-MB-231_Luc cells were injected orthotopically into the fourth mammary fat pad. Doxycycline was administered in the drinking water until tumors reached about 150mm3. Then, mice were randomized and doxycycline was withdrawn from the drinking water of half of the mice (n. 8 in each group). Tumors were allowed to grow until they reached about 700 mm3 and then surgically removed. Five weeks after removal of the primary tumor in vivo imaging was conducted. B. Volume of the tumors generated in A was followed using a caliper. The points represent average tumour volume at each time point +/- SD. **C.** Growth of the same tumors as in A and B, as determined by bioluminescence captured at approximately 9 weeks after injection (soon prior to surgery). Histograms represent the total photon flux emission of primary tumors per group. Values are mean +/- SD. **D.** Xenografts were removed soon after the analysis in C, formalin fixed and paraffin-embedded. Slices from the paraffin-embedded tumours were immunostainned with a monoclonal antibody against HER2. Fields are shown to appreciate the presence of positive cellular clusters in the absence of Dox. **E.** Representative luminescence images at 5 weeks after surgery (14 weeks after orthotopic injection) (left). Histograms representing the metastatic growth measured as total photon flux emission per group at the same time point. Values are mean +/- SD. P values were determined by Student t test, * $P < 0.05$ (right). The percentages above the plots represent how many animals per group developed metastasis.

Supplementary Information

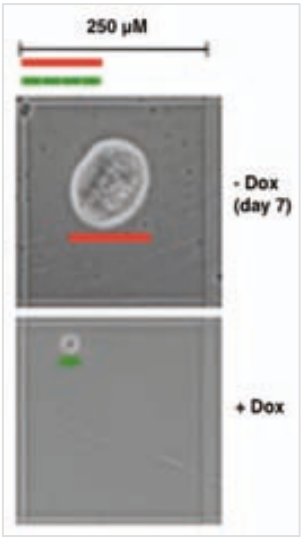

Supplementary Figure 1. Hyperthrophy of MCF7 cells expressing p95HER2: MCF7_tet-off_p95HER2 cells were harvested after one week in presence or absence of Dox, loaded into a Neubauer chamber and photographed.

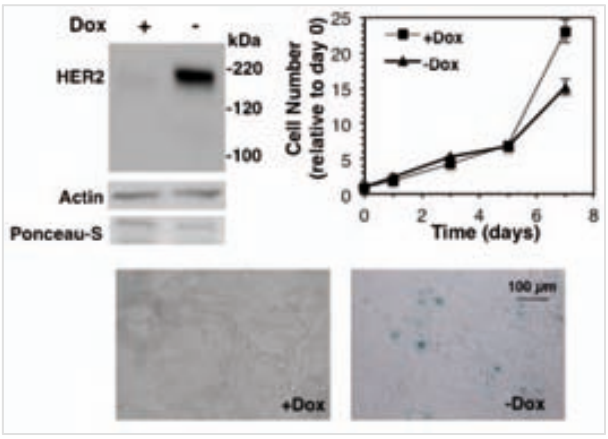

Supplementary Figure 2. MCF7 cells expressing HER2-FL: MCF7_tet-off_HER2-FL were subjected to the same procedure as in Fig. 3D

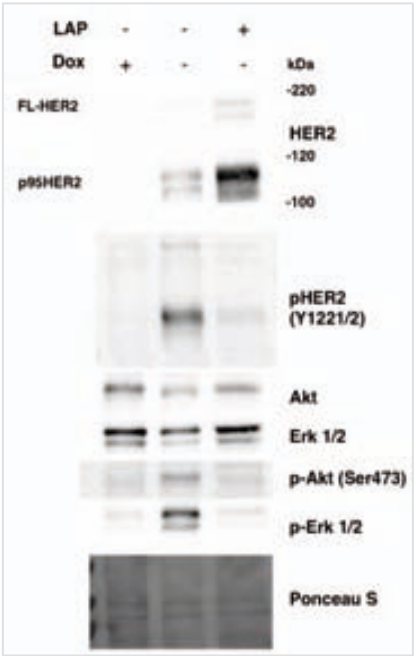

Supplementary Figure 3. Effect of lapatinib on senescent MCF7 cells: MCF7_tet-off_p95HER2 and MCF7_tet-off_HER2-FL were grown during one week in presence or absence of Dox and treated or not with Lap during the last 3,5 days. At this point cells were lysed and analyzed by WB with the indicated antibodies

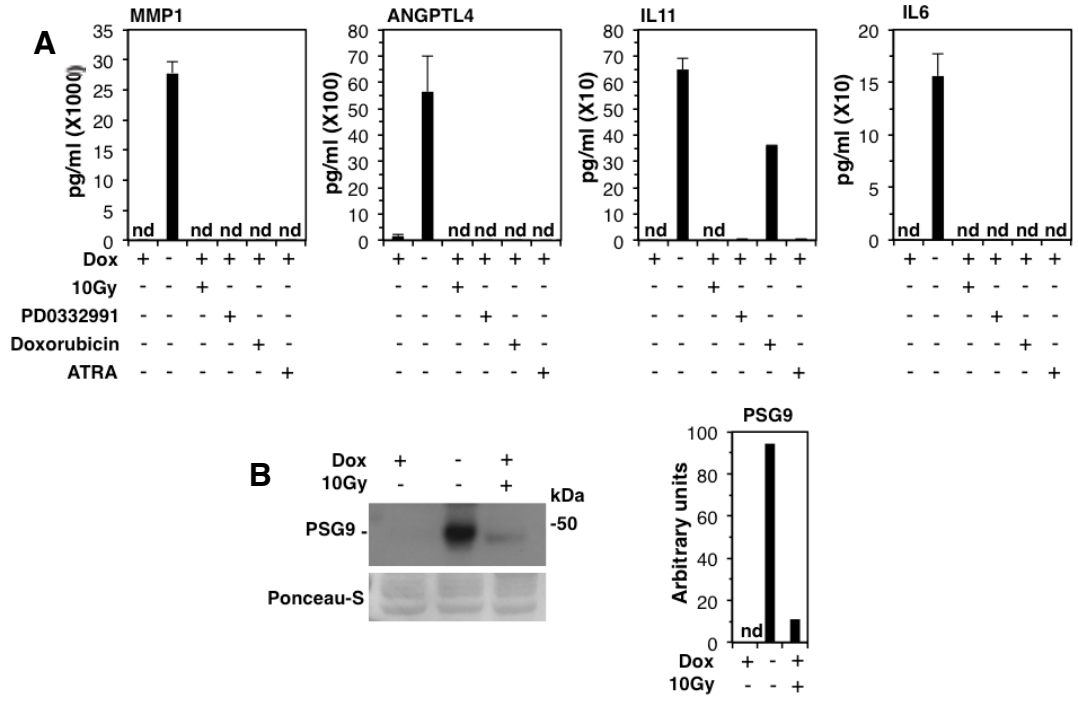

Supplementary Figure 4. Comparison of the secretion induced by different pro-senescent stimuli: **A.** MCF7_tet-off_p95HER2 grown in the presence of doxycyclin were irradiated with a dose of 10 Gy, treated with the CDK 4/6 inhibitor PD0332991, with Doxorubicin or with All-Trans Retinoic Acid (ATRA) to induce senescence (see Fig. 9A). Histograms represent the concentration of the indicated factors in the media conditioned during one week by senescent MCF7 cells obtained with the different treatments , in comparison with the same cells induced to OIS by p95HER2 and with their proliferating counterparts, as obtained by ELISA. B. Western Blot performed on the concentrated media conditioned by cell induced to senescence either by p95HER2 or by irradiation in comparison with proliferating cells (left). Quantification of the WB is also presented (right).

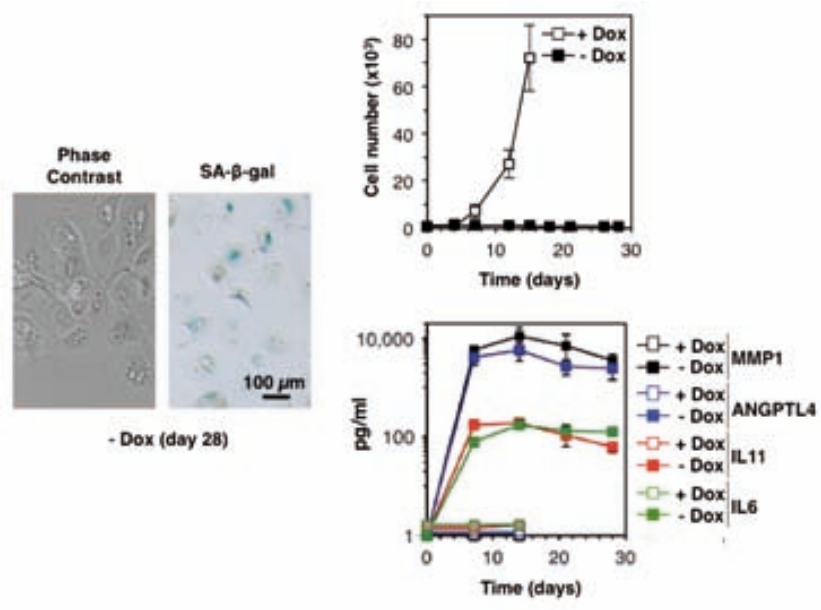

Supplementary Figure 5. Long-term secretory capacity of senescent MCF7 cells in vitro: A. MCF7 Tet-Off / p95HER2 cells were cultured with or without doxycycline and counted at the indicated time points. Each point of the curve represents the means ± SD of counting in three independent culture plates. **B.** In parallel to A conditioned media were collected at each time point. Curves represent the concentration of the indicated factors in the conditioned media as obtained by ELISA . P values were obtained by 2-tailed Student t test. * $P < 0.05$; *** $P < 0.001$; nd stands for not detectable. **C.** At day 28 in the same culture dish, senescent MCF7 cells were photographed, then fixed and immediately stained for SA-β-gal. Representative phase contrast microscopy images of unstained and stained cells, are shown.

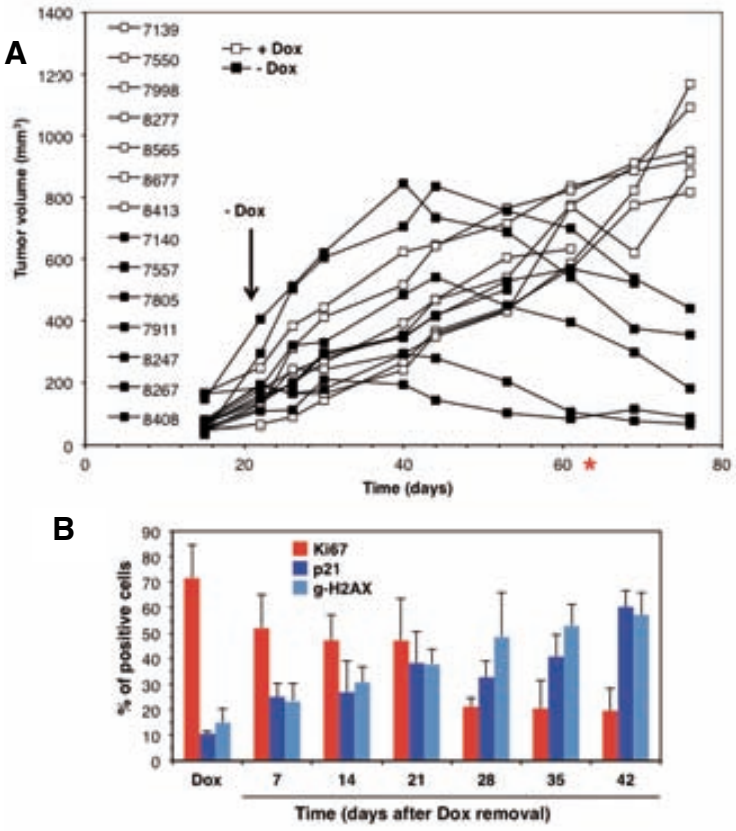

Supplementary Figure 6. p95HER2-induced senescence and proT-SASP in vivo: A. Volume of individual tumors at the indicated time points resulting in the average represented in the plot in Fig. 11A. **B.** Quantification of the immunohistochemical analysis whose representative pictures are shown in Fig. 11B. The number of positive cells for each staining at each time-point was quantified and the bars represent the averages of 3 independent determinations from 1 or 2 mice of the same group on at least two distant slices of each tumor.

gene name	log2FCp95HER2 (protein)	gene name	log2FCp95HER2 (protein)	gene name	log2FCp95HER2 (protein)	gene name	log2FCp95HER2 (protein)
TUBA4A	7.02	PLXNB2	3.46	LDLR	2.77	LOXL2	2.17
LAMC2	6.46	GOLM1	3.36	DBN1	2.74	MAN2B1	2.16
LUM	6.34	FN1	3.31	KRT81	2.74	RPL10A	2.16
MMP13	6.06	FAM20B	3.31	C19orf21	2.72	ITGA3	2.15
PLOD2	5.92	ICAM1	3.31	IL10RB	2.72	PSAP	2.15
MET	5.82	LIF	3.30	SMARCE1	2.72	AGRN	2.14
MMP1	5.51	LMO7	3.27	TRIP10	2.72	FAM3C	2.13
ERBB2	5.14	RAB27B	3.24	TGM2	2.69	IGFBP3	2.12
PLAUR	5.05	KLK6	3.18	MUC5AC	2.67	AFP	2.12
OSMR	4.85	S100A8	3.13	CEACAM5	2.67	ASAH1	2.12
PSG9	4.85	IL11	3.13	GNPTG	2.66	DIABLO	2.12
NOMO1	4.76	IL1RAP	3.13	PLOD1	2.65	DNAJC1	2.12
KRT80	4.67	KIAA1609	3.13	ATP6AP1	2.63	FURIN	2.12
VEGFC	4.39	LRP11	3.13	VASN	2.63	HOMER3	2.12
AREG	4.32	ENDOD1	3.13	LTBP3	2.57	IL18	2.12
BAIAP2L1	4.31	S100A9	3.08	ZNF185	2.55	PRPF40A	2.12
PTPRJ	4.23	CD55	3.07	MANF	2.48	QPRT	2.12
LCP1	4.14	CTBS	3.07	CTSL1	2.48	SDCBP2	2.12
PRSS22	4.07	VGF	3.06	PLA2G15	2.45	SRSF6	2.12
INHBA	4.00	CDH3	3.04	GALNT3	2.44	SSRP1	2.12
KIAA1199	3.99	PVR	3.02	HS6ST2	2.44	TOP1	2.12
UGGT1	3.98	GPRC5A	2.96	NME3	2.44	UBL4A	2.12
OLFML3	3.91	FSTL3	2.95	TJP2	2.44	YME1L1	2.12
B3GNT3	3.84	SEMA3B	2.95	CD44	2.41	TRAPPC3	2.12
ITGA2	3.82	LAMC1	2.94	DNM1L	2.38	FUT8	2.11
ASPH	3.73	LAMB3	2.94	GABARAPL2	2.38	ERAP1	2.11
FHL2	3.73	B4GALT3	2.94	STAT1	2.37	ATP1A1	2.10
PLG	3.73	B4GALT4	2.94	TOR1AIP1	2.36	CPE	2.10
ITGB1	3.61	EHD1	2.94	S100A14	2.34	DST	2.09
ANGPTL4	3.60	H2AFY	2.94	HMGB1	2.34	HEATR7B2	2.09
CPA4	3.60	PDLIM7	2.89	CTSB	2.31	IF2BL_HUMAN	2.09
DNAJC3	3.60	DSC2	2.86	QSOX1	2.29	MATN3	2.09
RELT	3.60	HYOU1	2.84	DSG2	2.28	IFI30	2.09
IDS	3.59	ULBP2	2.83	LAMA3	2.27	EPS8L1	2.08
ECM1	3.53	SLPI	2.81	GALNT2	2.26	EXD3	2.08
ANXA1	3.53	STC1	2.80	TFPI	2.26	PPL	2.07
SEMA7A	3.47	IL6	2.78	MESDC2	2.21	SERPINH1	2.05
DNAJB9	3.46	ERO1L	2.78	RHOC	2.19	HIST3H3	2.03
IL1RL1	3.46	LAMB1	2.77	PLOD3	2.18	EPPK1	2.01

Supplementary Table 2 (extract): Secretome of p95HER2-induced senescent MCF7 cells: This table reports the most up-regulated 154 proteins (log2FC > 2) out of the 361 more abundantly secreted by p95HER2-induced senescent MCF7 cells (see paragraph 3.5)

DISCUSSION

Chapter 4

Discussion

Back in 1957, George C. Williams proposed for the first time the concept of **antagonistic pleiotropy** to provide an evolutionary explanation for the process of aging (i.e. organismal senescence) [187]. Williams' original idea was that natural selection would not eliminate phenotypic traits that favor fitness during early-life (i.e. embryonic development or reproductive age), even if they are potentially detrimental in late-life [187]. The expression is a combination of three ancient greek terms: *antagonistēs,* meaning "opposite", *pleion*, meaning "several" and *tropos*, meaning "acquired/induced changes" (i.e. in our case "phenotypic traits"). Then, **pleiotropy** simply refers to "one single entity" (Williams choose "one gene") simultaneously governing (or implying) several different phenotypic traits. The term **antagonistic** indicates that such phenotypic traits have opposite effects (either beneficial or deleterious) when comparing different specific contexts. For almost historical reasons, the concept of antagonistic pleiotropy is classically approached from William's perspective (i.e. the perspective of evolutionary genetics). However, literally, antagonistic pleiotropy could simply refer to phenotypic aspects acting as a sort of double-edged sword. In such view, positive or negative effects of the analyzed phenotypes would be dictated by the biological contexts in which they develop. These conditions surely include homeostatic regulation, immune-surveillance and regenerative capacity of a given tissue. With respect to such properties, tissues and organs from a young and healthy individual are profoundly different from the ones of an old organism [227]. Arguably, this is true irrespectively of any environmental or evolutionary selective pressure. Specific factors (or cellular processes) beneficial in normal liver could reveal deleterious in a chronically inflamed liver (for example the senescent secretome, see paragraph 1.2.6 of the introduction). Specific process can be expected to be advantageous for the organism during early cancer development (i.e. in a predominantly normal tissue attempting to conserve its homeostasis) and become noxious in more advanced stages of the disease (i.e. in a tissue undergone malignant transformation). To our view, cellular senescence, particularly in regard to the influence of the SASP on tumor progression, fits pretty well this idea of age-independent of antagonistic pleiotropy. A study focused on RAS-induced liver

tumorigenesis strengthens the already well-established idea of a tumor-suppressive role of senescence in premalignant lesions [213]. In immuno-competent mice, RAS expression induces normal hepatocytes to enter OIS. The resulting SASP is proven to induce an adaptive immune response that effectively clears premalignant senescent hepatocytes. This response, designated as senescence immune-surveillance, is shown to be crucial in preventing malignant progression to hepatocellular carcinomas [183]. More recently, however, another report demonstrates that the SASP in the liver is not always beneficial. A specific obesity-induced gut microbial metabolite is also able to induce senescence in liver cells. In this case the SASP does not mediate any immune response but, on the contrary, is shown to actively promote liver cancer [194]. To date, at least in our knowledge, this is the first report providing a causal link between the senescence-secretome and cancer progression in a model of spontaneous tumorigenesis in vivo. Moreover, these two studies pose an interesting example of age-independent antagonistic pleiotropy in the liver, which is causally associated with the SASP. Work from Reddy et al. proves that different oncogenes, including constitutively active HER2, induce OIS in normal breast epithelial cells. In this case, there is no evidence for immune-surveillance of senescent premalignant cells in early breast tumor lesions. Such lesions, in fact, progress to fully blown mammary tumors within which senescent breast cancer cells are still readily detectable [216]. These results are suggestive of tissue-specific (or cell type-specific) differences in senescence immune-surveillance. Future understanding of the functional role of the senescence secretome produced within early breast tumor lesions, as well as in fully blown breast tumors, will be relevant. To this respect, our data about the SASP of breast epithelial cells induced to senescence by constitutively active HER2 can prove valuable in the future. The work reported in this thesis shows that p95HER2 induces OIS, which is accompanied by the secretion of several pro-tumorigenic factors. MCF7 cells efficiently form subcutaneous tumors in immuno-deficient mice. Upon induction of p95HER2-expression, cells within the tumor massively undergo OIS and, notably, components of the SASP become detectable in the plasma of the animals during more than one month (see Fig. 13). In contrast to our results, work from Scott Lowe and colleagues, shows a potent tumor suppressive effect of senescence in already formed tumors. Here, RAS-transformed hepatoma cells, in which p53 expression was inhibited, are subcutaneously injected and form a xenograft in the same immuno-deficient mice that we used. Subsequent restoration of p53 expression elicits a general senescence

response in the cells within the tumor. In this case, the resulting SASP induces an innate immune response, which leads to complete tumor shrinkage in about 2 weeks [184]. These results might reflect an intrinsic difference in the ability to evoke an immune response between mammary epithelial and hepatic senescent cells. Certainly, also differences associated with experimental settings cannot be discarded. However, the immune-modulating factors secreted by senescent hepatoma cells were not found in the secretome of senescent MCF7 cells (see Supp. Table 2). Some authors have previously hypothesized that the SASP could exert effects at sites distant from the one of its production [210]. p95HER2-expressing senescent within our subcutaneous tumors secrete IL11 and ANGPTL4, that are shown to reach the blood stream. These factors were previously shown to favor metastasis [228, 229]. Accordingly, we here present that the metastatic growth of reporter cells injected intracardiacally is increased in the presence of senescent subcutaneous tumors (see Fig. 15). p95HER2-expressing senescent cells secrete, among other factors, the already mentioned ANGPTL4, IL6 and MMP1 (see Fig. 9 and 10). MMPs produced by senescent cells alter the normal architecture of the mammary gland favoring spontaneous tumorigenesis [230, 231]. Moreover, they promote the growth of breast xenograft-tumors [232] and favor metastasis [233]. IL6 is able to stimulate Epithelial-to-Mesenchymal Transition (EMT) [124], an important step needed for metastatic spread from primary tumors. Data reported in this thesis demonstrates that p95HER2 expression is able to induce the pro-tumorigenic SASP also in already senescent irradiated MCF7 cells (see Fig. 8). Moreover, we obtained proof that γ-irradiation invariably induces senescence in proliferating MCF10A cells expressing either a vector control or p95HER2. Notably, the senescent growth arrest is accompanied by the production of a pro-tumorigenic secretome only when MCF10A cells express the oncogene (see Fig 9). To our view, if confirmed in vivo, this last result could imply particularly relevant clinical aspects. Radiotherapy and chemotherapy are commonly applied in breast cancer cases, sometimes prior to surgery [234, 235]. Both kinds of treatment are expected and actually known to induce senescence in a certain percentage of cells within the epithelial compartment of the tumor [217]. According to our results, proliferating cancer cells presenting over-activation of specific signaling pathways might be prone to develop a pro-tumorigenic SASP. Work currently ongoing in the lab is trying to confirm this hypothesis. If this proves to be the case, the administration of senescence-inducing cancer therapies would potentially generate a very undesirable situation. That is the co-existence,

during a variable time-lapse, of tumor cells not responding to (or not reached by) the treatment in the proximity of senescent cell actively producing a pro-tumorigenic SASP. Under these conditions, the non-senescent cells within the tumor might experience an acceleration in their malignant progression due to the effects of the senescence secretome. As a proof of principle, in this work we generated orthotopic xenograft-tumors formed by a mixture of MCF7 and reporter cells. Activating the expression of p95HER2, we induced senescence in the MCF7 compartment of the already formed tumors. After additional 3 weeks we surgically removed the primary tumors within which senescent and non-senescent cells had co-existed. The results clearly show increased metastatic spread and growth of reporter cells coming from partly senescent tumors (see Fig 16). Partly supporting our view, work presented in J.G. Jackson et al. shows that doxorubicin-induced senescence (compared to apoptosis) in transgenic mammary tumors correlates with worse clinical response. The study suggests that the resulting SASP would increase proliferation and survival of non-senescent cells within tumor. This would in turn impair the response to the drug and increase the rate of tumor relapse [236]. In summary, we show that constitutive HER2 signaling in senescent breast cancer cells activates and directly controls the production of a pro-tumorigenic SASP. Indeed, pharmacological inhibition of the receptor severely dampens the secretory phenotype of p95HER2-expressing senescent cells (see Fig. 8 and 9). Both the PI3K-AKT-mTOR pathway (see Fig. 11) and NFkB (see Fig. 10) activity are implicated in the generation of the HER2-driven senescence secretome. Senescent breast cancer cells expressing constitutively active HER2, likely through their secretome, exert a cell-non-autonomous prometastiatic effect. Given that HER2 over-activation occurs in a subset of breast cancers [54, 61, 60, 64, 70], the described effects could contribute to the progression of some breast cancers after neo-adjuvant DNA-damaging treatments. We propose that over-activation of certain signaling pathways highly increases the chances to develop a pro-tumorigenic SASP when cells within a fully blown tumor are induced to senescence. This implies that, despite initial clinical response, therapy-induced senescence might favor relapse and metastasis cell-non-autonomously after longer periods of time. This is probably the case in breast tumors, but the validity of this concept for other neoplastic tissues cannot be excluded. To add on this aspect, some retrospective study could eventually reveal interesting previously unpredicted correlations. These findings also suggest that, whenever possible, appropriate inhibitors able to dampen the SASP should be administered

together with senescence-inducing cancer treatments. Senescent cancer cells-targeted therapy in the period after conventional therapy could also represent an appealing novel opportunity [237]. Such interventions would restrain the detrimental effects of therapy-induced senescence and hopefully improve the long-term clinical outcome of cancer patients.

CONCLUSIONS

Chapter 5

Conclusions

1. **p95HER2 is an a constitutively active oncogenic variant of HER2**
   p95HER2 is a truncated version of HER2, which forms dimers covalently stabilized by intermolecular disulphide bonds. This results in the constitutive activation of the carboxy-terminal HER2 fragment, which acts as an oncogene. Upon p95HER2 expression, MEFs cells become able to generate xenografts, which are dependent on expression and activity of the truncated receptor.

2. **Breast cancer cells expressing p95HER2 undergo OIS**
   While increasing the proliferation of MCF10A cells, sustained expression of p95HER2 induces the proliferative arrest of MCF7, T47D and MDA-MB-453 cells. The arrest is accompanied by increased endogenous β-galactosidase activity at pH6, typically associated with premature senescence, in all cell lines. Further characterization of arrested MCF7 confirms different hallmarks of Oncogene Induced Senescence (OIS).

3. **p95HER2-induced senescent cells produce a proT-SASP**
   MCF7 cells undergoing OIS in response to p95HER2 expression secrete a plethora of factors, many of which possess widely reported protumorigenic functions. A subset of such secreted components (around 15%) results to be transcriptionally up-regulated and include MMP1, ANGPTL4, IL6, IL8 and IL11.

4. **p95HER2-activity is required to sustain the proT-SASP production**
   Inhibition of its kinase activity does not revert p95HER2-induced senescence but impairs the secretion of all factors analyzed. Thus, sustained p95HER2 signalling is required by cells undergoing OIS to produce at least part of the their proT-SASP. At the same time the oncogene activity is dispensable for the maintenance of the senescent state.

5. **NFkB activity mediates the generation of the p95HER2-induced SASP**
   Secretion of IL6 and IL8 in p95HER2-induced senescent cells is severely dampened by the constitutive Knock-Down of the NFkB subunit p65, which in turn does not alter the cell entry into senescence.

6. **PI3K and mTOR participate in the p95HER2-induced SASP production**
   Inhibition AKT and mTOR kinase activities result in reduced secretion of all factors analyzed.

7. **p95HER2 activates the proT-SASP in already senescent cells**
   MCF7 cells induced to senescence by irradiation do not secrete any component of the p95HER2-associated proT-SASP components. Nonetheless, if induced to express the HER2 fragment these senescent irradiated cells start producing the proT-SASP.

8. **The p95HER2-driven secretory response is specific of senescent cells**
   p95HER2 activity in proliferating MCF10A poorly increases their secretion while, in contrast, it induces the proT-SASP in the same cells when senescent in response to irradiation. This also implies that the SASP-inducing effect of p95HER2 is independent from its senescence-promoting activity.

9. **The p95HER2 drives senescence and proT-SASP in vivo**
   Activation of p95HER2 expression in already formed xenograft tumors induces senescence and its associated secretome also in vivo.

10. **p95HER2 senescent cells exert cell-non-autonomous prometastatic effect on both circulating and neighboring tumor cells**

    The metastatic growth of reporter cells injected intracardiacally is increased in animals carrying subcutaneous tumors formed by senescent p95HER2-expressing MCF7 cells.

    In addition, metastatic spread and growth of reporter cells is augmented when they come from mixed primary tumors in which a compartment of MCF7 cells is induced to senescence through p95HER2 expression.

MATERIALS and METHODS

Chapter 6

Materials and Methods

Cloning

All plasmid constructs of HER2 were derived from a cDNA clone identical to the published sequence gi:183986. The different cDNA constructs were made using standard PCR, sequencing, and cloning techniques.

Antibodies

Antibodies were from Dako (anti-Ki67), BD Biosciences (Rb), Cell Signaling (anti-p-HER2 (Y1221/1222), anti-p-p53 (Ser15), anti-p42/44 MAPK, Akt, p-p42/44 MAPK and p-Akt (Ser473), anti-mTOR and anti-p65 (NFkB)), Santa Cruz Biotechnology (anti-LAMP2, anti-53BP1 and anti-p53), NeoMarkers (anti-p21), Trevigen (anti-Actin), BioGenex (anti-HER2 [CB11]), Amersham (anti-rabbit immunoglobulin G [IgG] and anti-mouse IgG, both horseradish peroxidase linked), Invitrogen (anti-mouse-Alexa 488, anti-mouse-PE, anti-goat-Alexa 568).

Compounds

Lapatinib was kindly provided by GlaxoSmithKline, Research Triangle Park, NJ. Doxocyclin and doxorubicin were from Sigma-Aldrich. PD0332991 was from Selleckchem.

Kits

ELISA kits were used for determination of the corresponding factors in conditioned media or serum according to the manufacturer's indications. MMP1 and ANGPTL4 kits were from RayBiotech, the IL11 kit from R&D, the IL6 and IL8 kits from eBiosciences.

WST-1 Cell Proliferation Reagent was from Roche and was used to determine dehydrogenase activity

Cell culture

MCF7, T47D and MEFs Tet-Off cells (BD Biosciences) as well as normal MCF7 TeT-On (see below) , were maintained at 37°C and 5% CO2 in Dulbecco's minimal essential medium/F-12 (1:1) (Gibco) containing 10% fetal bovine serum (Gibco), 4 mM L-glutamine (PAA Laboratories), 0.2 mg/ml G418 (Gibco), and 1g/ml doxycycline (Sigma).

Tet-Off cells were transfected with FL-HER2 and p95HER2 expression plasmids by using FuGENE6 (Roche). Single stable clones with pUHD10-3h-based plasmid integrated were selected with 0.1 mg/ml hygromycin B (Invitrogen). Expression from pUHD10-3, encoding the cDNAs of HER2 and p95HER2, was induced by removing doxycyclin. First the cells were detached with 0.5% trypsin-EDTA (GIBCO) and washed three times by centrifugation, and the medium was changed 10-12 h after seeding in culture dishes. Homogeneity of the individual clones was checked by immunofluorescence and analyzed by confocal microscopy with an antibody against the cytoplasmic domain of HER2.

MCF7 Knock-Down for p65 (NFkB) were kindly provided by Dr. A. Cerrato.

MCF7_Tet-On_p95HER2 and vector control cells were obtained by lentiviral transduction of MCF7_p65-KD with the pInducer vector (kindly provided by Dr. A. Barriocanal) either empty or containing the cDNA coding p95HER2 .

MDA-MB-453 and MCF10A expressing p95HER2 were obtained by lentiviral transduction with the pLex vector (Thermofisher). MDA-MB-453 were maintained in L15 + Glutamax (Gibco) containing 10% FBS, 0.75 μg/ml Puromycin (Sigma. Vector control and p95HER2-expressing MCF10A were maintained in DMEM/F12, 10% FBS, 4mM L-Glutamine, 100uL1mg/mL Hidrocortison, 250uL1mg/mL Insulin, 100uL100mg/mL EGF and 0.75 μg/ml Puromycin. MDA-MB-231 / Luc were obtained by retroviral transduction as previously described [218].

Western blot and confocal microscopy

Extracts for immunoblots were prepared in modified radioimmunoprecipitation assay (RIPA) buffer (20 mM NaH2PO4/NaOH, pH 7.4, 150 mM NaCl, 1% Triton X-100, 5 mM EDTA, 100 mM phenylmethylsulfonyl fluoride, 25 mM NaF, 16 _g/ml aprotinin, 10 _g/ml leupeptin, and 1.3 mM Na3VO4), and protein concentrations were

determined with DC protein assay reagents (Bio-Rad). Samples were mixed with loading buffer (final concentrations: 62 mM Tris, pH 6.8, 12% glycerol, 2.5% sodium dodecyl sulfate [SDS]) with or without 5% beta-mercaptoethanol and incubated at 99°C for 5 min before loading and fractionation of 30 µg of protein by SDS-polyacrylamide gel electrophoresis

(PAGE). When indicated, specific signals in Western blots were quantified with the software ImageJ 1.38 (NIH).

Cells for immunofluorescence microscopy were seeded on glass coverslips, washed with phosphate-buffered saline, fixed with 4% formaldehyde for 20 min, and permeabilized with 0.2% Triton X-100 for 10 min. Phosphate-buffered saline with 1% Bovine Serum Albumin (BSA) was used for blocking and incubation with the different antibodies.

Proliferation assay

Proliferation was analyzed by cell counting. After trypsinization, viable cells determined by trypan blue dye exclusion, were counted on a Neubauer-chamber.

WST1 assay

The WST1 reagent was from Roche. $5x10^3$ cells were seeded in 96-well plates and the assay was carried out following the manufacturer indications

Metabolic labelling

Approximately $3x10^6$ cells were metabolically labelled with 500 μCi/ml [^{35}S]Translabel for 45 min in cysteine and methionine-free medium and lysed. Cell lysates were normalized by the number of cells and analyzed on SDS-polyacrylamide gels and fluorography.

Determination of cell volume

Cells were trypsinized, resuspended in complete medium and cell diameter was determined by direct measuring in a Neubauer chamber. Cell volume was approximated to the one of a sphere as 4/3 x (pi x cell radius^3) and five representative fields with 10-15 cells were analyzed.

Senescence-associated beta-galactosidase activity (SA-ß-gal)

Both cells and tissue slides were analyzed using senescence ß-galactosidase staining kit (Cell Signaling Technology) following the manufacturer indications. Cells were seeded as described above for confocal microscopy.

Cell irradiation

Cells were trypsinized, resuspended in complete medium and transferred to a fifteen-millilitre falcon tube. The tubes were immersed in water and kept vertical into a block of methacrylate at the moment of irradiation to improve precision and homogeneity. Irradiation was performed at the Radiotherapy Service of the Vall d'Hebron University Hospital (Barcelona) with a cobalt unit (Theraton 780-C, NCA) and a single total dose of 10 Gy was applied at the rate of 80 Gy/min.

ELISAs

The conditioned media were then collected, spun down at 200g for 5 min and transferred into clean tubes. Mice sera were obtained by complete exsanguinations and subsequent centrifugation using heparinized material. Concentration of all factors was determined according to the manufacturer instructions of each kit, normalized to cell number and expressed as pico-grams/mL per 25000 cells. All the experiments were performed at least three times and the results are represented as the means ± S.D.

Immunohistochemistry

Tumor xenografts were removed, fixed overnight with 4% formol and then paraffin-embedded. Sequential 5 μm thick slices where then obtained, hematoxylin-eosin stained and immunostained for Ki67, p21 (IHC) and g -H2AX (IF).

Xenografts

Mice were maintained and treated in accordance with institutional guidelines of Vall d'Hebron University Hospital Care and Use Committee. According to the experiment, p95HER2_MEFs alone, p95HER2_MCF7 alone or p95HER2_MCF7 mixed 1:1 with FLUC_MDA-MB-231 cells were injected. The injection was performed into the right flanks of 6- to 8-week-old female BALB/c athymic mice purchased from Charles Rivers Laboratories. The expression of p95HERs was repressed by adding doxycycline to the drinking water until tumors were ~150 mm3. Then mice were randomized and treated with or without doxycycline (50 mg/kg/day). Tumor

xenografts were measured with callipers every 3 days, and tumor volume was determined using the formula: (length × width2) × (pi/6). At the end of the experiment, the animals were anesthetized with a 1.5% isofluorane-air mixture and were killed by cervical dislocation. Results are presented as mean ± SD of tumor volume.

Metastatic colonization was monitored by in vivo bioluminescence imaging using the IVIS-200 imaging system from Xenogen as previously described (211).

Transcriptomic analysis

Expression analysis in MCF7 cells was performed using Affimetrix gene-chips HG U133 2.0, as previously described in (24).

Proteomic analysis

Cells expressing or not p95HER2 during five days were washed five times with serum-free medium and incubated for additional 48 hours in the absence of serum. The conditioned media were then collected, spun down at 200g for 5 minutes and transferred into clean tubes, filtered through a Nalgene 0.2 μm pore vacuum filter (Fisher #09-741-07) and concentrated using a 10 000 MWCO Millipore Amicon Ultra (Millipore #UFC901024) spinning down 15 mL at a time at 800g for 30 min until the final concentration was 1 mg/mL (~200- to 300-fold concentration). Protein concentration was determined with a Bio-Rad protein assay (Bio-Rad, #500-0006). Subsequent sample preparation and proteomic analysis was performed as previously described in (29).

Statistical analysis

Data are presented as averages ± SD and were analyzed by Student's t test when comparing two groups or ANOVA when comparing more than two groups. Results were considered to be statistically significant at $P < 0.05$. All statistical analyzes were performed using the SPSS 12.0 statistical software (SPSS, Inc.).

REFERENCES

References

1. Lacenere CJ, Sternberg PW. (2000). Regulation of EGF receptor signalling in the fruitfly D. melanogaster and the nematode C.elegans. Breast Dis. 11: 19–30.

2. Moghal N, Sternberg PW. (2003). The epidermal growth factor system in Caenorhabditis elegans. Exp Cell Res 284:150–159.

3. Yarden Y and Sliwkowski MX. (2001) Untangling the ErbB signalling network. Nature Reviews Molecular Cell Biology. **2**:127-137.

4. Gschwind A, Fischer OM, Ullrich A. (2004) The discovery of receptor tyrosine kinases: targets for cancer therapy. Nature Reviews. **4**(361-370).

5. Burden S, Yarden Y. (1997) Neuregulins and their receptors: a versatile signaling module in organogenesis and oncogenesis. Neuron. **18**(847-855).

6. Fowler KJ, Walker F, Alexander W, Hibbs ML, Nice EC, Bohmer RM, Mann GB, Thumwood C, Maglitto R, Danks JA, et al. (1995) Proc Natl Acad Sci U S A. 92(5):1465-9.

7. Xie W, Paterson AJ, Chin E, Nabell LM, Kudlow JE. (1997) Targeted expression of a dominant negative epidermal growth factor receptor in the mammary gland of transgenic mice inhibits pubertal mammary duct development. Mol Endocrinol. 1997 Nov;11(12):1766-81.

8. Jones FE, Stern DF. (1999) Expression of dominant-negative ErbB2 in the mammary gland of transgenic mice reveals a role in lobuloalveolar development and lactation. Oncogene 18(23):3481-90

9. Crone SA, Zhao YY, Fan L, Gu Y, Minamisawa S, Liu Y, Peterson KL, Chen J, Kahn R, Condorelli G, Ross J Jr, Chien KR, Lee KF. (2002) Nat Med 8(5):459-65.

9b. Andrechek ER, Hardy WR, Girgis-Gabardo AA, Perry RL, Butler R, Graham FL, Kahn RC, Rudnicki MA, Muller WJ. (2002) ErbB2 is required for muscle spindle and myoblast cell survival. Molecular and Cellular Biology. 22(13): p. 4714-4722.

10. Shih C, Padhy LC, Murray M, Weinberg RA. (1981). Transforming genes of carcinomas and neuroblastomas introduced into mouse fibroblasts. Nature 290: 261–264.

11. Schechter AL, Hung MC, Vaidyanathan L, Weinberg RA, Yang-Feng TL, Francke U et al. (1985). The neu gene: an erbB-homologous gene distinct from and unlinked to the gene encoding the EGF receptor. Science 229: 976–978.

12. Coussens L, Yang-Feng TL, Liao YC, Chen E, Gray A, McGrath J, Seeburg PH, Libermann TA, Schlessinger J, Francke U, et al. (1985) Tyrosine kinase receptor with extensive homology to EGF receptor shares chromosomal location with neu oncogene. Science. **230**(4730): p. 1132-1139.

13. Akiyama T, Sudo C, Ogawara H, Toyoshima K, Yamamoto T. (1986). The product of the human c-erbB-2 gene: a 185-kilodalton glycoprotein with tyrosine kinase activity. Science 232: 1644–1646.

14. Di Fiore PP, Pierce JH, Kraus MH, Segatto O, King CR, Aaronson SA. (1987). erbB-2 is a potent oncogene when overexpressed in NIH/3T3 cells. Science 237: 178–182.

15. Hudziak RM, Schlessinger J, Ullrich A. (1987). Increased expression of the putative growth factor receptor p185HER2 causes transformation and tumorigenesis of NIH 3T3 cells. Proc Natl Acad Sci USA 84: 7159–7163.

16. Chazin VR, Kaleko M, Miller AD, Slamon DJ. (1992). Transformation mediated by the human HER-2 gene independent of the epidermal growth factor receptor. Oncogene **7**: 1859–1866

17. Benz CC, Scott GK, Sarup JC, Johnson RM, Tripathy D, Coronado E et al. (1992). Estrogen-dependent, tamoxifen resistant tumorigenic growth of MCF-7 cells transfected withHER2/neu. Breast Cancer Res Treat 24: 85–95.

18. Muthuswamy SK, Li D, Lelievre S, Bissell MJ, Brugge JS.(2001). ErbB2, but not ErbB1, reinitiates proliferation and induces luminal repopulation in epithelial acini. Nat Cell Biol **3**: 785–792.

19. Woods Ignatoski KM, Grewal NK, Markwart S, Livant DL, Ethier SP. (2003). p38MAPK induces cell surface alpha4 integrin downregulation to facilitate erbB-2-mediated invasion. Neoplasia **5**: 128–134.

20. Finkle D, Quan ZR, Asghari V, Kloss J, Ghaboosi N, Mai E et al. (2004). HER2-targeted therapy reduces incidence and progression of midlife mammary tumors in female murine mammary tumor virus huHER2-transgenic mice. Clin Cancer Res 10: 2499–2511.

21. Siegel PM, Ryan ED, Cardiff RD, Muller WJ. (1999) Elevated expression of activated forms of Neu/ErbB-2 and ErbB-3 are involved in the induction of mammary tumors in transgenic mice: implications for human breast cancer. The EMBO Journal Vol.18 No.8 pp.2149–2164.

22. Siegel PM, Dankort DL, Hardy WR, Muller WJ. (1994) Novel activating mutations in the neu proto-oncogene involved in induction of mammary tumors. Mol Cell Biol. 14:7068–77.

23. Siegel PM, Muller WJ. (1996) Mutations affecting conserved cysteine residues within the extracellular domain of Neu promote receptor dimerization and activation. Proc Natl Acad Sci U S A;93:8878–83.

24. Pedersen K, Angelini PD, Laos S, Bach-Faig A, Cunningham MP, Ferrer-Ramon C, et al. (2009) A naturally occurring HER2 carboxy-terminal fragment promotes mammary tumor growth and metastasis. Mol Cell Biol 29:3319–31.

25. Burgess AW, Cho H-S, Elgenblot C, Ferguson KM, Garrett TPJ, Leahy DJ, Lemmon MA, Siwkowski MX, Ward CW, Yokoyama S. (2003) An open-and -shut case? Recent insights into the activation of EGF/ ErbB receptors Mol Cell. 12, 541–552.

26. Alvarado D, Klein DE**,** Lemmon MA (2009) ErbB2 resembles an autoinhibited invertebrate epidermal growth factor receptor. Nature Letter 461, 287-92

27. Cho HS, Mason K, Ramyar KX, Stanley AM, Gabelli SB, Denney DW Jr, Leahy DJ Cho, H. S. et al. (2003) Structure of the extracellular region of HER2 alone and in complex with the Herceptin Fab. Nature 421, 756–760.

28. Garrett TP, McKern NM, Lou M, Elleman TC, Adams TE, Lovrecz GO, Kofler M, Jorissen RN, Nice EC, Burgess AW, Ward CW. (2003) The crystal structure of a truncated ErbB2 ectodomain reveals an active conformation, poised to interact with other ErbB receptors. Mol. Cell 11,495–505.

29. Wehrman TS, Raab WJ, Casipit CL, Doyonnas R, Pomerantz JH, Blau HM. (2006) A system for quantifying dynamic protein interactions defines a role for Herceptin in modulating ErbB2 interactions. Proc. Natl Acad. Sci.USA 103,19063–19068

30. Miura GI, Buglino J, Alvarado D, Lemmon MA, Resh MD, Treisman JE. (2006) Palmitoylation of the EGFR ligand Spitz by Rasp increases Spitz activity by restricting its diffusion. Dev. Cell 10, 167–176.

31. Moasser MM. (2007) The oncogene HER2: its signaling and transforming functions and its role in human cancer pathogenesis. Oncogene 26(45):6469-87.

32. Ravichandran KS. (2001) Signaling via Shc family adapter proteins Oncogene 20(44):6322-30.

33. Shilo BZ. (2005) Regulating the dynamics of EGF receptor signaling in space and time. Development 132, 4017–4027.

34. Meyer-Hoffert U, Wingertszahn J, Wiedow O. (2004) Human Leukocyte Elastase Induces Keratinocytee Proliferation by Epidermal Growth factor Receptor Activation. Journal of investigative dermathology 123: 338-45.

35. Hynes NE, Lane HA. (2005) erbb receptors and cancer: the complexity of targeted inhibitors. Nature Reviews 5: 341-54

36. Slamon DJ, Godolphin W, Jones LA, Holt JA, Wong SG, Keith DE, Levin WJ, Stuart SG, Udove J, Ullrich A, et al. (1989) Studies of the HER-2/neu proto-oncogene in human breast and ovarian cancer. Science. 244(4905): p. 707-712.

37. Ross JS, Fletcher JA. (1998) The HER-2/neu oncogene in breast cancer: prognosic factor, predictive factor, and target for therapy. Stem Cells. 16: p. 413-428.

37b. Ross JS, Fletcher JA, Linette GP, Stec J, Clark E, Ayers M et al. (2003) The Her-2/neu gene and protein in breast cancer 2003: biomarker and target of therapy. Oncologist. **8**:307–325.

38. Gabos Z, Sinha R, Hanson J, Chauhan N, Hugh J, Mackey JR et al. (2006). Prognostic significance of human epidermal growth factor receptor positivity for the development of brain metastasis after newly diagnosed breast cancer. J Clin Oncol 24: 5658–5663.

39. Venter DJ, Tuzi NL, Kumar S, Gullick WJ. (1987). Overexpression of the c-erbB-2 oncoprotein in human breast carcinomas: immunohistological assessment correlates with gene amplification. Lancet **2**: 69–72.

40. Kallioniemi OP, Kallioniemi A, Kurisu W, Thor A, Chen LC, SmithHS et al. (1992). ERBB2 amplification in breast cancer analyzed by fluorescence in situ hybridization. Proc Natl Acad Sci USA 89: 5321–5325.

41. Lohrisch C, Piccart M. (2001). An overview of HER2. Semin Oncol 28: 3–11.

42. Tsuda H, Akiyama F, Terasaki H, Hasegawa T, Kurosumi M, Shimadzu M et al. (2001). Detection of HER-2/neu (c-erbB-2) DNA amplification in primary breast carcinoma. Interobserver reproducibility and correlation with immunohistochemical HER-2 overexpression. Cancer 92: 2965– 2974.

43. Latta EK, Tjan S, Parkes RK, O'Malley FP. (2002). The role of HER2/neu overexpression/amplification in the progression of ductal carcinoma in situ to invasive carcinoma of the breast. Mod Pathol 15: 1318–1325.

44. Carlsson J, Nordgren H, Sjostrom J, Wester K, Villman K, Bengtsson NO et al. (2004). HER2 expression in breast cancer primary tumours and corresponding metastases. Original data and literature review. Br J Cancer 90:2344–2348.

45. Park K, Han S, Kim HJ, Kim J, Shin E. (2006). HER2 status in pure ductal carcinoma in situ and in the intraductal and invasive components of invasive ductal carcinoma determined by fluorescence in situ hybridization and immunohistochemistry. Histopathology 48: 702–707.

46. Perou CM, Sorlie T, Eisen MB, van de RM, Jeffrey SS, Rees CA et al. (2000). Molecular portraits of human breast tumours. Nature 406: 747– 752.

47. Weigelt B, Hu Z, He X, Livasy C, Carey LA, Ewend MG et al. (2005). Molecular portraits and 70-gene prognosis signature are preserved throughout the metastatic process of breast cancer. Cancer Res 65: 9155–9158.

48. Mimura K, Kono K, Hanawa M, Mitsui F, Sugai H, Miyagawa N et al. (2005). Frequencies of HER-2/neu expression and gene amplification in patients withoesoph ageal squamous cell carcinoma. Br J Cancer 92:1253–1260.

49. Morrison C, Zanagnolo V, Ramirez N, Cohn DE, Kelbick N, Copeland L et al. (2006). HER-2 is an independent prognostic factor in endometrial cancer: association with outcome in a large cohort of surgically staged patients. J Clin Onc 24: 2376–2385.

50. Yano T, Doi T, Ohtsu A, Boku N, Hashizume K, Nakanishi M et al. (2006). Comparison of HER2 gene amplification assessed by fluorescence in situ hybridization and HER2 protein expression assessed by immunohistochemistry in gastric cancer. Oncol Rep 15: 65–71.

51. Hirsch FR, Varella-Garcia M, Franklin WA, Veve R, Chen L, Helfrich B et al. (2002). Evaluation of HER-2/neu gene amplification and protein expression in non-small cell lung carcinomas. Br J Cancer 86: 1449–1456.

52. Khan AJ, King BL, SmithBD, SmithGL, DiGiovanna MP, Carter D et al. (2002). Characterization of the HER-2/neu oncogene by immunohistochemical and fluorescence in situ hybridization analysis in oral and oropharyngeal squamous cell carcinoma. Clin Cancer Res **8**: 540–548.

53. Latif Z, Watters AD, Dunn I, Grigor KM, Underwood MA, Bartlett JM. (2003). HER2/neu overexpression in the development of muscle- invasive transitional cell carcinoma of the bladder. Br J Cancer 89: 1305–1309.

54. Bose R, Kavuri SM, Searleman AC, Shen W, Shen D, Koboldt DC, Monsey J, Goel N, Aronson AB, Li S, Ma CX, Ding L, Mardis ER, Ellis MJ. (2012) Activating HER2 Mutations in HER2 Gene Amplification Negative Breast Cancer. Cancer Discovery 3:224-237.

55. Shigematsu H, Takahashi T, Nomura M, Majmudar K, Suzuki M, Lee H, et al. (2005) Somatic mutations of the HER2 kinase domain in lung adenocarcinomas. Cancer Res 65:1642–6.

56. Bargmann CI, Hung MC, Weinberg RA. (1986). Multiple independent activations of the neu oncogene by a point mutation altering the transmembrane domain of p185. Cell. 45: 649–657.

57. Weiner DB, Liu J, Cohen JA, Williams WV, Greene MI. (1989b). A point mutation in the neu oncogene mimics ligand induction of receptor aggregation. Nature 339:230–231.

58. Muller WJ, Sinn E, Pattengale PK, Wallace R, Leder P. (1988). Single-step induction of mammary adenocarcinoma in transgenic mice bearing the activated c-neu oncogene. Cell 54: 105–115.

59. Bouchard L, Lamarre L, Tremblay PJ, Jolicoeur P. (1989). Stochastic appearance of mammary tumors in transgenic mice carrying the MMTV/c-neu oncogene. Cell 57: 931–936.

60. Serra V, Vivancos A, Puente XS, Felip E, Silberschmidt D, Caratù G, Parra JL, De Mattos-Arruda L, Grueso J, Hernández-Losa J, Arribas J, Prudkin L, Nuciforo P, Scaltriti M, Seoane J, Baselga J. (2013) Clinical response to a lapatinib-based therapy of a Li-Fraumeni Syndrome patient with a novel HER2-V659E mutation. Cancer Discovery 3(11):1238-44. doi: 10.1158/2159-8290.

61. Stephens P, Hunter C, Bignell G, Edkins S, Davies H, Teague J, et al. (2004) Lung cancer: intragenic ERBB2 kinase mutations in tumours . Nature 431:525–6.

62. Mazières J, Peters S, Lepage B, Cortot AB, Barlesi F, Beau-Faller M, Besse B, Blons H, Mansuet-Lupo A, Urban T, Moro-Sibilot D, Dansin E, Chouaid C, Wislez M, Diebold J, Felip E, Rouquette I, Milia JD, Gautschi O. (2013) Lung Cancer That Harbor a HER2 Mutation: Epidemiologic Characteristics and Therapeutic Perspectives. J Clin Oncol 31(16):1997-2003.

63. Siegel PM, Ryan ED, Cardiff RD, Muller WJ. (1999) Elevated expression of activated forms of Neu/ErbB-2 and ErbB-3 are involved in the induction of mammary tumors in transgenic mice: implications for human breast cancer. EMBO J 18: 2149–2164.

64. Castiglioni F, Tagliabue E, Campiglio M, Pupa SM, Balsari A, Menard S. (2006) Role of exon-16-deleted HER2 in breast carcinomas. Endocr Relat Cancer 13:221–32.

65. Alajati A, N Sausgruber, Aceto N, Duss S, Sarret S, Voshol H, Bonenfant D, Bentires-Alj M. (2013) Mammary Tumor Formation and Metastasis Evoked by a HER2 Splice Variant Cancer Res. 73(17): 5320-27.

66. Ursini-Siegel J, Schade B, Cardiff RD, Muller WJ. (2007) Insights from transgenic mouse models of ERBB2-induced breast cancer. Nat Rev Cancer 7:389–97.

67. Mitra D, Brumlik MJ, Okamgba SU, Zhu Y, Duplessis TT, Parvani JG, et al. (2009). An oncogenic isoform of HER2 associated with locally disseminated breast cancer and trastuzumab resistance. Mol Cancer Ther 8:2152–62.

68. Anido J, Scaltriti M, Bech-Serra JJ, Josefat BS, Rojo Todo F, Baselga J, Arribas J. (2006). Biosynthesis of tumorigenic HER2 C-terminal fragments by alternative initiation of translation. EMBO J. 25:3234–3244.

69. Garcia-Castillo J, Pedersen K, Angelini PD, Bech-Serra JJ, Colome N, Cunningham MP, et al. (2009) HER2 carboxy-terminal fragments regulate cell migration and cortactin phosphorylation. J Biol Chem 284:25302–13.

70. Parra-Palau JL, Pedersen K, Peg V, Scaltriti M, Angelini PD, Escorihuela M, et al. (2010) A major role of p95/611-CTF, a carboxy-terminal fragment of HER2, in the downmodulation of the ER in HER2-positive breast cancers. Cancer Res 70:8537–46.

71. Molina MA, Saez R, Ramsey EE, Garcia-Barchino MJ, Rojo F, Evans AJ, Albanell J, Keenan EJ, Lluch A, Garcia-Conde J, Baselga J, Clinton GM. (2002) NH(2)-terminal truncated HER-2 protein but not full-length receptor is associated with nodal metastasis in human breast cancer. Clin. Cancer Res. 8:347–353.

72. Saez, R, Molina MA, Ramsey EE, Rojo F, Keenan EJ, Albanell J, Lluch A, Garcia-Conde J, Baselga J, Clinton GM. (2006) p95HER-2 predicts worse outcome in patients with HER-2-positive breast cancer. Clin. Cancer Res. 12:424–431.

73. Lin YZ, Clinton GM. (1991) A soluble protein related to the HER-2 proto-oncogene product is released from human breast carcinoma cells. Oncogene 6:639–643.

74. Chandarlapaty S, Scaltriti M, Angelini PD, Ye Q, Guzman M, Hudis CA, Norton L, Solit DB, Arribas J, Baselga J, Rosen N. (2010) Inhibitors of HSP90 block p95-HER2 signaling in Trastuzumab-resistant tumors and suppress their growth. Oncogene 29(3):325-34.

75. Scaltriti M, Chandarlapaty S, Prudkin L, Aura C, Jimenez J, Angelini PD, et al. (2010) Clinical benefit of lapatinib-based therapy in patients with human epidermal growth factor receptor 2-positive breast tumors coexpressing the truncated p95HER2 receptor. Clin Cancer Res 16:2688–95

76. Sperinde J, Jin X, Banerjee J, Penuel E, Saha A, Diedrich G, et al. (2010) Quantitation of p95HER2 in paraffin sections by using a p95-specific antibody and correlation with outcome in a cohort of trastuzumab treated breast cancer patients. Clin Cancer Res 16:4226–35.

77. Ocana A, Vera-Badillo F, Seruga B, Templeton A, Pandiella A, Amir E. (2013) HER3 overexpression and survival in solid tumors: a meta-analysis. J Natl Cancer Inst 105(4):266-73.

78. Jaiswal BS, Kljavin NM, Stawiski EW, Chan E, Parikh C, Durinck S, Chaudhuri S, Pujara K, Guillory J, Edgar KA, Janakiraman V, Scholz RP, Bowman KK, Lorenzo M, Li H, Wu J, Yuan W, Peters BA, Kan Z, Stinson J, Mak M, Modrusan Z, Eigenbrot C, Firestein R, Stern HM, Rajalingam K, Schaefer G, Merchant MA, Sliwkowski MX, de Sauvage FJ, Seshagiri S. (2013) Oncogenic ERBB3 mutations in human cancers. Cancer Cell. 23(5): 603-17

79. Umelo IA, Noeparast A, Chen G, Renard M, Geers C, Vansteenkiste J, Teugels E, de Grève J. (2013) A novel HER3/ERBB3 driver mutation in Non-Small Cell Lung Cancer. Annals of Oncology 24 (Supplement 1): i7–i17.

80. Kew TY, Bell JA, Pinder SE, Denley H, Srinivasan R, Gullick WJ, Nicholson RI, Blamey RW, Ellis IO. (2000). c-ErbB4 protein expression in human breast cancer. Br. J. Cancer 82, 1163–1170

81. Gilbertson RJ, Perry RH, Kelly PJ, Pearson AD, Lunec J. (1997) Prognostic significance of HER2 and HER4 coexpression in childhood medulloblastoma. Cancer Res. 57, 3272–3280.

82. Soung YH, Lee JW, Kim SY, Wang YP, Jo KH, Moon SW, Park WS, Nam SW, Lee JY, Yoo NJ, Lee SH. (2006) Somatic mutations of the ERBB4 kinase domain in human cancer. Int J Cancer 118(6): 1426-9.

83. Ni CY, Murphy MP, Golde TE, Carpenter G. (2001) gamma -Secretase cleavage and nuclear localization of ErbB-4 receptor tyrosine kinase. Science 294: 2179–2181.

84. Lee HJ, Jung KM, Huang YZ, Bennett LB, Lee JS, Mei L, Kim TW. (2002) Presenilin dependent gamma-secretase-like intramembrane cleavage of ErbB4. J Biol Chem 277:6318–6323

85. Williams C, Allison J, Vidal G, Burow M, Beckman B, et al. (2004) The ERBB4/HER4 receptor tyrosine kinase regulates gene expression by functioning as a STAT5A nuclear chaperone. J Cell Biol 167: 469–478.

86. Zhu Y, Sullivan LL, Nair SS, Williams CC, Pandey AK, Marrero L, Vadlamudi RK, Jones FE. (2006) Coregulation of Estrogen Receptor by ERBB4/HER4 Establishes a Growth-Promoting Autocrine Signal in Breast Tumor Cells. Cancer Res 66: 7991–7998.

87. Hollmen M, Liu P, Kurppa K, Wildiers H, Reinvall I, Vandorpe T, Smeets A, Deraedt A, Vahlberg T, Joensuu H, Leahy DJ, Schoffski P, Elenius K. (2012) Proteolytic Processing of ErbB4 in Breast Cancer PLoS ONE 7(6): e39413

88. Hayflick L, Moorhead PS. (1961) The serial cultivation of human diploid cell strains. Exp. Cell Res. 25:585–621

89. Hayflick L. (1965) The limited in vitro lifetime of human diploid cell strains. Exp. Cell Res. 37:614–36

90. Beausejour CM, Krtolica A, Galimi F, Narita M, Lowe SW, et al. (2003) Reversal of human cellular senescence: roles of the p53 and p16 pathways. EMBO J. 22:4212–22

91. DimriGP, Lee X, Basile G, Acosta M, Scott G, et al. (1995) A novel biomarker identifies senescent human cells in culture and in aging skin in vivo. Proc. Natl. Acad. Sci. USA 92:9363–67

92. Campisi J, d'Adda di Fagagna F. (2007). Cellular senescence: when bad things happen to good cells. Nat. Rev. Mol. Cell Biol. **8**, 729–740.

93. Blagosklonny MV. (2003) Cell senescence and hypermitogenic arrest. EMBO Rep. 4:358–62

94. Serrano M, Lin AW, McCurrach ME, Beach D, Lowe SW. (1997) Oncogenic ras provokes premature cell senescence associated with accumulation of p53 and p16INK4a. Cell 88:593–602

95. Bihani T, Chicas A, Lo CP, Lin AW. (2007) Dissecting the senescence-like program in tumor cells activated by Ras signaling. J Biol Chem. 282(4):2666-75.

96. Braig M, Schmitt CA. (2006) Oncogene-induced senescence: putting the brakes on tumor development Cancer Res. 66:2881–84

97. Campisi J. (2005) Suppressing cancer: the importance of being senescent. Science 309:886–87

98. Prieur A, Peeper DS. (2008) Cellular senescence in vivo: a barrier to tumorigenesis. Curr. Opin. Cell Biol. 20:150–55

99. Trost TM, Lausch EU, Fees SA, Schmitt S, Enklaar T, et al. (2005) Premature senescence is a primary fail-safe mechanism of ERBB2- driven tumorigenesis in breast carcinoma cells. Cancer Res. 65:840–49

100. Alimonti A, Nardella C, Chen Z, Clohessy JG, Carracedo A, et al. (2010) Anovel type of cellular senescence that can be enhanced in mouse models and human tumor xenografts to suppress prostate tumorigenesis. J. Clin. Investig. 120:681–93

101. Moiseeva O, Mallette FA, Mukhopadhyay UK, Moores A, Ferbeyre G. (2006) DNA damage signaling and p53-dependent senescence after prolonged beta-interferon stimulation. Mol. Biol. Cell 17:1583–92

102. Takahashi A, Ohtani N, Yamakoshi K, Iida S, Tahara H, et al. (2006) Mitogenic signalling and the p16INK4a-Rb pathway cooperate to enforce irreversible cellular senescence. Nat. Cell Biol. 8:1291–97

103. Deng Q, Liao R, Wu BL, Sun P. (2004) High intensity ras signaling induces premature senescence by activating p38 pathway in primary human fibroblasts. J. Biol. Chem. 279:1050–59.

104. Bartkova J, Rezaei N, Liontos M, Karakaidos P, Kletsas D, et al. (2006) Oncogene-induced senescence is part of the tumorigenesis barrier imposed by DNA damage checkpoints. Nature 444:633–37.

105. Di Micco R, Fumagalli M, Cicalese A, Piccinin S, Gasparini P, Luise C, Schurra C, Garre M, Nuciforo PG, Bensimon A, Maestro R, Pelicci PG, d'Adda di Fagagna F. (2006) Oncogene-induced senescence is a DNA damage response triggered by DNA hyper-replication. Nature Letters 444(30): 638-642.

106. Mallette FA, Gaumont-Leclerc MF, Ferbeyre G. (2007) The DNA damage signaling pathway is a critical mediator of oncogene-induced senescence. Genes Dev. 21:43–48.

107. Olovnikov AM. (1971) Principle of marginotomy in template synthesis of polynucleotides. Dokl Akad Nauk SSSR 201:1496–1499.

108. Watson JD. (1972) Origin of concatemeric T7 DNA. Nat New Biol 239: 197–201.

109. D'Adda di Fagagna F, Reaper PM, Clay-Farrace L, Fiegler H, Carr P, Von Zglinicki T, Saretzki G, Carter NP, Jackson SP. (2003) A DNA damage checkpoint response in telomere-initiated senescence. Nature 426: 194–198.

110. Fumagalli M, Rossiello F, Clerici M, Barozzi S, Cittaro D, et al. (2012) Telomeric DNA damage is irreparable and causes persistent DNA-damage-response activation. Nat. Cell Biol. 14:355–65.

111. Kurz DJ, Decary S, Hong Y, Erusalimsky JD. (2000) Senescence- associated **β**-galactosidase reflects an increase in lysosomal mass during replicative ageing of human endothelial cells. J. Cell Sci. 113:3613–22

112. Denoyelle C, Abou-Rjaily G, Bezrookove V, Verhaegen M, Johnson TM, Fullen DR, Pointer JN, Gruber SB, Su LD, Nikiforov MA, et al. (2006) Anti-oncogenic role of the endoplasmic reticulum differentially activated by mutations in the MAPK pathway. Nat Cell Biol 8: 1053– 1063.

113. Gamerdinger M, Hajieva P, Kaya AM, Wolfrum U, Hartl FU, Behl C.(2009). Protein quality control during aging involves recruitment of the macroautophagy pathway by BAG3. EMBO J. 28, 889–901.

114. Young AR, Narita M, Ferreira M, Kirschner K, Sadaie M, Darot JF, Tavare S, Arakawa S, Shimizu S, Watt FM, Narita M. (2009). Autophagy mediates the mitotic senescence transition. Genes Dev. 23, 798–803.

115. Narita M, Young AR, Arakawa S, Samarajiwa SA, Nakashima T, Yoshida S, Hong S, Berry LS, Reichelt S, Ferreira M, Tavaré S, Inoki K, Shimizu S, Narita M (2011). Spatial coupling of mTOR and autophagy augments secretory phenotypes. Science 20;332(6032):966-70.

116. Debacq-Chainiaux F, Erusalimsky JD, Campisi J, Toussaint O. [2009). Protocols to detect senescence-associated **b**-galactosidase (SA-**b**gal) activity, a biomarker of senescent cells in culture and in vivo. Nat Protoc 4: 1798–1806.

117. Lee BY, Han JA, Im JS, Morrone A, Johung K, Goodwin EC, Kleijer WJ, DiMaio D, Hwang ES. (2006). Senescence-associated **b**-galactosidase is lysosomal **b**-galactosidase. Aging Cell 5: 187–195.

118. Dominic G. Hildebrand, Simon Lehle, Andreas Borst, Sebastian Haferkamp, Frank Essmann, Klaus Schulze-Osthoff (2013). α -Fucosidase as a novel convenient biomarker for cellular senescence. Cell Cycle 12(12): 1922 - 1927

119. Kulju, K. S., & Lehman, J. M. (1995). Increased p53 protein associated with aging in human diploid fibroblasts. Experimental Cell Research, 217, 336–345.

120. Serrano M, Lin AW, McCurrach ME, Beach D, Lowe SW. (1997). Oncogenic ras provokes premature cell senescence associated with accumulation of p53 and p16INK4a. Cell, 88, 593–602.

121. Narita, M., Nunez, S., Heard, E., Lin, A. W., Hearn, S. A., Spector, D. L., et al. (2003). Rb-mediated heterochromatin formation and silencing of E2F target genes during cellular senescence. Cell,113, 703–716.

121b.Narita M. et al. (2006) A novel role for high-mobility group A proteins in cellular senescence and heterochromatin formation. Cell. 126, 503–514

122. Shelton DN, Chang E, Whittier PS, Choi D, Funk WD. (1999). Microarray analysis of replicative senescence. Current Biology. 9, 939–945.

123. Serrano M, Blasco MA. (2001). Putting the stress on senescence. Current Opinion in Cell Biology, 13, 748–753.

124. Coppe, JP, Patil CK, Rodier, F, Sun Y, Munoz DP, Goldstein J, Nelson PS, Desprez PY, and Campisi J. (2008). Senescence-associated secretory phenotypes reveal cell-nonautonomous functions of oncogenic RAS and the p53 tumor suppressor. PLoS Biol. **6**, 2853–2868.

125. Kuilman T, Peeper DS. (2009). Senescence-messaging secretome: SMS-ing cellular stress. Nat. Rev. Cancer **9**, 81–94.

126. Levine AJ, Oren M. (2009) The first 30 years of p53: growing ever more complex. Nat. Rev. Cancer 9:749–58

127. Campisi J. (2013) Aging, cellular senescence, and cancer. Annu Rev Physiol. 75:685-705.

128. Uto K, Inoue D, Shimuta K, Nakajo N, Sagata N. (2004) Chk1, but not Chk2, inhibits Cdc25 phosphatases by a novel common mechanism. EMBO J. 23(16):3386-96

129. Bonner WM, Redon CE, Dickey JS, Nakamura AJ, Sedelnikova OA, Stéphanie Solier and Yves Pommier (2008) γH2AX and cancer. Nature Reviews Cancer 8, 957-967.

130. Toledo LI,Murga M, Gutierrez-Martinez P, Soria R, Fernandez-Capetillo O. (2008) ATR signaling can drive cells into senescence in the absence of DNA breaks. Genes Dev. 22:297–302.

131. Shieh SY, Ideda M, Taya Y, Prives C. (1997) DNA damage-induced phosphorylation of p53 alleviates inhibition by MDM2. *Cell* **91**, 325–334.

132. Hewitt G, Jurk D, Marques FD, Correia-Melo C, Hardy T, Gackowska A, Anderson R, Taschuk M, Mann J, Passos JF. (2012) Telomeres are favoured targets of a persistent DNA damage response in ageing and stress-induced senescence. Nat Commun. Feb 28;3:708.

133. Di Micco R, Sulli G, Dobreva M, Liontos M, Botrugno OA, Gargiulo G, dal Zuffo R, Matti V, d'Ario G, Montani E, Mercurio C, Hahn WC, Gorgoulis V, Minucci S, d'Adda di Fagagna F. (2011) Interplay between oncogene-induced DNA damage response and heterochromatin in senescence and cancer Nature Cell Biology **13**, 292-302.

134. Zhang, R. et al. (2005) Formation of macroH2A-containing senescence-associated heterochromatin foci and senescence driven by ASF1a and HIRA. Dev. Cell 8, 19–30.

135. Ye X et al. (2007) Definition of pRB- and p53-dependent and -independent steps in HIRA/ASF1a-mediated formation of senescence-associated heterochromatin foci. Mol. Cell Biol. 27, 2452–2465.

136. Herbig U, Ferreira M, Condel L, Carey D, Sedivy JM. (2006) Cellular senescence in aging primates. Science 311:1257.

137. Rodier F, Munoz DP, Teachenor R, Chu V, Le O, et al. (2011) DNA-SCARS: distinct nuclear structures that sustain damage-induced senescence growth arrest and inflammatory cytokine secretion. J. Cell Sci.124:68–81

138. Freund A, Patil PK, Campisi J. (2011) p38MAPK is a novelDNAdamage response-independent regulator of the senescence-associated secretory phenotype. EMBO J. 30:1536–48

139. Roussel MF. (1999) The INK4 family of cell cycle inhibitors in cancer Oncogene 18(38):5311-7.

140. Ogara MF, Sirkin PF, Carcagno AL, Marazita MC, Sonzogni SV, Ceruti JM, Cánepa ET. (2013) Chromatin Relaxation-Mediated Induction of p19INK4d Increases the Ability of Cells to Repair Damaged DNA PLoS ONE 8(4):e61143.

141. Carcagno AL, Giono LE, Marazita MC, Castillo DS, Pregi N, Cánepa ET. (2012) E2F1 induces p19INK4d, a protein involved in the DNA damage response, following UV irradiation. Mol Cell Biochem. 366(1-2):123-9.

142. Jacobs JJ, de Lange T. (2004). Significant role for p16INK4a in p53-independent telomere-directed senescence. Curr. Biol. 14, 2302–2308.

143. Wang Y, Schulte BA, Larue AC, Ogawa M, Zhou D. (2006). Total body irradiation selectively induces murine hematopoietic stemcell senescence. Blood 107, 358–366.

144. Zindy F, Quelle DE, Roussel MF, Sherr CJ. (1997a). Expression of the p16INK4a tumor suppressor versus other INK4 family members during mouse development and aging. Oncogene, 15, 203-211.

145a.Hara E, Smith R, Parry D, Tahara H, Stone S, Peters G. Regulation of p16CDKN2 expression and its implications for cell immortalization and senescence. (1996). Mol. Cell. Biol., 16, 859 ± 867.

145b.Fujita K, Mondal AM, Horikawa I, Nguyen GH, Kumamoto K, Sohn JJ, Bowman ED, Mathe EA, Schetter AJ, Pine SR, et al. (2009) p53 isoforms **D**133p53 and p53**b** are endogenous regulators of replicative cellular senescence. Nat Cell Biol 11: 1135–1142.

145. Chang BD, Broude EV, Fang J, Kalinichenko TV, Abdryashitov R, Poole JC, Roninson IB. (2000) p21Waf1/Cip1/Sdi1-induced growth arrest is associated with depletion of mitosis-control proteins and leads to abnormal mitosis and endoreduplication in recovering cells. Oncogene. 19:2165-2170.

146. Majumder PK, Grisanzio C, O'Connell F, Barry M, Brito JM, Xu Q, Guney I, Berger R, Herman P, Bikoff R, Fedele G, Baek WK, Wang S, Ellwood-Yen K, Wu H, Sawyers CL, Signoretti S, Hahn WC, Loda M, Sellers WR. (2008) A prostatic intraepithelial neoplasia-dependent p27 Kip1 checkpoint induces senescence and inhibits cell proliferation and cancer progression. Cancer Cell. 14(2):146-55.

147. Giovannini C, Gramantieri L, Minguzzi M, Fornari F, Chieco P, Grazi GL, Bolondi L. (2012) CDKN1C/P57 is regulated by the Notch target gene Hes1 and induces senescence in human hepatocellular carcinoma. Am J Pathol. 181(2):413-22.

148. Tsugu A, Sakai K, Dirks PB, Jung S, Weksberg R, Fei YL, Mondal S, Ivanchuk S, Ackerley C, Hamel PA, Rutka JT. (2000) Expression of p57(KIP2) potently blocks the growth of human astrocytomas and induces cell senescence. Am J Pathol. 157(3):919-32.

149. Lin, H-K et al. (2010). Skp2 targeting suppresses tumorigenesis by Arf–p53-independent cellular sensescence. Nature 464, 374–379

150. Senturk S, Mumcuoglu M, Gursoy-Yuzugullu O, Cingoz B, Akcali KC, Ozturk M. (2010). Transforming growth factor-beta induces senescence in hepatocellular carcinoma cells and inhibits tumor growth. Hepatology 52(3):966-74.

151. James DeGregori (2004). The Rb network. Journal of Cell Science 117, 3411-3413 Published by The Company of Biologists

152. DeGregori J. (2002). The genetics of the E2F family of transcription factors: shared functions and unique roles. Biochim. Biophys. Acta 1602,131-150.

153. Trimarchi JM, Lees JA. (2002). Sibling rivalry in the E2F family. Nat. Rev. Mol. Cell. Biol. 3, 11-20.

154. Stevaux O, Dyson NJ. (2002). A revised picture of the E2F transcriptional network and RB function. Curr. Opin. Cell Biol. 14, 684-691.

155. Braig M et al. (2005) Oncogene-induced senescence as an initial barrier in lymphoma development. Nature 436, 660–665.

156. Adams PD. (2009) Healing and Hurting: Molecular Mechanisms, Functions, and Pathologies of Cellular Senescence. Molecular Cell 36, 2-14

157. Simboeck E, Di Croce L. (2013) p16INK4a in cellular senescence. AGING 5, 8: 590-1

158. Shay JW, Pereira-Smith OM, Wright WE. (1991). A role for both RB and p53 in the regulation of human cellular senescence. Experimental Cell Research, 196, 33–39.

159. Bond JA, Wyllie FS, Wynford-Thomas D. (1994). Escape from senescence in human diploid fibroblasts induced directly by mutant p53. Oncogene, 9, 1885–1889.

160. Kortlever RM, Higgins PJ, Bernards R (2006) Plasminogen activator inhibitor-1 is a critical downstream target of p53 in the induction of replicative senescence Nat Cell Biol. 8(8): 877-884.

161. Gire V, Wynford-Thomas D. (1998). Reinitiation of DNA synthesis and cell division in senescent human fibroblasts by microinjection of anti-p53 antibodies. Molecular and Cellular Biology 18, 1611–1621.

162. Voorhoeve PM, Agami R. (2003). The tumor-suppressive functions of the human INK4A locus. Cancer Cell, 4, 311-319.

163. Wei W, Herbig U, Wei S, Dutriaux A, Sedivy JM. (2003). Loss of retinoblastoma but not p16 function allows bypass of replicative senescence in human fibroblasts. EMBO Report, 4,1061–1065.

164. Dannenberg JH, van Rossum A, Schuijff L, te Riele H. (2000). Ablation of the retinoblastoma gene family deregulates G(1) control causing immortalization and increased cell turnover under growth-restricting conditions. Genes & Development, 14, 3051–3064.

165. Sage J, Mulligan GJ, Attardi LD, Miller A, Chen S, Williams B, Theodorou E, Jacks T. (2000). Targeted disruption of the three Rb-related genes leads to loss of G(1) control and immortalization. Genes & Development,14, 3037–3050.

166. Brown JP, Wei W, Sedivy JM. (1997). Bypass of senescence after disruption of p21CIP1/WAF1 gene in normal diploid human fibroblasts. Science, 277, 831–834.

167. Chicas A, Wang X, Zhang C, McCurrach M, Zhao Z, Mert O, Dickins RA, Narita M, Zhang M, Lowe SW. (2010). Dissecting the unique role of the retinoblastoma tumor suppressor during cellular senescence. Cancer Cell 17,376–387.

168. Dirac AM, Bernards R. (2003). Reversal of senescence in mouse fibroblasts through lentiviral suppression of p53. Journal of Biological Chemistry, 278, 11731-11734.

169. Pantoja C, Serrano M. (1999). Murine fibroblasts lacking p21 undergo senescence and are resistant to transformation by oncogenic Ras. Oncogene, 18, 4974-4982.

170. Smogorzewska A, de Lange T. (2002). Different telomere damage signaling pathways in human and mouse cells. EMBO Journal, 21, 4338–4348.

171. Ben-Porath I, Weinberg RA. (2005) The signals and pathways activating cellular senescence. The International Journal of Biochemistry & Cell Biology 37 961-976.

172. (same as ref. 168).

173. Coppe JP, Rodier F, Patil CK, Freund A, Desprez PY, Campisi J. (2011) The tumor suppressor and aging biomarker p16INK4a induces cellular senescence without the associated inflammatory secretory phenotype. J. Biol. Chem. 286:36396–403

174. Novakova Z, Hubackova S, Kosar M, Janderova-Rossmeislova L, Dobrovolna J, et al. (2010) Cytokine expression and signaling in drug-induced cellular senescence. Oncogene 29:273–84.

175. Rodier F, Coppe JP, Patil CK, Hoeijmakers WA, Munoz DP, et al. (2009) Persistent DNA damage signalling triggers senescence-associated inflammatory cytokine secretion. Nat. Cell Biol. 11:973–79

176. Pazolli E, Alspach E, Milczarek A, Prior J, Piwnica-WormsD, Stewart SA. (2012) Chromatin remodeling underlies the senescence-associated secretory phenotype of tumor stromal fibroblasts that supports cancer progression. Cancer Res. 72:2251–61.

177. Bavik C, Coleman I, Dean JP, Knudsen B, Plymate S, Nelson PS. (2006) The gene expression program of prostate fibroblast senescence modulates neoplastic epithelial cell proliferation through paracrine mechanisms. Cancer Res. 66:794–802

178. Kuilman T, Michaloglou C, Vredeveld LC, Douma S, van Doorn R, Desmet CJ, Aarden LA, Mooi WJ, Peeper DS. (2008). Oncogene-induced senescence relayed by an interleukin-dependent inflammatory network. Cell 133, 1019–1031.

179. Acosta JC, et al. (2008) Chemokine signaling via the CXCR2 receptor reinforces senescence. Cell.133(6):958–961.

180. Wajapeyee N, Serra RW, Zhu X, Mahalingam M, Green MR. (2008) Oncogenic BRAF induces senescence and apoptosis through pathways mediated by the secreted protein IGFBP7. Cell 132, 363–374.

181. McLoughlin RM, Jenkins BJ, Grail D, Williams AS, Fielding CA, Parker CR, Ernst M, Topley N, Jones SA. Rachel M. (2005) IL-6 trans-signaling via STAT3 directs T cell infiltration in acute inflammation PNAS 102 (27) 9589-9594

182. Hoenicke L, Zender L. (2012) Immune surveillance of senescent cells-biological significance in cancer- and non-cancer pathologies. Carcinogenesis 33(6): 1123-1126

183. Xue W et al. (2007) Senescence and tumour clearance is triggered by p53 restoration in murine liver carcinomas. Nature, 445, 656-660.

184. Acosta JC, Banito A, Wuestefeld T, et al. (2013) A complex secretory program orchestrated by the inflammasome controls paracrine senescence. Nature Cell Biology. 15(8):978-90.

185. Andreasen PA, Egelund R, Petersen HH. (2000). The plasminogen activation system in tumor growth, invasion, and metastasis. Cell Mol. Life Sci. 57, 25-40

186. Williams GC. (1957) Pleiotropy, natural selection, and the evolution of senescence. *Evolution* 11:398-411.

187. Storer et al. (2013) Senescence Is a Developmental Mechanism that Contributes to Embryonic Growth and Patterning. Cell 155, 1-12

188. Muñoz-Espın et al., (2013). Programmed Cell Senescence during Mammalian Embryonic Development, Cell 155, 1–15,

189. Krizhanovsky V, Yon M, Dickins RA, Hearn S, Simon J, et al. 2008. Senescence of activated stellate cells limits liver fibrosis. Cell 134:657–67

190. Jun JI, Lau LF. (2010) Thematricellular proteinCCN1induces fibroblast senescence and restricts fibrosis in cutaneous wound healing. Nat. Cell Biol. 12:676–85.

191. Freund A, Orjalo A, Desprez PY, Campisi J. (2010) Inflammatory networks during cellular senescence: causes and consequences. Trends Mol. Med. 16:238–48

192. Coppe JP, Desprez PY, Krtolica A, Campisi J. 2010. The senescence-associated secretory phenotype: the dark side of tumor suppression. Annu. Rev. Pathol. Mech. Dis. 5:99–118.

193. Yoshimoto S, Loo TM, Atarashi K, Kanda H, Sato S, Oyadomari S, Iwakura Y, Oshima K, Morita H, Hattori M, Honda K, Ishikawa Y, Hara E, Ohtani N. (2013). Obesity-induced gut microbial metabolite promotes liver cancer through senescence secretome. Nature Letter 499 97-104.

194. Wang C, Jurk D, Maddick M, Nelson G, Martin-Ruiz C, von Zglinicki T. (2009) DNA damage response and cellular senescence in tissues of aging mice. Aging Cell **8**, 311–323.

195. Krishnamurthy J, Torrice C, Ramsey MR, Kovalev GI, Al-Regaiey K, Su L, Sharpless NE. (2004). Ink4a/Arf expression is a biomarker of aging. J. Clin. Invest. 114, 1299–1307.

196. R Ressler S, Bartkova J, Niederegger H, Bartek J, Scharffetter-Kochanek K, Jansen-Dürr P, Wlaschek M. (2006). p16INK4A is a robust in vivo biomarker of cellular aging in human skin. Aging Cell **5**, 379–389.

197. Burd CE, Sorrentino JA, Clark KS, Darr DB, Krishnamurthy J, Deal AM, Bardeesy N, Castrillon DH, Beach DH, Sharpless NE. (2013) Monitoring Tumorigenesis and Senescence In Vivo with a p16INK4a-Luciferase Model Cell 152, 340-351

198. Sedelnikova OA, Horikawa I, Zimonjic DB, Popescu NC, Bonner WM, Barrett JC. 2004. Senescing human cells and ageing mice accumulate DNA lesions with unrepairable double-strand breaks. Nat. Cell Biol. 6:168–70

199. McElhaney JE, Effros RB. (2009) Immunosenescence: What does it mean to health outcomes in older adults? Curr. Opin. Immunol. 21:418–24

200. Shaw AC, Joshi S, Greenwood H, Panda A, Lord JM. (2010) Aging of the innate immune system. Curr. Opin. Immunol. 22:507–13.

201. Le Garff-Tavernier M, Beziat V, Decocq J, Siguret V, Gandjbakhch F, et al. (2010) Human NK cells display major phenotypic and functional changes over the life span. Aging Cell 9:527–35.

202. Bitto A, Sell C, Crowe E, Lorenzini A, Malaguti M, et al. (2010) Stress-induced senescence in human and rodent astrocytes. Exp. Cell Res. 316:2961–68.

203. Salminen A, Ojala J, Kaarniranta K,Haapasalo A, Hiltunen M, Soininen H. (2011) Astrocytes in the aging brain express characteristics of senescence-associated secretory phenotype. Eur. J. Neurosci. 34:3–11.

204. Erusalimsky JD, Kurz DJ. (2005) Cellular senescence in vivo: its relevance in ageing and cardiovascular disease. Exp. Gerontol. 40:634–42.

205. Gorenne I, KavurmaM, Scott S, Bennett M. (2006) Vascular smoothmuscle cell senescence in atherosclerosis. Cardiovasc. Res. 72:9–17

206. Roberts S, Evans EH, Kletsas D, Jaffray DC, Eisenstein SM. (2006) Senescence in human intervertebral discs. Eur. Spine J. 15:312–16

207. Shane Anderson A, Loeser RF. (2010) Why is osteoarthritis an age-related disease? Best Pract. Res. Clin. Rheumatol. 24:15–26

208. Velarde MC, Flynn JM, Day NU, Melov S, Campisi J. (2012) Mitochondrial oxidative stress caused by Sod2 deficiency promotes cellular senescence and aging phenotypes in the skin. Aging 4:3–12

209. Campisi J, Andersen JK, Kapahi P, Melov S. (2011) Cellular senescence: a link between cancer and age-related degenerative disease? Semin. Cancer Biol. 21:354–59.

210. Angelini PD, Zacarias Fluck MF, Pedersen K, Parra-Palau JL, Guiu M, Bernadó Morales C, Vicario R, Luque-García A, Navalpotro NP, Giralt J, Canals F, Gomis RR, Tabernero J, Baselga J, Villanueva J, Arribas J. (2013) Constituve HER2 Signaling Promotes Breast Cancer Metastasis through Cellular Senescence. Cancer Res; 73(1): 450-58

211. Lee SL, Hong SW, Shin JS, Kim JS, Ko SG, Hong NJ, et al. (2009) p34SEI-1 inhibits doxorubicin-induced senescence through a pathway mediated by protein kinase C-delta and c-Jun-NH2-kinase 1 activation in human breast cancer MCF7 cells. Mol Cancer Res 7:1845–53.

212. Collado M, Blasco M, Serrano M. (2007) Cellular Senescence in Cancer and Aging. Cell 130: 223-34

213. Hartman ZC, Yang XY, Glass O, Lei G, Osada T, Dave SS, Morse MA, Clay TM, Lyerly HK. (2011). HER2 Overexpression Elicits a Proinflammatory IL-6 Autocrine Signaling Loop That Is Critical for Tumorigenesis. Cancer Res; 71(13): 4380-91

214. Demidenko ZN, Zubova SG, Bukreeva EI, Pospelov VA, Pospelova TV, Blagosklonny MV. (2009) Rapamycin decelerates cellular senescence. Cell Cycle. 8:1888-1895.

215. Reddy JP, Peddibhotla S, Bu W, Zhao J, Haricharan S, Du YC, et al. (2010). Defining the ATM-mediated barrier to tumorigenesis in somatic mammary cells following ErbB2 activation. Proc Natl Acad Sci U S A 107:3728–33.

216. te Poele RH, Okorokov AL, Jardine L, Cummings J, Joel SP. (2002) DNA damage is able to induce senescence in tumor cells in vitro and in vivo. Cancer Res. 62 :1876-83.

217. Padua D, Zhang XH, Wang Q, Nadal C, Gerald WL, Gomis RR, et al. (2008) TGFbeta primes breast tumors for lung metastasis seeding through angiopoietin-like 4. Cell 133:66–77.

218. Liu J, Xiong W, Baca-Regen L, Nagase H, Baxter BT. (2003) Mechanism of inhibition of matrix metalloproteinase-2 expression by doxycycline in human aortic smooth muscle cells. J Vasc Surg. 38(6):1376-83.

219. Hanemaaijer R, Visser H, Koolwijk P, Sorsa T, Salo T, Golub LM, van Hinsbergh VW. (1998) Inhibition of MMP synthesis by doxycycline and chemically modified tetracyclines (CMTs) in human endothelial cells. Adv Dent Res. 12(2):114-8.

220. Charlesworth B. (1994). Evolution in Age-Structured Populations. Cambridge: Cambridge University Press.

221. Charlesworth B. (1996) Evolution of senescence: Alzheimer's disease and evolution. Curr. Biol. **6**, 20–22.

222. Leroi AM, Bartke A, De Benedictis G, Franceschi C, Gartner A, Gonos ES, Fedei ME, Kivisild T, Lee S, Kartaf-Ozer N, Schumacher M, Sikora E, Slagboom E, Tatar M, Yashin AI, Vijg J, Zwaan B. (2005) What evidence is there for the existence of individual genes with antagonistic pleiotropic effects? Mech. Ageing Dev. 126, 421–429.

223. Flatt T, Promislow DEL. (2007) Still pondering an age-old question. Science 318, 1255–1256.

224. Blagosklonny MV. (2010) Revisiting the antagonistic pleiotropy theory of aging: TOR-driven program and quasi-program. Cell Cycle **9**, 3151–3156.

225. Giaimo S, d'Adda di Fagagna F. (2012) Is cellular senescence an example of antagonistic pleiotropy? Aging Cell 11, 378-383.

226. Lopez-Otın C, Blasco MA, Partridge L, Serrano M, Kroemer G. (2013) The Hallmarks of Aging. Cell 153: 1194-1217.

227. Ren L, Wang X, Dong Z, Liu J, Zhang S. (2013) Bone metastasis from breast cancer involves elevated IL-11 expression and the gp130/STAT3 pathway. Med Oncol. 30(3):634.

228. Padua D, Zhang XH, Wang Q, Nadal C, Gerald WL, Gomis RR, Massagué J. (2008) TGFbeta primes breast tumors for lung metastasis seeding through angiopoietin-like 4. Cell. 133(1):66-77.

229. Parrinello S, Coppe JP, Krtolica A, Campisi J. (2005) Stromal-epithelial interactions in aging and cancer: Senescent fibroblasts alter epithelial cell differentiation. J. Cell Sci. 118:485–96

230. Tsai KK, Chuang EY, Little JB, Yuan ZM. (2005) Cellular mechanisms for low-dose ionizing radiationinduced perturbation of the breast tissue microenvironment. Cancer Res. 65:6734–44

231. Liu D, Hornsby PJ. (2007) Senescent Human Fibroblasts Increase the Early Growth of Xenograft Tumors via Matrix Metalloproteinase Secretion. Cancer Res 67: (7): 3117-26

232. Capparelli C, Guido C, Whitaker-Menezes D, Bonuccelli G, Balliet R, Pestell TG, Goldberg AF, Pestell RG, Howell A, Sneddon S, Birbe R, Tsirigos A, Martinez-Outschoorn U, Sotgia F, Lisanti MP. (2012) Autophagy and senescence in cancer-associated fibroblasts metabolically supports tumor growth and metastasis via glycolysis and ketone production. Cell Cycle. 11(12):2285-302.

233. Calitchi E, Kirova YM, Otmezguine Y, Feuilhade F, Piedbois Y, Le Bourgeois JP. (2001) Long-term results of neoadjuvant radiation therapy for breast cancer. Int J Cancer. 96(4):253-9.

234. Schott AF, Hayes DF. (2012) Defining the Benefits of Neoadjuvant Chemotherapy for Breast Cancer . J Clin Onc 30(15):1747-9.

235. Jackson JG, Pant V, Li Q, Chang LL, Quintás-Cardama A, Garza D, Tavana O, Yang P, Manshouri T, Li Y, El-Naggar AK, Lozano G. (2012). p53-Mediated Senescence Impairs the Apoptotic Response to Chemotherapy and Clinical Outcome in Breast Cancer. Cancer Cell. 21, 793–806

236. Dörr JR, Yu Y, Milanovic M, Beuster G, Zasada C, Däbritz JH, Lisec J, Lenze D, Gerhardt A, Schleicher K, Kratzat S, Purfürst B, Walenta S, Mueller-Klieser W, Gräler M, Hummel M, Keller U, Buck AK, Dörken B, Willmitzer L, Reimann M, Kempa S, Lee S, Schmitt CA. (2013) Synthetic lethal metabolic targeting of cellular senescence in cancer therapy. Nature 501(7467):421-5.

Clinical Trials

NeoAltto: Neo ALTTO (Neoadjuvant Lapatinib and/or Trastuzumab Treatment Optimisation) Study. ClinicalTrials.gov Identifier: NCT00553358.

GeparQuattro: GeparQuattro: Combination Chemotherapy With or Without Capecitabine and/or Trastuzumab Before Surgery in Treating Women With Stage I, Stage II, or Stage III Breast Cancer. ClinicalTrials.gov Identifier: NCT00288002.

PUBLICATIONS

List of publications

1. Pedersen K, Angelini PD, Laos S, Bach-Faig A, Cunningham MP, Ferrer-Ramon C, et al. (2009) A naturally occurring HER2 carboxy-terminal fragment promotes mammary tumor growth and metastasis. Mol Cell Biol 29:3319–31.

2. Garcia-Castillo J, Pedersen K, Angelini PD, Bech-Serra JJ, Colome N, Cunningham MP, et al. (2009) HER2 carboxy-terminal fragments regulate cell migration and cortactin phosphorylation. J Biol Chem 284:25302–13.

3. Parra-Palau JL, Pedersen K, Peg V, Scaltriti M, Angelini PD, Escorihuela M, et al. (2010) A major role of p95/611-CTF, a carboxy-terminal fragment of HER2, in the downmodulation of the ER in HER2-positive breast cancers. Cancer Res 70:8537–46.

4. Chandarlapaty S, Scaltriti M, Angelini PD, Ye Q, Guzman M, Hudis CA, Norton L, Solit DB, Arribas J, Baselga J, Rosen N. (2010) Inhibitors of HSP90 block p95-HER2 signaling in Trastuzumab-resistant tumors and suppress their growth. Oncogene 29(3):325-34.

5. Scaltriti M, Chandarlapaty S, Prudkin L, Aura C, Jimenez J, Angelini PD, et al. (2010) Clinical benefit of lapatinib-based therapy in patients with human epidermal growth factor receptor 2-positive breast tumors coexpressing the truncated p95HER2 receptor. Clin Cancer Res 16:2688–95

6. Angelini PD, Zacarias Fluck MF, Pedersen K, Parra-Palau JL, Guiu M, Bernadó Morales C, Vicario R, Luque-García A, Navalpotro NP, Giralt J, Canals F, Gomis RR, Tabernero J, Baselga J, Villanueva J, Arribas J. (2013) Constituve HER2 Signaling Promotes Breast Cancer Metastasis through Cellular Senescence. Cancer Res; 73(1): 450-58

Patents

1. Method for diagnosing cancers expressing the HER2 receptor or its truncated variants
   Patent number: 8389227
   Type: Grant
   Filed: June 5, 2009
   Issued: March 5, 2013
   Assignees: Fundacio Privada Institut de Recerca Hospital Universitari VallHebron, Fundacio Privada Institucio Catalana de Recera I Estudis Avancats, Fundacio Privada Institut d'Investigacio Oncologica de Vall Hebron
   Inventors: Joaquin Arribas Lopez, Kim Pedersen, Pier-Davide Angellini, Josep Liuis Parra Palau, Sirle Laos, Jose Baselga Torres

2. Antibodies Against HER2 Truncated Variant CTF-611
   Application number: 20110135653
   Type: Application
   Filed: December 6, 2010
   Issued: June 9, 2011
   Assignees: the law, operating under the law
   Inventors: Joaquin Arribas Lopez, Kim Pedersen, Pier-Davide Angellini, Josep Lluis Parra Palau, Jose Baselga Torres

Constitutive HER2 Signaling Promotes Breast Cancer Metastasis through Cellular Senescence

Pier Davide Angelini, Mariano F. Zacarias Fluck, Kim Pedersen, et al.

Cancer Res 2013;73:450-458.

Cancer Research

Constitutive HER2 Signaling Promotes Breast Cancer Metastasis through Cellular Senescence

Pier Davide Angelini[1,5], Mariano F. Zacarias Fluck[1], Kim Pedersen[1], Josep Lluís Parra-Palau[1], Marc Guiu[4], Cristina Bernadó Morales[1], Rocio Vicario[1], Antonio Luque-García[1], Nerea Peiró Navalpotro[2], Jordi Giralt[2], Francesc Canals[1], Roger R. Gomis[3,4], Josep Tabernero[2], José Baselga[2], Josep Villanueva[1], and Joaquín Arribas[1,2,5]

Abstract

Senescence, a terminal cell proliferation arrest, can be triggered by oncogenes. Oncogene-induced senescence is classically considered a tumor defense barrier. However, several findings show that, under certain circumstances, senescent cells may favor tumor progression because of their secretory phenotype. Here, we show that the expression in different breast epithelial cell lines of p95HER2, a constitutively active fragment of the tyrosine kinase receptor HER2, results in either increased proliferation or senescence. In senescent cells, p95HER2 elicits a secretome enriched in proteases, cytokines, and growth factors. This secretory phenotype is not a mere consequence of the senescence status and requires continuous HER2 signaling to be maintained. Underscoring the functional relevance of the p95HER2-induced senescence secretome, we show that p95HER2-induced senescent cells promote metastasis *in vivo* in a non–cell-autonomous manner. *Cancer Res; 73(1); 450–8. ©2012 AACR.*

Introduction

Senescence, an irreversible cell proliferation arrest, can be triggered by an excessive number of cell divisions or a variety of stressors, including oncogenes. Oncogene-induced senescence (OIS) constitutes an antitumor barrier that impedes the expansion of early neoplastic cells before they become malignant (1, 2). However, senescent cells remain metabolically active and, through a robust secretory machinery (3), release a wealth of factors, collectively termed senescence-associated secretory phenotype (SASP) or senescence messaging secretome (SMS), (4, 5). This senescence secretome includes components necessary to establish and maintain the senescence program (5) and, in addition, chemotactic factors that mediate the clearance of senescent cells *in vivo* by attracting cellular components of the immune system belonging both to the innate and to the adaptive immune response (6–8). However, the frequent presence of protumorigenic factors in the senescence secretome has led several authors to propose that, under certain circumstances, OIS may contribute to tumor progression in a cell nonautonomous manner (4, 5).

Authors' Affiliations: [1]Preclinical Research, [2]Clinical Research Programs, Vall d'Hebron Institute of Oncology (VHIO); [3]Institució Catalana de Recerca i Estudis Avançats (ICREA); [4]Oncology Program, Institute for Research in Biomedicine Barcelona, Barcelona; and [5]Department of Biochemistry and Molecular Biology, Universitat Autonoma de Barcelona, Bellaterra, Spain

Note: Supplementary data for this article are available at Cancer Research Online (http://cancerres.aacrjournals.org/).

Corresponding Author: Joaquín Arribas, Preclinical Research Program, Vall d'Hebron Institute of Oncology (VHIO), Psg. Vall d'Hebron 119-129, Barcelona 08035, Spain. Phone: 34-93-2746026; Fax: 34-93-4893884; E-mail: jarribas@vhio.net

doi: 10.1158/0008-5472.CAN-12-2301

The receptor tyrosine kinase HER2 is a prototypic proto-oncogene overexpressed in approximately 20% of breast cancers. HER2-positive tumors constitute a group of breast cancers with specific biologic features and therapeutic options (9). The expression of neu, an oncogenic mutant form of HER2, leads to premature senescence (10); however, very little is known about the relevance of this observation in the progression and treatment of HER2-positive breast tumors.

A subgroup of HER2-positive breast cancers express a heterogeneous group of 80 to 115 kDa carboxy-terminal fragments of HER2 collectively known as HER2 CTFs or p95HER2 (11). Compared with tumors expressing only full-length HER2, p95HER2-positive tumors exhibit worse prognosis and a higher likelihood to metastasize (12, 13). One of the HER2 CTFs, the 100- to 115-kDa p95HER2 fragment (also known as 611-CTF), is a constitutively active form of HER2 because of its ability to form homodimers maintained by disulphide bonds (14).

Here, we show that expression of 110- to 115-kDa p95HER2/611-CTF (hereafter referred to as p95HER2) can induce the onset of OIS in different breast cancer cells. Notably, p95HER2-induced senescent cells, likely due to their distinct secretory phenotype, increase the ability of proliferating breast cancer cells to metastatize.

Materials and Methods

Materials

Antibodies were from Dako (anti-Ki67), BD Biosciences (Rb), Cell Signaling (anti-P-HER2 (Y1221/1222), anti-Ras, anti-P-p53 (Ser15), Santa Cruz Biotechnology (anti-p21, anti-53BP1 and anti-p53), BioGenex [anti-HER2 (CB11)], Amersham [anti-rabbit IgG and anti-mouse IgG, both horseradish peroxidase (HRP)-linked], Invitrogen (anti-mouse-Alexa 488, anti-mouse-

PE, anti-goat-Alexa 568), and Millipore (anti-gamma-H2AX). Lapatinib was kindly provided by GlaxoSmithKline.

Doxorubicin was from Sigma-Aldrich. MMP1, ANGPTL4 (RayBiotech), interleukin (IL)-11 (R&D), and IL-6 (eBiosciences) ELISA kits were used for determination of the corresponding factors in conditioned media or serum according to the manufacturer's indications.

Cell culture

MCF7 Tet-Off/p95HER2, MCF7 Tet-Off/HER2, and T47D/p95HER2 cells were transfected as previously described (14).

p95HER2_MDA-MB-453 and p95HER2_MCF10A were obtained by retroviral transduction with p95HER2. p95HER2_MDA-MB-453 were maintained in L15 + GlutaMAX (Gibco) containing 10% FBS, 0.75 μg/mL puromycin (Sigma), and 1 μmol/L lapatinib (Tykerb, GlaxoSmithKline), whereas p95HER_MCF10A were maintained in Dulbecco's Modified Eagle's Media (DMEM):F-12, 10% FBS, 4 mmol/L L-glutamine, and 0.75 μg/mL puromycin.

MDA-MB-231/Luc were obtained by retroviral transduction as previously described (15).

Western blot and confocal microscopy

Western blot and confocal microscopy were carried out as previously described (14).

Proliferation assay

Proliferation was analyzed by cell counting. After trypsinization, viable cells determined by trypan blue dye exclusion were counted on a Neubauer chamber.

WST1 assay

The WST1 reagent was from Roche. A total of 5×10^3 cells were seeded in 96-well plates and the assay was conducted following the manufacturer's indications.

Metabolic labeling

Approximately 3×10^6 cells were metabolically labeled with 500 μCi/mL [^{35}S]Translabel for 45 minutes in cysteine and methionine-free medium and lysed. Cell lysates were normalized by the number of cells and analyzed on SDS-PAGE and fluorography.

Determination of cell volume

Cells were trypsinized, resuspended in complete medium, and cell diameter was determined by direct measuring in a Neubauer chamber. Cell volume was approximated to the one of a sphere as $4/3 \times (\pi \times \text{cell radius}^3)$ and 5 representative fields with 10 to 15 cells were analyzed.

Senescence-associated β-galactosidase activity

Both cells and tissue slides were analyzed using senescence β-galactosidase staining kit (Cell Signaling Technology) following the manufacturer's indications.

Cell irradiation

Cells were trypsinized, resuspended in complete medium, and transferred to a 15-mL falcon tube. About 10 Gy γ-irradiation dose was applied at Radiotherapy Service of the Vall d'Hebron University Hospital (Barcelona, Spain) with a cobalt unit (Theraton 780-C, NCA) at a dose rate of 80 cGy/min and the total dose was 10 Gy in a single dose.

ELISAs

The conditioned media were collected, spun down at $200 \times g$ for 5 minutes, and transferred into clean tubes. Mice sera were obtained by complete exsanguinations and subsequent centrifugation using heparinized material. Concentration of all factors was determined according to the manufacturer's instructions of each kit, normalized to cell number, and expressed as pg/mL/25,000 cells. All the experiments were carried out at least 3 times, and the results are represented as the means ± SD.

Immunohistochemistry

Tumor xenografts were removed, fixed overnight with 4% formol, and then paraffin-embedded. Sequential 5-μm thick slices where then obtained, hematoxylin and eosin stained, and immunostained for Ki67, p21 (immunohistochemistry), and γ-H2AX (immunofluorescence).

Xenografts

Mice were maintained and treated in accordance with institutional guidelines of Vall d'Hebron University Hospital Care and Use Committee. p95HER2_MCF7 Tet-Off cells were injected into the right flanks of 6- to 8-week-old female BALB/c athymic mice purchased from Charles Rivers Laboratories. The expression of p95HERs was repressed by adding doxycycline to the drinking water until tumors were about 150 mm^3. Then mice were randomized and treated with or without doxycycline (50 mg/kg/d). Tumor xenografts were measured with calipers every 3 days, and tumor volume was determined using the formula: $(\text{length} \times \text{width}^2) \times (\pi/6)$. At the end of the experiment, the animals were anesthetized with a 1.5% isofluorane–air mixture and were killed by cervical dislocation. Results are presented as mean ± SD of tumor volume.

Metastatic colonization was monitored by *in vivo* bioluminescence imaging using the IVIS-200 Imaging System from Xenogen as previously described (16).

Transcriptomic analysis

Expression analysis in both MCF7 was conducted using Affymetrix gene chips HG U133 2.0, as previously described (14).

Proteomic analysis

Cells expressing or not p95HER2 during 5 days were washed 5 times with serum-free medium and incubated for additional 48 hours in the absence of serum. The conditioned media were then collected, spun down at $200 \times g$ for 5 minutes, transferred into clean tubes, filtered through a Nalgene 0.2-μm pore vacuum filter (Fisher #09-741-07), and concentrated using a 10 000 MWCO Millipore Amicon Ultra (Millipore #UFC901024) spinning down 15 mL at a time at $800 \times g$ for 30 minutes until the final concentration was 1 mg/mL (~200- to 300-fold concentration). Protein concentration was determined with

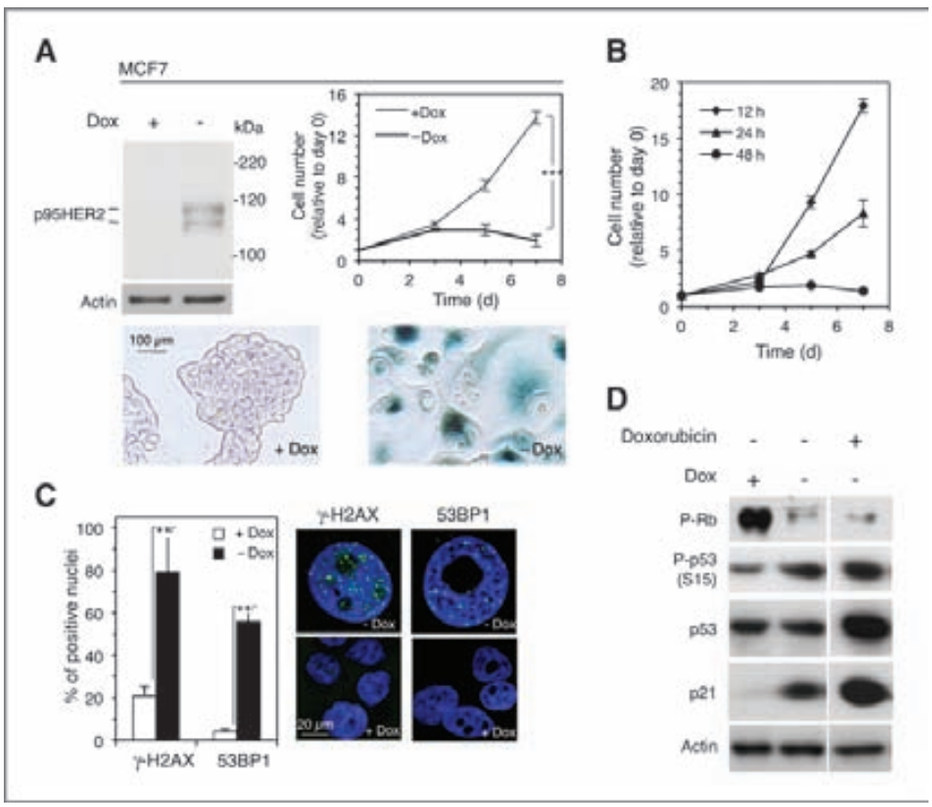

Figure 1. Expression of p95HER2 in MCF7 cells results in premature senescence. A, top left, MCF7 Tet-off/p95HER2 cells were treated with or without doxycycline (Dox) for 7 days. Then, cells were lysed and the cell lysates were analyzed by Western blotting with antibodies against HER2. Note that p95HER2 is expressed as 2 bands; previous characterization of these bands showed that the fast migrating one is an intracellular precursor and the slow migrating one is the fully glycosylated form that is transported to the cell surface (14). Top right, the same cells were cultured with or without doxycycline and counted at the indicated time points. *P* values were obtained by 2-tailed Student *t* test. ***, $P < 0.001$. Bottom, the same cells treated with or without doxycycline were cultured for 7 days, fixed, and stained for β-galactosidase activity. B, the same cells as in A were treated without doxycycline for 12, 24, or 48 hours. Then, doxycycline was added back and cells were counted at the indicated time points. C, right, the same cells treated as in A were fixed, stained with antibodies specific for γ-H2AX or 53BP1, and the number of positive nuclei was quantified. The bars represent the averages of 3 independent experiments ±SD. *P* values were obtained by 2-tailed Student *t* test. **, $P < 0.01$. Left, representative nuclei are shown. D, MCF7 Tet-off/p95HER2 were treated with 0.5 μmol/L of doxorubicin and doxycycline as indicated. Then, cells were lysed and the cell lysates were analyzed by Western blotting with the indicated antibodies.

a Bio-Rad protein assay (Bio-Rad, #500-0006). Subsequent sample preparation and proteomic analysis were conducted as previously described (17).

Statistical analysis

Data are presented as averages ± SD and were analyzed by the Student *t* test when comparing 2 groups or ANOVA when comparing more than 2 groups. Results were considered to be statistically significant at $P < 0.05$. All statistical analyses were conducted using the SPSS 12.0 Statistical Software (SPSS, Inc.).

Results

Effect of p95HER2 expression in different breast epithelial cell lines

In MCF10A, a nontransformed immortalized mammary epithelial cell line, the expression of p95HER2 accelerated cell proliferation (Supplementary Fig. S1A). In contrast, in MCF7, MDA-MB-453, or T47D, the expression of the HER2 fragment resulted in a marked proliferation arrest and increased levels of the senescence-associated β-galactosidase activity (SA-β-gal; Fig. 1A; Supplementary Fig. S1B and S1C), 2 phenotypes associated with OIS.

OIS is irreversible and it is characterized by the activation of the DNA damage response (DDR). The proliferation arrest was irreversible after 48 hours of p95HER2 expression (Fig. 1B), and it was accompanied by the upregulation of 2 markers of the activation of the DDR: γ-H2AX (the phosphorylated form of histone H2AX) and 53BP1 (tumor suppressor p53-binding protein; Fig. 1C).

OIS is regulated by p53 and/or pRb pathways and results in an increased expression of cyclin-dependent kinase inhibitors (CDKI). The expression of p95HER2 resulted in the activation of both pathways and in the upregulation of the CDKI p21 (Fig. 1D). As a control, we showed that treatment with the DNA-damaging agent doxorubicin, which promotes senescence in MCF7 cells (18), led to comparable results (Fig. 1D).

Senescent cells remain metabolically active (1). We observed that the metabolic activity of MCF7 cells expressing p95HER2 was higher than that of proliferating nonexpressing cells as judged by the WST1 assay, which it is frequently used to

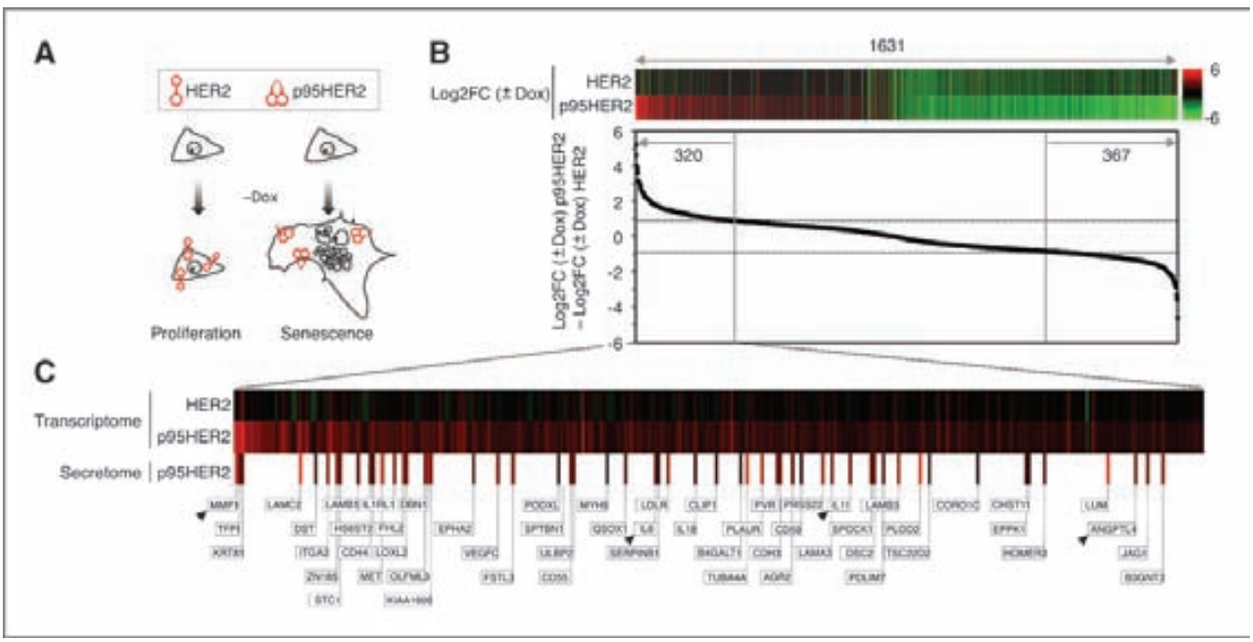

Figure 2. p95HER2-induced senescence secretome. A, schematic drawing to illustrate the different outcomes of the expression of full-length HER2 or p95HER2 in MCF7 cells. B, transcriptomic analysis on MCF7 Tet-off cells expressing p95HER2 or HER2 and treated with or without doxycycline during 60 hours. Top, heatmap of the 1,631 genes regulated by p95HER2 (i.e., genes encoding transcripts with $\log_2$FC > 0.9 or <−0.9 comparing cells treated without and with doxycycline). Bottom, to identify genes regulated by p95HER2 but not by HER2, we ordered the 1,631 genes according to the result of subtracting the $\log_2$FC in cells expressing HER2 from the $\log_2$FC in cells expressing p95HER2 [$\log_2$FC (± Dox) p95HER2 − $\log_2$FC (±Dox) HER2]. The number of genes with a $\log_2$FC (±Dox) p95HER2 − $\log_2$FC (±Dox) HER2 above or below 0.9 and −0.9, respectively, are shown. C, top, heatmap of the 320 genes transcriptionally upregulated by p95HER2 but not by HER2. Bottom lane, heatmap of the gene products as determined by the proteomic analysis conducted comparing the secretomes of MCF7 Tet-off/p95HER2 cells treated with and without doxycycline (see Supplementary Table S2). Arrows mark genes chosen for the validation of the analysis.

determine cell proliferation but, in reality, it measures dehydrogenase activity (Supplementary Fig. S2A). Furthermore, p95HER2 expression led to an increased rate of protein biosynthesis (Supplementary Fig. S2B). This enhanced metabolic activity is the likely cause of the remarkable hypertrophy experimented by p95HER2-expressing cells (Supplementary Fig. S2C and S2D).

Collectively, these results showed that expression of p95HER2 in different breast cancer cells leads to OIS.

p95HER2-induced senescence secretome

While expression of p95HER2 in MCF7 cells results in OIS (Fig. 1), the expression of full-length HER2 does not prevent the proliferation of the same cells (Supplementary Fig. S1D, see also Fig. 2A). The majority of genes regulated by p95HER2 are also regulated by full-length HER2. However, a group of genes is specifically regulated by the constitutively active HER2 fragment (14). Therefore, to identify components of the secretome specific of the senescence state, we focused in genes regulated by p95HER2 but not by HER2 (Fig. 2B; Supplementary Table S1). Of the 1,631 genes regulated by p95HER2 ($-.9 > \log_2$FC > 0.9), 944 were also regulated by HER2, whereas 2 groups of 320 and 367 genes were more acutely up- or downregulated, respectively, by p95HER2 (Fig. 2B).

Nearly one fifth of the genes preferentially upregulated by p95HER2 encode for transmembrane proteins or secreted factors and therefore they could contribute to the secretome of p95HER2-induced senescent cells. To validate and extend this observation, we compared the secretome of p95HER2-induced senescent MCF7 cells with that of control MCF7 cells through label-free proteomics. We identified 361 proteins whose levels increased ($\log_2$FC > 0.9) in p95HER2-induced senescent cells (Supplementary Table S2). Fifty-five of the corresponding genes were transcriptionally upregulated in p95HER2-induced senescent cells (Fig. 2C; Supplementary Table S3). Many of these secreted factors, such as matrix metalloproteases 1 (MMP1), angiopoietin-like 4 ANGPTL4, IL-11, and IL-6, are well-characterized protumorigenic factors (19, 20). Analysis of the levels of these factors by ELISA confirmed their increased secretion by p95HER2-induced senescent cells and their absence in the media conditioned by cells expressing HER2 (see Fig. 3A).

The p95HER2-induced senescence secretome is regulated by HER2 signaling

The secretory phenotype is considered one of the hallmarks of premature senescence (21). Therefore, it could be speculated that the secretory phenotype of p95HER2-induced senescent cells is a consequence of the senescence status and not a consequence of the expression of p95HER2. To test this possibility, we used the HER2 tyrosine kinase inhibitor lapatinib. As expected, lapatinib did not revert the senescence phenotype (Supplementary Fig. S3); nevertheless, the inhibitor impaired the production of the factors analyzed (Fig. 3A), strongly

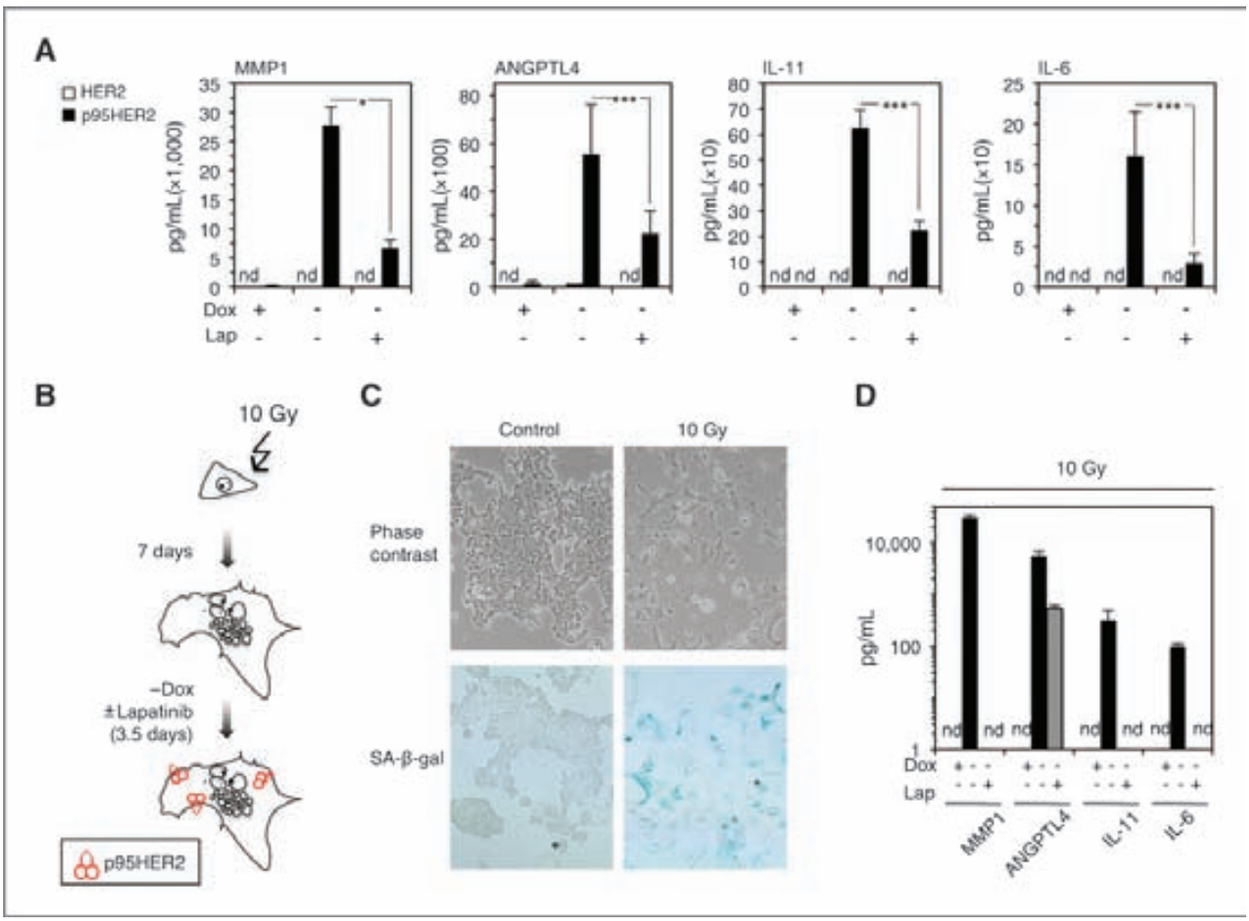

Figure 3. Effect of inhibition of HER2 signaling on the p95HER2-induced senescence secretome. A, results of ELISAs to determine the concentration of the indicated factors in the conditioned media of MCF7 Tet-off/p95HER2 and MCF7 Tet-off/HER2 treated with or without doxycycline and lapatinib (Lap) as indicated. *P* values were obtained by 2-tailed Student *t* test. *, $P < 0.05$; ***, $P < 0.001$. nd, not detectable. B, MCF7 Tet-off/p95HER2 treated with doxycycline were irradiated with 10 Gy. One week after irradiation, control or irradiated cells were fixed and stained for β-galactosidase (β-gal) activity. Representative phase contrast microscopy images are shown. C, schematic drawing showing the protocol used; see text for details. D, results of ELISAs to determine the concentration of the indicated factors in the conditioned media of irradiated MCF7 Tet-off/p95HER2 treated with or without doxycycline and or lapatinib.

suggesting that their efficient secretion requires continuous p95HER2 signaling. To confirm this conclusion, we induced cellular senescence by irradiation (Fig. 3B and C). Irradiation-induced senescent cells did not secrete detectable levels of any of the factors analyzed (Fig. 3D), but induction of p95HER2 in irradiation-induced senescent cells resulted in a secretory phenotype similar to that of p95HER2-induced senescent cells (Fig. 3C and D). As a further control, we showed that treatment with lapatinib blocked the secretion of MMP1, IL-11, and IL-6 and impaired the secretion ANGPTL4 (Fig. 3D). We concluded that, in addition to trigger senescence, the expression of active p95HER2 is required to maintain the p95HER2-induced senescence secretome. However, the maintenance of the senescence state and the composition of the senescence secretome are regulated independently.

Dynamics of the p95HER2-induced senescence secretome *in vitro* and *in vivo*

Characterization of the dynamics of the senescence secretome induced by p95HER2 in MCF7 cells showed that *in vitro* senescent cells continue secreting high levels of IL-6, IL-11, MMP1, and ANGPTL4 for at least 1 month (Fig. 4A and B). This result indicates that p95HER2-induced senescent cells could constitute a long-lasting reservoir of protumorigenic factors *in vivo*. To test this hypothesis, we injected MCF7 Tet-Off p95HER2 cells into nude mice and when the tumors reached about 150 mm^3, we removed doxycycline from the drinking water of the animals to allow the expression of p95HER2 (Fig. 3C). The subsequent analysis of xenograft samples showed the efficient onset of senescence *in vivo* after about 21 days of expression of p95HER2 as judged by the decrease of the cell proliferation marker Ki67, increase in the percentage of cells positive for p21, γ-H2AX, and SA-β-gal (Fig. 3D; Supplementary Fig. S4A). Consistently, the xenografts expressing p95HER2 grew for about 30 days, probably because of the increase in cell size, and then stabilized (Fig. 3C). Furthermore, cells obtained from xenografts expressing p95HER2 displayed the typical morphology of senescent cells (Supplementary Fig. S4B and S4C). A time course determination of the plasma levels of ANGPTL4 and IL-11 in mice carrying senescent cells

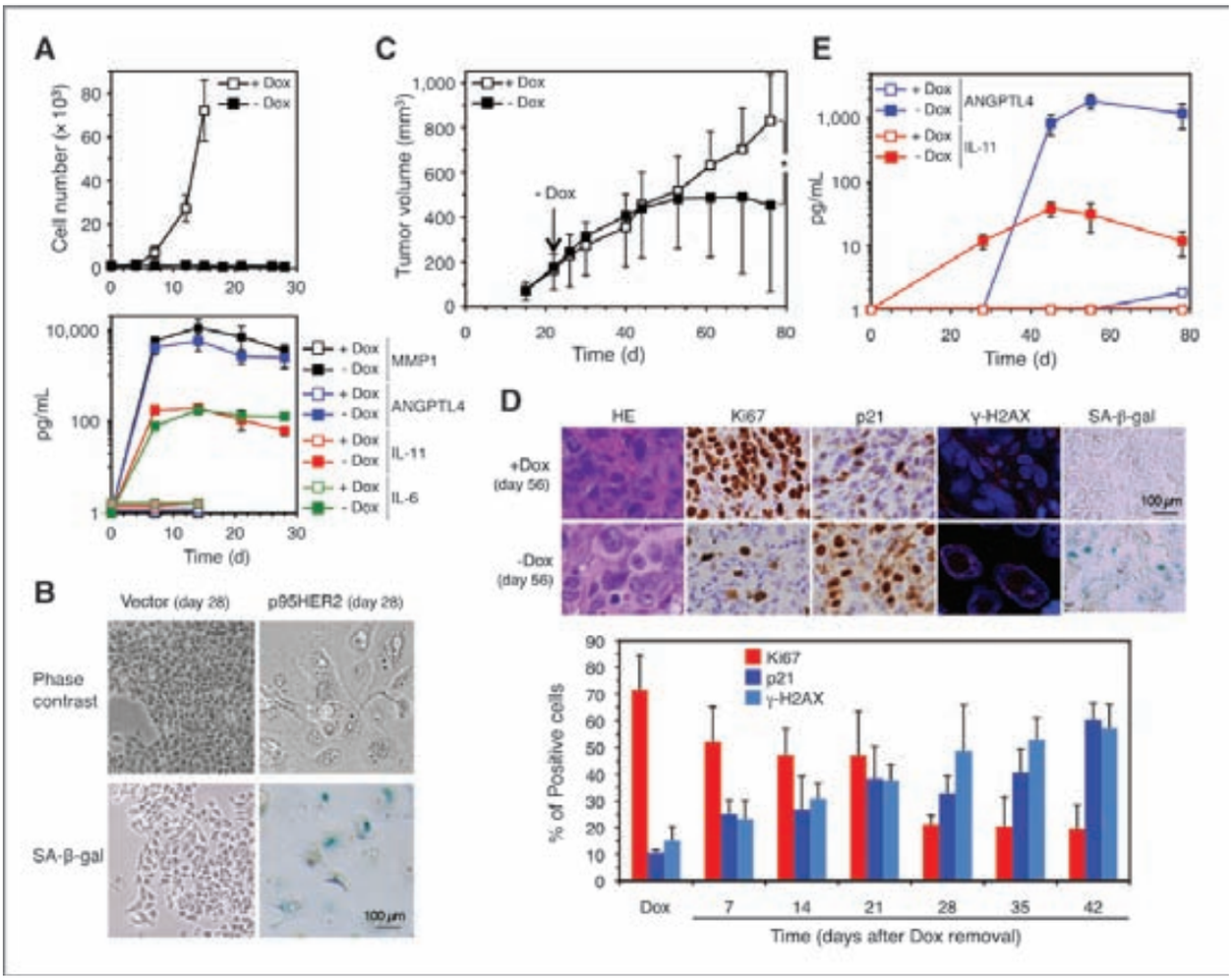

Figure 4. Dynamics of the p95HER2-induced senescence secretome *in vitro* and *in vivo*. A, top, MCF7 Tet-off/p95HER2 cells were treated with or without doxycycline for the indicated periods of time and counted. The points represent the mean ± SD of 3 independent experiments. Bottom, results of ELISAs to determine the concentration of the indicated factors in the conditioned media of the same cells treated as above. The results are represented as the averages ± SD of 3 independent experiments. B, the same cells treated as in A for the indicated periods of time were fixed and immediately stained for β-galactosidase activity. Representative phase contrast microscopy images are shown. C, a total of 3×10^6 MCF7 Tet-off/p95HER2 cells were injected subcutaneously into the flank of nude mice. Doxycycline was administered in the drinking water until tumors reached about 150 mm^3, then mice were randomized and doxycycline was withdrawn from the drinking water of half of the mice ($n = 12$ in each group). The points represent average tumor volume at each time point ± SD. *P* values were obtained by 2-tailed Student *t* test. *, $P < 0.05$. D, the xenografts from mice treated as in C were surgically removed, fixed, and stained for β-galactosidase activity or paraffin-embedded. Hematoxylin eosin (HE) staining or immunostaining for the indicated markers were conducted in serial slices from the paraffin-embedded tumors. The number of positive cells was quantified and the bars represent the averages of 3 independent determinations from 2 mice. Representative fields are shown. E, results of ELISAs to determine the concentration of the indicated factors in the sera of mice treated as in C and exsanguinated at the indicated time points. The points represent the averages of determinations from 3 mice ± SD.

expressing p95HER2 showed that the senescence secretome is also displayed *in vivo* during long periods of time (Fig. 4E).

These results show that the p95HER2-induced senescence cells are long lived *in vitro* and *in vivo* and that they continuously secrete protumorigenic factors.

p95HER2-induced senescent cells favor metastasis cell nonautonomously

MDA-MB-231, a cell line established from the pleural fluid of a patient with advanced metastatic breast cancer, is a widely used experimental model of breast cancer metastasis. Injection of MDA-MB-231 cells carrying luciferase as reporter into the hearts of nude mice results in colonization of bones, brain, or lungs that can be monitored *in vivo* by bioluminescence imaging (22).

The increase in plasma levels of different prometastatic factors (Fig. 4E) suggests that the presence of p95HER2-induced senescent cells in the primary tumor contributes to metastasis in a systemic manner. To this aim, we injected MDA-MB-231/Luc cells intracardially in mice carrying subcutaneous MCF7 Tet-off/p95HER2 xenografts and treated them with or without doxycycline. Although in both conditions, 100% of the mice developed metastases, the metastatic cells that colonized target organs in mice carrying p95HER2-

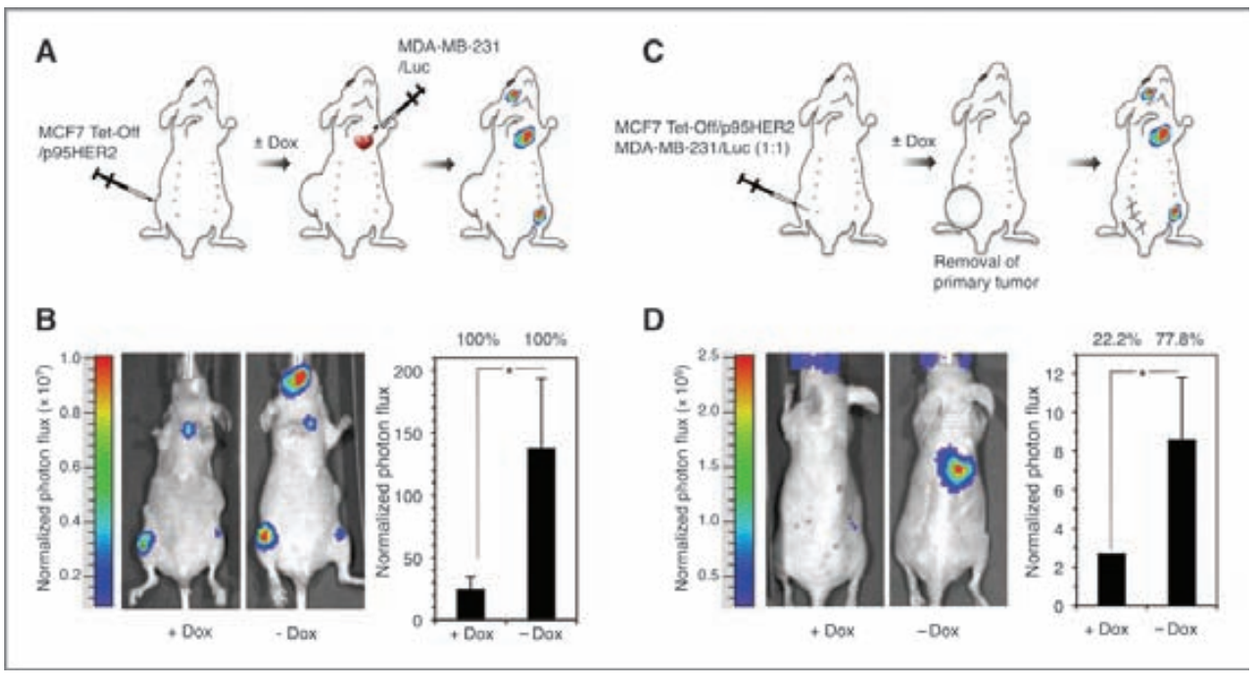

Figure 5. p95HER2-induced senescent cells promote metastasis cell nonautonomously. A, schematic drawing showing the protocol used. Briefly, 3×10^6 MCF7 Tet-off/p95HER2 cells were injected subcutaneously into the flank of nude mice. Doxycycline was administered in the drinking water until tumors reached about 150 mm^3. Then, mice were randomized and doxycycline was withdrawn from the drinking water of half of the mice ($n = 5$ in each group). Two weeks after removal of doxycycline from one of the groups, 2.5×10^5 MDA-MB-231/Luc were injected intracardially in all mice and, after 35 days, *in vivo* imaging was conducted. B, left, representative luminescence images at 6 weeks after intracardiac injection. Right, metastatic growth determined by total photon flux at the same time point. Values are mean ± SD. *P* values were determined by Student *t* test. *, $P < 0.05$. The percentages represent the numbers of mice with metastasis. C, schematic drawing showing the protocol used. Briefly, 1.5×10^6 MCF7 Tet-off/p95HER2 mixed with 1.5×10^6 MDA-MB-231/Luc cells were injected orthotopically into the fourth mammary fat pad. Doxycycline was administered in the drinking water until tumors reached about 150 mm^3. Then, mice were randomized and doxycycline was withdrawn from the drinking water of half of the mice ($n = 8$ in each group). Tumors were allowed to grow until they reached about 700 mm^3, then they were surgically removed. Forty days after removal of the primary tumor *in vivo* imaging was conducted. D, left, representative luminescence images at 14 weeks after orthotopic injection. Right, metastatic growth determined by total photon flux at the same time point. Values are mean ± SD. *P* values were determined by Student *t* test. *, $P < 0.05$. The percentages represent the numbers of mice with metastasis.

induced senescent cells gave rise to bigger metastasis, as measured by total photon flux emission (Fig. 5A and B). This result shows that the p95HER2-induced senescent cells, likely through the secretion of prometastatic factors, act in a systemic fashion increasing the metastatic growth of cells that have reached the target organs. As a control, we ruled out that the observed results were due to the effect of the removal of doxycycline on MDA-MB-231/Luc cells (Supplementary Fig. S5).

Many of the factors secreted by senescent cells are likely to exert their functions locally. For example, cell surface and secreted proteases tend to cleave extracellular components in close proximity to the producing cell. Therefore, we analyzed the metastatic behavior of MDA-MB-231/Luc cells coinjected orthotopically with MCF7 Tet-off/p95HER2 cells. The presence in the primary tumor of p95HER2-induced senescent cells did significantly increase the metastatic ability of MDA-MB-231 cells (Fig. 5C and D). This result was likely not due only to the differences in the growth rate of the primary tumor, as shown by tumor volume and luminescence (Supplementary Fig. S6). Therefore, p95HER2-induced senescent cells prime proliferating breast tumor cells for metastasis.

Discussion

The main argument supporting a positive contribution of senescence to tumor progression is the existence of the senescence secretome, which is enriched in protumorigenic cytokines, growth factors, and proteases. Accordingly, *in vitro*, the secretome of senescent cells increases cell proliferation (23, 24), angiogenesis, and invasion (21). *In vivo*, it favors the growth of some xenografts (25, 26). An alternative explanation for the existence of the senescence secretome is compatible with the consideration of senescence as a pure intrinsic antitumor barrier. Such consideration is based on subcutaneous xenograft experiments carried out in nude mice. In this model, RAS-transformed hepatoma cells induced to senescence by p53 restoration secrete chemotactic cytokines, including Csf1, Mcp1, Cxcl1, and IL-15, which induce an innate immune response by attracting neutrophils, macrophages, and natural killer cells (7, 27). This inflammatory response leads to complete tumor regression in about 2 weeks due to a prompt clearance of senescent cells. In contrast, p95HER2-induced senescent cells last months in nude mice (Fig. 4). The most likely explanation to reconcile these results is that the composition of the senescence secretome induced by p53 restoration in RAS-transformed hepatoma cells is different from

that of p95HER2-induced senescent cells. While the former includes cytokines that attracts cellular components of the innate immune system, the latter lacks such cytokines. Supporting this conclusion, we have not detected the expression of Csf1, Mcp1, Cxcl1, or IL-15 in the secretome of p95HER2-induced senescent cells (see Supplementary Tables S1–S3).

Using immunocompetent mice, a recent report shows that the adaptive immune system rapidly clears Ras-induced hepatocarcinoma senescent cells from early tumor lesions (8). However, in line with our conclusions with nude mice, it has been shown that senescent cells expressing an oncogenic form of HER2 are long lived *in vivo*, also in immunocompetent mice (28). Therefore, these reports also support that clearance of senescent cells *in vivo* depends on the oncogene that induced senescence, presumably because of the differences in senescence secretomes.

The strict control of the senescence secretome by oncogenes that would reconcile the apparently disparate results aforementioned is strongly supported by different evidence presented in this report. On one hand, the inhibition of HER2 signaling impairs the secretory phenotype of p95HER2-induced senescent cells (Fig. 3). On the other hand, induction of senescence by γ-irradiation leads to a secretome different to that of p95HER2-induced senescent cells, and expression of p95HER2 in irradiation-induced senescent cells results in a secretome similar to that of p95HER2-induced senescent cells (Fig. 3). Therefore, our data show that the composition of the senescence secretome, and thus the cell nonautonomous effects of senescent cells, depends on the specific cause that drives senescence.

In summary, we propose that different oncogenes might lead to senescent cells that, despite showing many common features, are very different with respect to their secretory phenotype. The secretome elicited by constitutive HER2 signaling in senescent cell exerts a prometastic effect that could contribute to the progression of some breast cancers.

Disclosure of Potential Conflicts of Interest

J. Baselga is a consultant/advisory board member of Roche Genentech. No potential conflicts of interest were disclosed by the other authors.

Authors' Contributions

Conception and design: P.-D. Angelini, J. Arribas
Development of methodology: P.-D. Angelini, M. Zacarías-Fluck, K. Pedersen, J. Giralt, F. Canals, R.R. Gomis, J. Villanueva, J. Arribas
Acquisition of data (provided animals, acquired and managed patients, provided facilities, etc.): P.-D. Angelini, M. Zacarias-Fluck, K. Pedersen, J.-L. Parra-Palau, M. Guiu, C. Bernadó-Morales, R. Vicario, A. Luque-García, N. Peiró-Navalpotro
Analysis and interpretation of data (e.g., statistical analysis, biostatistics, computational analysis): P.-D. Angelini, M. Zacarías-Fluck, J. Tabernero, J. Baselga, J. Arribas
Writing, review, and/or revision of the manuscript: P.-D. Angelini, M. Zacarías-Fluck, J. Arribas
Study supervision: J. Arribas

Acknowledgments

The authors thank Dr. Manuel Serrano for helpful discussions, the constant support of the UCTS and animal facilities (Vall d'Hebron Institut de Recerca), Drs. Ana Pujol and Yolanda Fernández-Amurgo for the *in vivo* luminescence experiments, and Dr. Agueda Martinez-Barriocanal for critical reading of the manuscript.

Grant Support

This work was supported by the Instituto de Salud Carlos III (Intrasalud PI081154 and the Network of Cooperative Cancer Research (RTICC-RD06/0020/0022), the Breast Cancer Research Foundation (BCRF).

The costs of publication of this article were defrayed in part by the payment of page charges. This article must therefore be hereby marked *advertisement* in accordance with 18 U.S.C. Section 1734 solely to indicate this fact.

Received June 13, 2012; revised September 24, 2012; accepted October 19, 2012; published online January 3, 2013.

References

1. Collado M, Serrano M. Senescence in tumours: evidence from mice and humans. Nat Rev Cancer 2010;10:51–7.
2. Reddy JP, Li Y. Oncogene-induced senescence and its role in tumor suppression. J Mammary Gland Biol Neoplasia 2011;16:247–56.
3. Narita M, Young AR, Arakawa S, Samarajiwa SA, Nakashima T, Yoshida S, et al. Spatial coupling of mTOR and autophagy augments secretory phenotypes. Science 2011;332:966–70.
4. Rodier F, Campisi J. Four faces of cellular senescence. J Cell Biol 2011;192:547–56.
5. Kuilman T, Peeper DS. Senescence-messaging secretome: SMS-ing cellular stress. Nat Rev Cancer 2009;9:81–94.
6. Ventura A, Kirsch DG, McLaughlin ME, Tuveson DA, Grimm J, Lintault L, et al. Restoration of p53 function leads to tumour regression *in vivo*. Nature 2007;445:661–5.
7. Xue W, Zender L, Miething C, Dickins RA, Hernando E, Krizhanovsky V, et al. Senescence and tumour clearance is triggered by p53 restoration in murine liver carcinomas. Nature 2007;445:656–60.
8. Kang TW, Yevsa T, Woller N, Hoenicke L, Wuestefeld T, Dauch D, et al. Senescence surveillance of pre-malignant hepatocytes limits liver cancer development. Nature 2011;479:547–51.
9. Baselga J, Swain SM. Novel anticancer targets: revisiting ERBB2 and discovering ERBB3. Nat Rev Cancer 2009;9:463–75.
10. Trost TM, Lausch EU, Fees SA, Schmitt S, Enklaar T, Reutzel D, et al. Premature senescence is a primary fail-safe mechanism of ERBB2-driven tumorigenesis in breast carcinoma cells. Cancer Res 2005;65:840–9.
11. Arribas J, Baselga J, Pedersen K, Parra-Palau JL. p95HER2 and breast cancer. Cancer Res 2011;71:1515–9.
12. Molina MA, Saez R, Ramsey EE, Garcia-Barchino MJ, Rojo F, Evans AJ, et al. NH(2)-terminal truncated HER-2 protein but not full-length receptor is associated with nodal metastasis in human breast cancer. Clin Cancer Res 2002;8:347–53.
13. Saez R, Molina MA, Ramsey EE, Rojo F, Keenan EJ, Albanell J, et al. p95HER-2 predicts worse outcome in patients with HER-2-positive breast cancer. Clin Cancer Res 2006;12:424–31.
14. Pedersen K, Angelini PD, Laos S, Bach-Faig A, Cunningham MP, Ferrer-Ramon C, et al. A naturally occurring HER2 carboxy-terminal fragment promotes mammary tumor growth and metastasis. Mol Cell Biol 2009;29:3319–31.
15. Ponomarev V, Doubrovin M, Serganova I, Vider J, Shavrin A, Beresten T, et al. A novel triple-modality reporter gene for whole-body fluorescent, bioluminescent, and nuclear noninvasive imaging. Eur J Nucl Med Mol Imaging 2004;31:740–51.
16. Minn AJ, Gupta GP, Siegel PM, Bos PD, Shu W, Giri DD, et al. Genes that mediate breast cancer metastasis to lung. Nature 2005;436:518–24.
17. Lawlor K, Nazarian A, Lacomis L, Tempst P, Villanueva J. Pathway-based biomarker search by high-throughput proteomics profiling of secretomes. J Proteome Res 2009;8:1489–503.
18. Lee SL, Hong SW, Shin JS, Kim JS, Ko SG, Hong NJ, et al. p34SEI-1 inhibits doxorubicin-induced senescence through a pathway mediated by protein kinase C-delta and c-Jun-NH2-kinase 1 activation in human breast cancer MCF7 cells. Mol Cancer Res 2009;7:1845–53.

19. Kang Y, Siegel PM, Shu W, Drobnjak M, Kakonen SM, Cordon-Cardo C, et al. A multigenic program mediating breast cancer metastasis to bone. Cancer Cell 2003;3:537–49.
20. Kishimoto T. Interleukin-6: from basic science to medicine–40 years in immunology. Annu Rev Immunol 2005;23:1–21.
21. Coppe JP, Patil CK, Rodier F, Sun Y, Munoz DP, Goldstein J, et al. Senescence-associated secretory phenotypes reveal cell-nonautonomous functions of oncogenic RAS and the p53 tumor suppressor. PLoS Biol 2008;6:2853–68.
22. Padua D, Zhang XH, Wang Q, Nadal C, Gerald WL, Gomis RR, et al. TGFbeta primes breast tumors for lung metastasis seeding through angiopoietin-like 4. Cell 2008;133:66–77.
23. Bavik C, Coleman I, Dean JP, Knudsen B, Plymate S, Nelson PS. The gene expression program of prostate fibroblast senescence modulates neoplastic epithelial cell proliferation through paracrine mechanisms. Cancer Res 2006;66:794–802.
24. Coppe JP, Desprez PY, Krtolica A, Campisi J. The senescence-associated secretory phenotype: the dark side of tumor suppression. Annu Rev Pathol 2010;5:99–118.
25. Liu D, Hornsby PJ. Senescent human fibroblasts increase the early growth of xenograft tumors via matrix metalloproteinase secretion. Cancer Res 2007;67:3117–26.
26. Ohanna M, Giuliano S, Bonet C, Imbert V, Hofman V, Zangari J, et al. Senescent cells develop a PARP-1 and nuclear factor-{kappa}B-associated secretome (PNAS). Genes Dev 2011;25:1245–61.
27. Krizhanovsky V, Yon M, Dickins RA, Hearn S, Simon J, Miething C, et al. Senescence of activated stellate cells limits liver fibrosis. Cell 2008;134:657–67.
28. Reddy JP, Peddibhotla S, Bu W, Zhao J, Haricharan S, Du YC, et al. Defining the ATM-mediated barrier to tumorigenesis in somatic mammary cells following ErbB2 activation. Proc Natl Acad Sci U S A 2010;107:3728–33.

A Naturally Occurring HER2 Carboxy-Terminal Fragment Promotes Mammary Tumor Growth and Metastasis

Kim Pedersen, Pier-Davide Angelini, Sirle Laos, Alba Bach-Faig, Matthew P. Cunningham, Cristina Ferrer-Ramón, Antonio Luque-García, Jesús García-Castillo, Josep Lluis Parra-Palau, Maurizio Scaltriti, Santiago Ramón y Cajal, José Baselga and Joaquín Arribas

Mol. Cell. Biol. **2009, 29(12):3319. DOI: 10.1128/MCB.01803-08.**
Published Ahead of Print 13 April 2009.

MOLECULAR AND CELLULAR BIOLOGY, June 2009, p. 3319–3331 Vol. 29, No. 12
0270-7306/09/$08.00+0 doi:10.1128/MCB.01803-08

A Naturally Occurring HER2 Carboxy-Terminal Fragment Promotes Mammary Tumor Growth and Metastasis▽†

Kim Pedersen,[1] Pier-Davide Angelini,[1,2] Sirle Laos,[1] Alba Bach-Faig,[1] Matthew P. Cunningham,[1] Cristina Ferrer-Ramón,[1] Antonio Luque-García,[1] Jesús García-Castillo,[1] Josep Lluis Parra-Palau,[1] Maurizio Scaltriti,[1] Santiago Ramón y Cajal,[1] José Baselga,[1] and Joaquín Arribas[1,2,3]*

Medical Oncology Research Program, Research Institute Foundation and Vall d'Hebron Institute of Oncology, Vall d'Hebron University Hospital, Psg. Vall d'Hebron 119-129, 08035 Barcelona, Spain[1]; Department of Biochemistry and Molecular Biology, Autonomous University of Barcelona, Campus de la UAB, 08193 Bellaterra, Spain[2]; and Institució Catalana de Recerca i Estudis Avançats, 08010 Barcelona, Spain[3]

Received 25 November 2008/Returned for modification 3 February 2009/Accepted 3 April 2009

HER2 is a tyrosine kinase receptor causally involved in cancer. A subgroup of breast cancer patients with particularly poor clinical outcomes expresses a heterogeneous collection of HER2 carboxy-terminal fragments (CTFs). However, since the CTFs lack the extracellular domain that drives dimerization and subsequent activation of full-length HER2, they are in principle expected to be inactive. Here we show that at low expression levels one of these fragments, 611-CTF, activated multiple signaling pathways because of its unanticipated ability to constitutively homodimerize. A transcriptomic analysis revealed that 611-CTF specifically controlled the expression of genes that we found to be correlated with poor prognosis in breast cancer. Among the 611-CTF-regulated genes were several that have previously been linked to metastasis, including those for MET, EPHA2, matrix metalloproteinase 1, interleukin 11, angiopoietin-like 4, and different integrins. It is thought that transgenic mice overexpressing HER2 in the mammary glands develop tumors only after acquisition of activating mutations in the transgene. In contrast, we show that expression of 611-CTF led to development of aggressive and invasive mammary tumors without the need for mutations. These results demonstrate that 611-CTF is a potent oncogene capable of promoting mammary tumor progression and metastasis.

HER2 (ErbB2) is a type I transmembrane protein that belongs to the epidermal growth factor receptor (EGFR, ErbB1, HER1) family. Two additional members, HER3 and -4 (ErbB3 and -4), complete this family. When an EGF-like ligand binds to HER1, -3, or -4, its extracellular domain adopts the so-called open conformation, which allows the formation of homo- or heterodimers (5). Despite not binding any ligand, HER2 readily interacts with other ligand-bound HER receptors because its extracellular domain is constitutively in an open conformation (10).

At the cell surface, dimerization of the extracellular domains leads to interaction between the intracellular kinases of the HER receptors and subsequent transphosphorylation of tyrosine residues in the C-terminal tails. The phosphotyrosines act as docking sites for proteins that initiate signals which are transduced to the nucleus through different pathways, including the mitogen-activated protein kinases (MAPKs), phosphoinositide-3-kinase-activated Akt, Src, and phospholipase C gamma (PLCgamma) pathways. These signaling circuitries control the expression of target genes that act coordinately to modify key aspects of cellular biology, including proliferation, migration, survival, and differentiation (7).

In addition to the canonical mode, HER receptors or fragments of them are capable of direct signaling. For example, a nuclear carboxy-terminal fragment (CTF) encompassing the entire cytoplasmic domain of HER4 has been shown to regulate gene transcription (22, 39). The CTF of HER4 is generated at the plasma membrane by the sequential action of two types of proteolytic enzymes known as the alpha- and gamma-secretases. Alpha-secretases cleave in the juxtamembrane region, releasing the extracellular domain. The transmembrane stub left behind is a substrate of the gamma-secretase complex, which through regulated intramembrane proteolysis releases the intracellular domain (20, 28).

Several reports have shown that full-length HER2 can also be transported to the nucleus and regulate gene expression directly (40). Although the mechanism of transport is not fully understood, a nuclear localization signal (NLS), which consists of a cluster of basic amino acids that overlaps with the transmembrane stop transfer signal, has been identified in the intracellular juxtamembrane region of HER2 (15, 41). Nuclear transport of HER2 relies on interactions between this NLS, the receptor importin beta 1, and the nuclear pore protein Nup358 (12).

In addition to its proposed function in the nucleus as a full-length molecule, HER2 is also cleaved by alpha-secretases, and the resulting transmembrane-cytoplasmic fragment is known as P95 (21, 31, 44, 45). To date, cleavage of P95 by the gamma-secretase has not been reported. Since P95 lacks the extracel-

* Corresponding author. Mailing address: Medical Oncology Research Program, Vall d'Hebron University Hospital, Psg. Vall d'Hebron 119-129, 08035 Barcelona, Spain. Phone: 34 93 274 6026. Fax: 34 93 489 3884. E-mail: jarribas@ir.vhebron.net.

† Supplemental material for this article may be found at http://mcb.asm.org/.

▽ Published ahead of print on 13 April 2009.

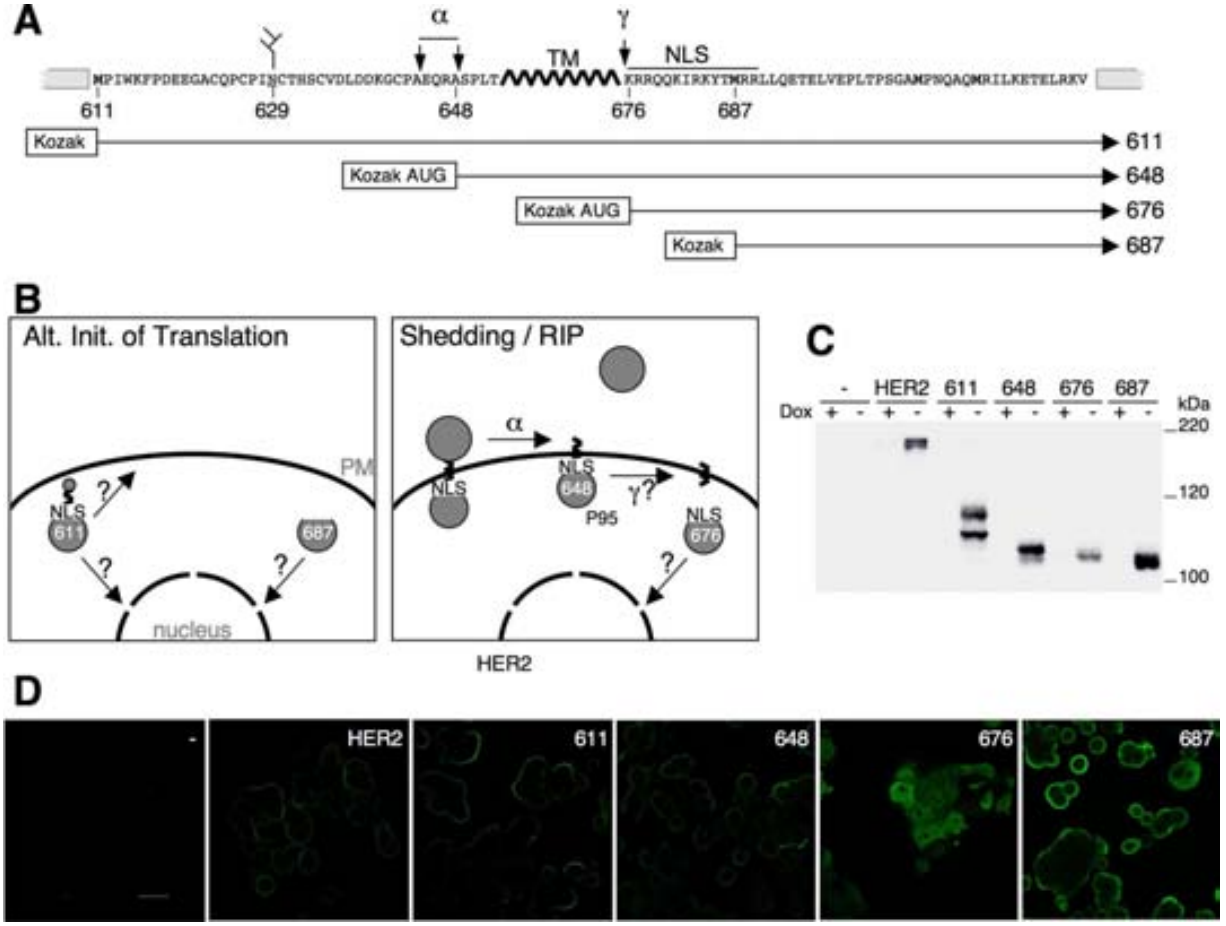

FIG. 1. Generation and characterization of cellular models expressing individual CTFs of HER2. (A) Schematic showing the primary sequence of the juxtamembrane regions of HER2, the alpha-secretase cleavage sites (α), the transmembrane domain (TM), a putative gamma-secretase cleavage site (γ), the NLS, the N-glycosylated Asn-629, and the position of amino acid residues 611, 648, 676, and 687 (corresponding to the N termini of the HER2 CTFs). The schematics below the sequence represent cDNA constructs used for expression of the different CTFs. (B) Schematic depicting the different HER2 CTFs generated by alternative initiation of translation (left) and proteolytic processing (right). (C) Expression from the cDNA constructs shown in panel A. MCF7 Tet-Off clones stably transfected with the empty vector (-) or with the vector containing the cDNA of HER2 or 611-, 648-, 676-, or 687-CTF under the control of a Tet/Dox-responsive element were kept with or without doxycycline (Dox) for 24 h, lysed, and analyzed by Western blotting with an antibody against the cytoplasmic domain of HER2. (D) The MCF7 clones stably transfected with vector (-), HER2, or 611-, 648-, 676-, or 687-CTF, as in panel C, were analyzed 24 h after induction of expression with a confocal microscope by indirect immunofluorescence with an antibody against the cytoplasmic domain of HER2. The bar in the first photo from the left represents 30 μm.

lular domain, it is not predicted to form stable hetero- or homodimers. Nevertheless, P95 has been suggested to be active (6, 25, 42).

We have recently identified alternative initiation of translation as an additional mechanism that generates CTFs of HER2 (1). Initiation of translation from a methionine codon located upstream (Fig. 1A, methionine 611) or downstream (methionine 687) of the transmembrane domain leads to the synthesis of two different CTFs. Although preliminary evidence suggested that CTFs generated by translation are active, as in the case of P95, the mechanism of activation has not been determined.

Breast cancer patients expressing CTFs of HER2 are more likely to develop nodal metastasis (26) and have worse prognoses than those predominantly expressing the full-length receptor (32). Furthermore, the presence of CTFs seems to be relevant for the treatment of breast cancer patients, since ~90% of the tumors expressing CTFs are resistant to treatment with the anti-HER2 antibody trastuzumab (Herceptin) (33). However, the CTFs expressed in tumors have not been characterized, and it is not known if they arise from proteolysis and/or alternative initiation of translation. Furthermore, since the activities of the different CTFs have not been analyzed, their individual contributions to the malignant phenotype are not known.

We hypothesized that a functional analysis of HER2 CTFs not only could shed light on noncanonical signaling by receptor tyrosine kinases, it could also help to explain why CTFs contribute to poor prognosis in breast cancer. We found that one of the CTFs, 611-CTF, incorporated into the secretory pathway independently of a classic signal peptide and reached the plasma membrane, where it led to hyperactivation of several oncogenic signaling pathways. 611-CTF specifically controlled the expression of genes that predict poor prognosis in breast

cancer patients. These included the receptor tyrosine kinases MET and EPHA2, the matrix metalloproteinase 1 (MMP1), several integrins, interleukin 11 (IL-11), and angiopoietin-like 4 (ANGPTL4). The mechanism of activation of 611-CTF involved the formation of constitutive homodimers by intermolecular disulfide bonding. The cysteines involved are located in a small region not present in the other CTFs, providing an explanation for the unique hyperactivity of 611-CTF in the absence of most of the extracellular domain. Confirming the relevance of these results in vivo, and in contrast to full-length HER2 that requires activating mutations to become oncogenic, expression of wild-type 611-CTF in the mouse mammary gland led to the development of aggressive tumors. In addition, the tumors induced by 611-CTF metastasized to the lung with high frequency. These results suggest that 611-CTF plays a causal role in the progression and invasion of human breast cancers and that the expression of this CTF should be taken into account in the design of future anti-HER2 therapies.

MATERIALS AND METHODS

Materials. All plasmid constructs of HER2 were derived from a cDNA clone identical to the published sequence gi:183986. The different cDNA constructs were made using standard PCR, sequencing, and cloning techniques.

Antibodies were from Cell Signaling (anti-P-HER2 [no. 2249], anti-P-Erk1/2 [no. 9101], anti-Erk1/2 [no. 9102], anti-P-Jnk [no. 9251], anti-P-Akt [no. 9275 and 9271], anti-Akt [no. 9272], anti-P-Src [no. 2101], and anti-P-PLCg1 [no. 2821]), BD Biosciences (anti-ITGA2, anti-ITGA5, and anti-ITGB1), Santa Cruz Biotechnology (anti-MET and anti-PHLDA), Upstate (anti-EphA2), Trevigen (anti-GAPDH), Abcam (anti-LDH), BioGenex (anti-HER2 [CB11]), Amersham (anti-rabbit immunoglobulin G [IgG] and anti-mouse IgG, both horseradish peroxidase linked), and Invitrogen (anti-mouse IgG linked to Alexa Fluor 488).

Lapatinib was kindly provided by GlaxoSmithKline, Research Triangle Park, NJ.

Cell culture. MCF7 Tet-Off cells (BD Biosciences) were maintained at 37°C and 5% CO_2 in Dulbecco's minimal essential medium/F-12 (1:1) (Gibco) containing 10% fetal bovine serum (Gibco), 4 mM L-glutamine (PAA Laboratories), 0.2 mg/ml G418 (Gibco), and 1 μg/ml doxycycline (Sigma). The BT474 cells were cultured in the same medium but without G418 and doxycycline. Cells were transfected with the various expression plasmids by using FuGENE6 (Roche). Single stable clones with pUHD10-3h-based plasmids integrated were selected with 0.1 mg/ml hygromycin B (Invitrogen). Expression from pUHD10-3 h-encoded cDNAs of HER2 and CTFs was induced by removing doxycycline. First the cells were detached with 0.5% trypsin-EDTA (GIBCO) and washed three times by centrifugation, and the medium was changed 10 h after seeding in culture dishes. Homogeneity of the individual clones was checked by immunofluorescence confocal microscopy with an antibody against the cytoplasmic domain of HER2. Two independently selected stable clones (i.e., -A and -B in Fig. S6 in the supplemental material) were used in the experiments presented throughout this report.

P95 was induced in BT474 cells by treatment with 0.75 mM APMA (4-aminophenyl mercuric acetate) for 20 min, with or without 1 h of pretreatment with 1 mM of the inhibitor 1,10-phenanthroline.

Biochemical methods. Extracts for immunoblots were prepared in modified radioimmunoprecipitation assay (RIPA) buffer (20 mM NaH_2PO_4/NaOH, pH 7.4, 150 mM NaCl, 1% Triton X-100, 5 mM EDTA, 100 mM phenylmethylsulfonyl fluoride, 25 mM NaF, 16 μg/ml aprotinin, 10 μg/ml leupeptin, and 1.3 mM Na_3VO_4), and protein concentrations were determined with DC protein assay reagents (Bio-Rad). Samples were mixed with loading buffer (final concentrations: 62 mM Tris, pH 6.8, 12% glycerol, 2.5% sodium dodecyl sulfate [SDS]) with or without 5% beta-mercaptoethanol and incubated at 99°C for 5 min before fractionation of 15 μg of protein by SDS-polyacrylamide gel electrophoresis (PAGE). Specific signals in Western blots were quantified with the software ImageJ 1.38 (NIH).

Cells for immunofluorescence microscopy seeded on glass coverslips were washed with phosphate-buffered saline, fixed with 4% paraformaldehyde for 20 min, and permeabilized with 0.2% Triton X-100 for 10 min. For blocking and antibody binding, we used phosphate-buffered saline with 1% bovine serum albumin, 0.1% saponin, and 0.02% NaN_3, and for mounting, we used Vectashield with DAPI (4′,6′-diamidino-2-phenylindole) (Vector Laboratories).

Glycosylation was examined by incubating ON at 37°C modified RIPA cell lysate (15 μg of protein) with or without 1 μl (1 unit) of *N*-glycosidase F (Roche).

Membrane and cytosolic fractionation of breast tumor tissue samples was achieved by ultracentrifugation precipitation of membranes. While frozen, the samples were cut in small pieces, mixed with separation buffer (50 mM Tris, pH 7.4, 150 mM NaCl, 250 mM sucrose, 10 mM EDTA, 1 mM phenylmethylsulfonyl fluoride, 5 mM NaF, 10 μg/ml aprotinin, 10 μg/ml leupeptin, 1 μg/ml pepstatin, and 1 mM Na_3VO_4), and homogenized with a Polytron instrument and a 22-gauge needle. Then, nonbroken material and organelles were removed by centrifugation three times, each for 10 min at 10,000 × *g*. The cleared lysates were centrifuged for 1 h at 100,000 × *g*. The resulting supernatants containing the cytosolic proteins were collected and centrifuged for an additional 1 h at 100,000 × *g* to remove traces of membrane proteins. The pellets from the first 1 h of centrifugation containing the membranes were washed in separation buffer containing an additional 1 M NaCl, in order to release membrane interacting proteins. Membranes were then recovered by centrifugation again for 1 h at 100,000 × *g* and finally suspended in modified RIPA buffer. For Western analysis, we used 50 μg of cytosolic proteins and a volume of membrane protein samples corresponding to the same percentage of the input.

Transcriptomic analysis of cell line model. For the transcriptomic analysis, we purified total RNA (Qiagen; RNeasy) from the MCF7 Tet-Off stable clones seeded 15 or 60 h earlier in the presence or absence of doxycycline. For immunoblot analyses, the same cells were seeded in parallel dishes (see Fig. S6 in the supplemental material). For the 15-h time point, we used the following clones: -A and -B (vector), H2-A and H2-B (HER2), 611-A and 611-B (611-CTF), 676-A and 676-B (676-CTF), and 687-A and 687-B (687-CTF). The following clones were used for the 60-h time point: -A (vector), H2-A (HER2), 611-A (611-CTF), 676-A (676-CTF), and 687-A (687-CTF). The integrity of the total RNA samples was validated in an Agilent BioAnalyzer Nanochip before amplification with a one-cycle target labeling protocol and by analysis on Affymetrix GeneChip expression probe arrays (Human Genome U133 Plus 2.0) at the UCTS facility in Vall d'Hebron University Hospital. For the 15-h samples, the RNA preparations were run twice, independently on arrays. For the 60-h samples, except for clones 676-A and 687-A, two independent RNA preparations of each condition were analyzed. Except for the first array run of the 15-h samples of clone H2-A, the RNA samples from clones in the presence and absence of doxycycline were analyzed completely in parallel at the facility. The data files of in total 56 arrays were analyzed in the program ArrayAssist 5.5.1 (Stratagene) with probe levels normalized by the RMA (robust multichip average) algorithm. Consistency of the data sets was verified by determining how many of the 54,675 probe sets varied more than twofold when comparing the doxycycline presence and absence data from a clone in the same array run (see Table SII, column 5, in the supplemental material). In the case of the 60-h samples of clones 676-A and 687-A, only 1 and 21 probe sets representing 0 and 17 genes, respectively, varied more than twofold. For the rest of the conditions, we took advantage of the experimental duplication to determine the number of probe sets with more than twofold differences in pairwise *t* tests with a P of <0.05 (see Table SII, column 7, in the supplemental material). Expression of 611-CTF for 15 and 60 h, and HER2 for 60 h, led to significant changes of 120, 690, and 150 probe sets, respectively, representing in total 624 different genes. Subsequently, all probe sets of these genes with more than twofold changes in at least one of the conditions were exported to Excel, where the average *n*-fold induction for each gene in each condition was calculated (see Table SI in the supplemental material).

Transcriptomic analysis of publicly available data on primary breast tumors. For expression analysis in breast tumors, we downloaded the gene array data with GEO accession numbers GSE1456 and GSE3494. The GSE1456 data set consists of 159 profiles of primary breast tumors collected at the Karolinska Hospital in Sweden from 1 January 1994 to 31 December 1996, with clinicopathological information available on all patients. The GSE3494 data set consists of 251 profiles of primary breast tumors collected in Uppsala County in Sweden from 1 January 1987 to 31 December 1989, with clinicopathological information available on 236 of the patients. The two data sets had been obtained by RNeasy Mini kit (Qiagen) extraction of total RNA followed by Affymetrix U133 A and B array analysis. The Excel files of all samples with patient information from the two data sets were opened as two independent projects with RMA normalization without baseline transformation in the program GeneSpring GX 9.0. Of the 624 genes identified as regulated by 611-CTF and HER2 in our cell line model, 599 represented by 1,416 probe sets were found in the U133 data. Without filtering for minimum detection threshold or expression variation, we exported all values

of the 1,416 probe sets from the 159- and 236-profile data sets to Excel. Here the data sets were baseline and $\log_2$ transformed and then fused to give a data set of 395 profiles. The HER2 status of the original 159-profile, but not the 236-profile, data set was available. In the 236-profile data set, we defined patients as HER2 positive if the value of at least one of the three different probe sets targeting HER2 was more than 2.5 times higher than its total average. If this definition had been applied to the 159-profile data set, five tumors would have been classified as false positive and another five as false negative with respect to the determinations made by the pathologist. In order to examine the importance of different subsets of genes regulated in our cell line analysis, we extracted all probe set values representing the chosen genes in all 395 tumor profiles and performed unsupervised hierarchical average linkage clustering with correlation-centered similarity metrics in the program Cluster (Michael Eisen, Stanford University). Clustering results were imported in the program Treeview in order to save heatmaps as .bmp files and dendrograms as .ps files. Kaplan-Meier survival analyses of clustered groups were done with the Excel add-in XLSTAT 2008.

TG mice. Transgenic (TG) 611 and TG 687 mice were engineered by cloning the sequences encoding 687-CTF and 611-CTF into the multiple cloning site II downstream of the Rous sarcoma virus-enhanced mouse mammary tumor virus long terminal repeat of the pMB vector (a kind gift from Marcos Malumbres, CNIO, Madrid, Spain). Founder lines were generated by microinjecting linearized plasmid DNA into fertilized oocytes harvested from superovulated FVB mice in the Centre of Animal Biotechnology and Gene Therapy (Centre de Biotecnologia Animal i Teràpia Gènica, Universitat Autònoma de Barcelona). Founder mice were genotyped by Southern hybridization analysis. After identification of founder animals, routine colony maintenance was performed by PCR genotyping. The male and female FVB/N-Tg(MMTVneu)202J mice were obtained from the Jackson Laboratory (Bar Harbor, ME).

Whole mounts and histology. Mammary glands were mounted on glass slides, fixed overnight in 4% paraformaldehyde, and transferred to 70% ethanol. The slides were rinsed in water for 5 min and stained in a filtered solution of 0.2% carmine for 24 h. Glands were then dehydrated sequentially with decreasing concentrations of ethanol and then defatted and stored in methyl salicylate. For histological analysis, fixed glands were blocked in paraffin, sectioned, and stained with hematoxylin and eosin.

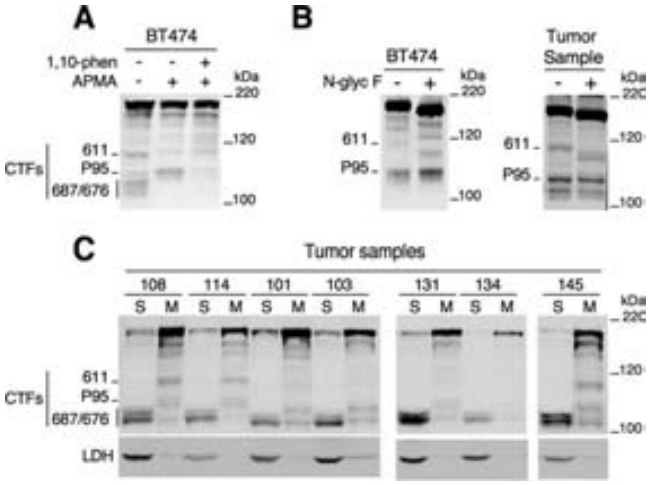

FIG. 2. Characterization of CTFs from BT474 cells and breast cancer samples. (A) BT474 cells were treated with APMA, 1,10-phenanthroline, and/or control solvent, as indicated. Cell lysates were analyzed by Western blotting with an antibody against the cytoplasmic domain of HER2. (B) Lysates of BT474 cells treated with APMA and membrane fraction from tumor sample 108 were incubated overnight with or without *N*-glycosidase F, followed by Western blot analysis with an antibody against the cytoplasmic domain of HER2. (C) Tissue samples of human mammary tumors were fractionated, and equal amounts of total soluble (S) and membrane (M) fractions were analyzed by Western blotting with an antibody against the cytoplasmic domain of HER2 or, as a control, with an antibody against the cytosolic protein LDH.

RESULTS

Generation of a cellular model to characterize CTFs of HER2. Alternative initiation of translation of the mRNA encoding HER2 from methionine codons 611 and 687 leads to synthesis of two CTFs that differ by only 76 amino acids (1). However, this sequence could be functionally relevant because it contains a short extracellular region, a transmembrane domain, and a NLS (Fig. 1A and B).

Proteolytic shedding of the HER2 extracellular domain occurs by alpha-secretase cleavage after alanine 645 or arginine 647 (44). This cleavage generates a CTF, P95, with five to eight extracellular amino acid residues. Many products of the alpha-secretases are subsequently cleaved by the gamma-secretase complex. A putative gamma-secretase cleavage of P95 would generate an intracellular soluble fragment starting around lysine 676 and containing the NLS (Fig. 1A and B).

To individually express the different CTFs, we constructed plasmids with the corresponding cDNAs (Fig. 1A) under the control of a promoter repressible by the tetracycline analog doxycycline and transfected them into MCF7 cells. This cell line expresses low levels of HER2 and undetectable levels of CTFs and has been widely used to study signaling pathways involved in tumor progression.

Western blot analysis of stable clones confirmed that each cDNA construct produced a characteristic set of CTFs (Fig. 1C). Detailed characterization of these HER2 isoforms by immunofluorescence microscopy (Fig. 1D; also see Fig. S1 in the supplemental material) and a variety of biochemical techniques (see Fig. S2 in the supplemental material) showed that CTFs containing the transmembrane domain, 611- and 648-CTFs, were efficiently delivered to the cell surface plasma membrane. The two 611-CTF species corresponded to an intracellular precursor and a glycosylated cell surface transmembrane form. The 676- and 687-CTFs were soluble and localized to the cytoplasm and nucleus. Consistent with the presence of a NLS, the nuclear levels of 676-CTF were higher than those of 687-CTF (see Fig. S1 and S2 in the supplemental material).

Collectively these results demonstrated that the cell lines generated constitute an appropriate model to characterize the different CTFs of HER2.

CTFs expressed in human breast tumors. To determine the type of CTFs expressed by breast tumor cells, we compared them with CTFs from the transfected cell lines. First, we analyzed BT474 cells, which are derived from a human mammary carcinoma, because they overexpress HER2 as well as several CTFs (6, 9). Analysis by Western blotting showed that one of the CTFs expressed comigrated with transfected 611-CTF (Fig. 2A; also data not shown). Another fragment was identified as P95 because it migrated as 648-CTF and could be upregulated by APMA, a mercurial compound known to activate the metalloproteases that cleave HER2 (26). Furthermore, this upregulation could be blocked by 1,10-phenanthroline, a classic metalloprotease inhibitor that prevents the shedding of HER2 (8, 25). APMA treatment induced the disappearance of the low-molecular-weight fragments that comigrated with 676- and 687-CTFs (Fig. 2A). This effect was likely due to cell permeabilization by the mercurial compound.

611-CTF includes the N-glycosylated Asn-629, which is absent in P95 (Fig. 1A; also see Fig. S2 in the supplemental

TABLE 1. Levels of expression of CTFs in breast tumor tissue samples[a]

Tumor sample no.	CTF	Ratio of CTF/HER2 (100)
108	611	15.0 ± 4.3
	P95	9.4 ± 4.1
	687/676	29.7 ± 19.0
114	611	15.3 ± 5.7
	P95	14.2 ± 4.1
	687/676	37.3 ± 4.9
101	611	3.8 ± 1.7
	P95	8.9 ± 3.0
	687/676	22.3 ± 4.6
103	611	ND
	P95	15.6 ± 7.1
	687/676	38.3 ± 11.1
131	611	ND
	P95	ND
	687/676	105 ± 15.8
134	611	ND
	P95	ND
	687/676	51.6 ± 11.4
145	611	31.2 ± 7.5
	P95	20.6 ± 6.1
	687/676	62.6 ± 16.6

[a] Lysates from the indicated tumors (see Fig. 2C) were analyzed by Western blotting with an antibody against the cytoplasmic domain of HER2. The Western blots were quantified, and the results were normalized to HER2 in the same sample. The averages of three independent determinations ± standard deviations are shown. ND, not detectable.

material). Thus, to further support the identifications made in Fig. 2A, we analyzed the N-glycosylation status of the CTFs from BT474 cells treated with APMA. The result of N-glycosidase F treatment was consistent with the identification of 611-CTF and P95 (Fig. 2B, left panel).

Next, we extended the analysis to human mammary tumor tissue samples selected on the basis of their high HER2 expression. Like with the BT474 cells, we identified the different CTFs from tumor samples by comparing their electrophoretic migration patterns with those of the transfected CTFs (see Fig. S3 in the supplemental material; also data not shown). Fractionation of the tumor samples showed that, as expected, the fragments identified as 611-CTF and P95 were membrane bound, while the CTFs comigrating with the 676- and 687-CTFs were largely soluble (Fig. 2C). Treatment with N-glycosidase F confirmed that the candidate 611-CTF was glycosylated, while P95 was not (Fig. 2B, right panel). These results showed that tumor samples contain both P95 and a fragment identical to that generated by alternative initiation of translation from methionine 611, as well as different soluble fragments that migrate as 676- and 687-CTFs.

In addition to malignant epithelial cells overexpressing HER2 and CTFs, the tumors contain a variety of stromal cell types that do not express, or express low levels of, HER2 and CTFs. Furthermore, the levels of total HER2 in individual epithelial tumor cells vary considerably, as seen in immunohistochemistry analyses (see, for example, reference 26). Nevertheless, the average levels of HER2 in tumors as determined by Western analysis appear less variable and similar to the expression level in our HER2 MCF7 stable transfectant (see Fig. S4 in the supplemental material). Thus, to quantitatively compare the expression of individual CTFs, we normalized their

TABLE 2. Levels of expression of CTFs in the cell lines used in this study[a]

Cell line	Ratio of CTF/HER2 (100)
HER2-A	100
611-A	182.1 ± 21.8
611-B	34.9 ± 5.6
648-A	103.1 ± 26.1
676-A	31.3 ± 4.2
687-A	113.7 ± 16.6

[a] Lysates from the indicated cell lines (see Fig. S6 in the supplemental material) were analyzed by Western blotting with an antibody against the cytoplasmic domain of HER2. The Western blots were quantified, and the results were normalized to the level in the HER2 clone. The averages of five independent determinations ± standard deviations are shown.

levels to the level of HER2 in the same tumor sample or cell line (Tables 1 and 2, respectively).

Transduction of signals by CTFs in cell lines. Activation of the intrinsic tyrosine kinase activity of HER2 leads to autophosphorylation and subsequent activation of signal transduction pathways. Incubation of immunoprecipitated CTFs with [γ-^{32}P]ATP led to radioactive labeling in all cases (see Fig. S5 in the supplemental material). Thus, all the model CTFs appear to be correctly folded and endowed with kinase activity.

We then monitored the statuses of specific components of the MAPK, Akt, Src, and PLCgamma signal transduction pathways (Fig. 3A). Expression of HER2 led to a progressive time-dependent accumulation of active components of these pathways (Fig. 3B; also see Fig. S6 in the supplemental material). Within the time frame chosen, the activation induced by HER2 did not reach a plateau. In contrast, 611-CTF induced a rapid and acute increase in the levels of active components that later decreased (P-Erk1/2, P-Akt, and P-Jnk) or reached a plateau (P-Src). In cells expressing 648-CTF, the activation was kinetically comparable to that in cells expressing 611-CTF, but the intensity was clearly lower (Fig. 3; also see Fig. S6 in the supplemental material).

Importantly, the signaling activation was nearly identical in cells expressing two different levels of 611-CTFs (see Fig. S6, clone 611-A and 611-B in the supplemental material; also data not shown). Despite expressing levels that differed by ~5-fold, the subsequent increases in phosphorylated signal transducers were kinetically and quantitatively similar. This result indicates that signal saturation was reached at relatively low levels of 611-CTF. The level of 611-CTF expressed in the 611-B cell line was comparable to those found in human mammary tumors (Table 1, tumor 145, and Table 2). Thus, pathophysiological levels of 611-CTF expression are signaling competent.

Even at the latest time point examined, expression of soluble 676- or 687-CTF did not lead to any changes in the statuses of the signal transducers (Fig. 3; also see Fig. S6 in the supplemental material). Therefore, neither cytoplasmic nor nuclear CTFs were able to activate, directly or indirectly, the MAPK, Akt, PLCgamma, or Src pathway.

611-CTF regulates the expression of a group of genes that correlates with poor prognosis in breast cancer patients. Despite engaging the same pathways, the activation levels of signal transduction by HER2 and transmembrane CTFs,

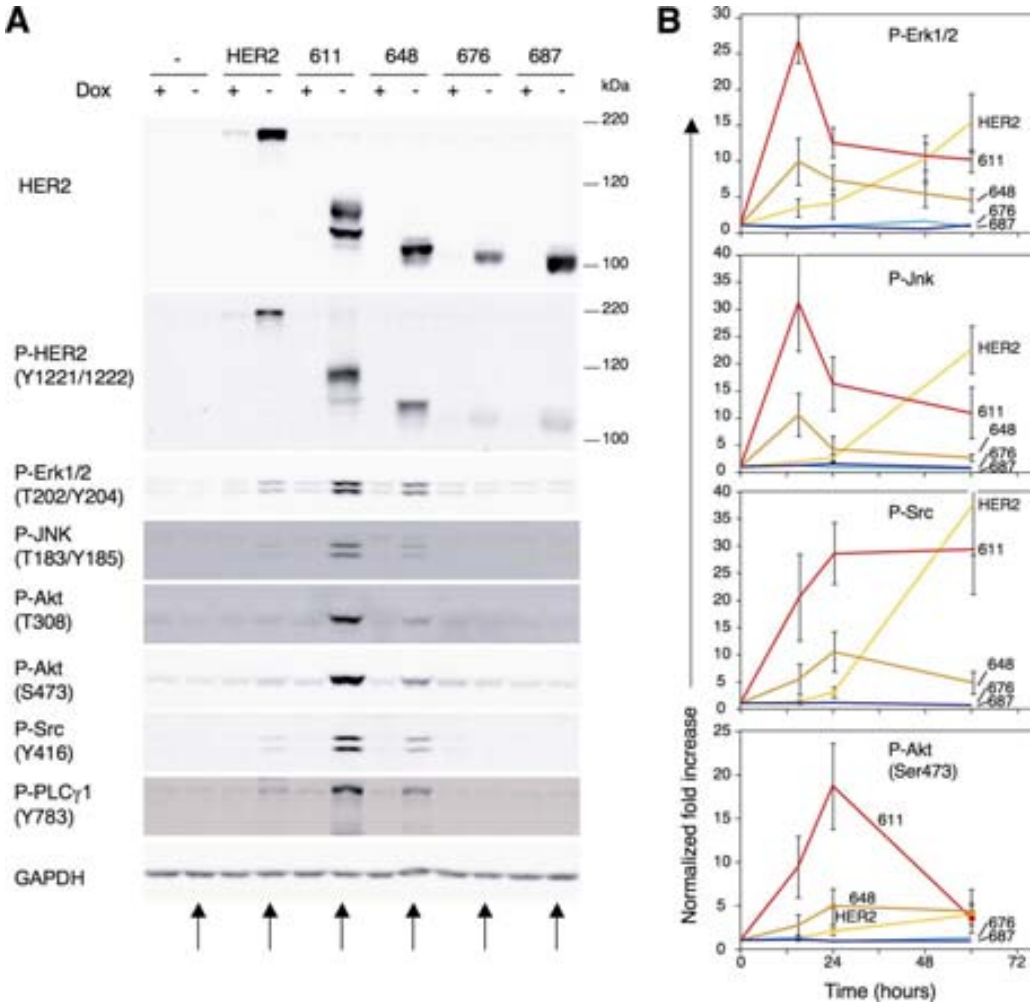

FIG. 3. Activation of signal transduction pathways in cells expressing the different CTFs. (A) The MCF7 clones stably transfected with vector (-), HER2, or 611-, 648-, 676-, or 687-CTF, as in Fig. 1C, were washed with media with or without doxycycline (Dox), cultured for 24 h, lysed, and analyzed by Western blotting with the indicated antibodies. Lanes marked with an arrow were used for quantification. GAPDH, glyceraldehyde-3-phosphate dehydrogenase. (B) Western blot signals from the expressed constructs and the indicated phosphoproteins in the three independent experiments described for panel A (and in Fig. S6 in the supplemental material) at different time points were quantified. The level of each phosphoprotein was divided by the level of expressed HER2 or CTF in the same sample, followed by normalization to the level of phosphoprotein in cells transfected with empty vector. The averages are presented as bars ± standard deviations.

particularly 611-CTF, were kinetically and quantitatively different (Fig. 3B). Thus, 611-CTF might regulate the expression of a distinct group of genes. To test this, we analyzed the transcriptome of cells expressing HER2 or 611-CTF at different time points. In addition, as an unbiased way to examine the possible activities of soluble nuclear or cytoplasmic CTFs, we included in the analysis cells expressing 676- or 687-CTF.

Consistent with the kinetic analyses, we found that 611-CTF expression led to a rapid regulation of gene expression and produced a change in the transcriptome of MCF7 cells that was far more profound than that induced by HER2 (Fig. 4A; also see Fig. S7A and Table SI in the supplemental material). In contrast, virtually no transcripts were affected by the expression of 676- or 687-CTF. The technical quality of the gene arrays was validated by verifying the regulation of several transcripts with real-time quantitative PCR (see Fig. S7B in the supplemental material).

Regulation of gene transcription is not always followed by corresponding changes in protein levels. We therefore sought validation of the increased expression of some gene products by Western blot analysis. Confirming the existence of genes specifically regulated by 611-CTFs, MET, MMP1, and the cell adhesion molecule integrin alpha 2 were not upregulated by HER2 (Fig. 4B; also see Fig. S8 in the supplemental material). Conversely, integrin alpha 5 was preferentially upregulated by HER2. Finally, PHLDA1, EPHA2, and integrin beta 1 were upregulated by both HER2 and 611-CTF, although as expected, to a higher extent by the latter. Part of these results was validated in a different cell line (see Fig. S9 in the supplemental material).

Hierarchical clustering of induction levels of the 624 genes

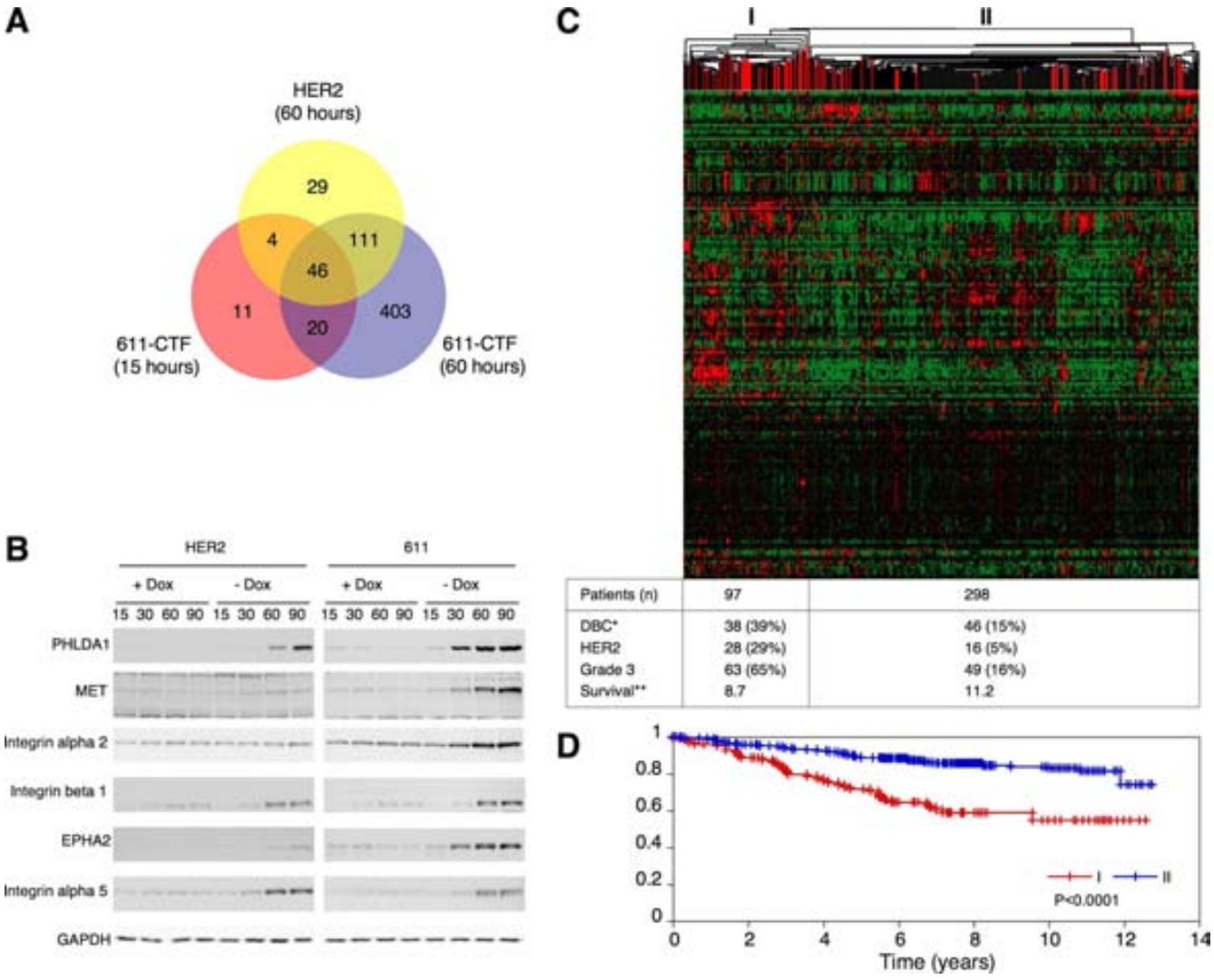

FIG. 4. Transcriptomic analysis with HER2 and 611-CTF. (A) Venn diagram showing the number and overlap of genes regulated after 15 or 60 h of expression of 611-CTF or HER2 in MCF7. The identities and *n*-fold induction of in total 624 genes in the seven different groups are listed in Table SI in the supplemental material. GAPDH, glyceraldehyde-3-phosphate dehydrogenase. (B) Cells of the MCF7 clones stably transfected with HER2 or 611-CTF were washed with media with or without doxycycline (Dox), cultured for 15, 30, 60, or 90 h, lysed, and analyzed by Western blotting with the indicated antibodies. (C) Unsupervised hierarchical clustering of 395 primary breast tumors from two independent publicly available studies, on the basis of expression levels of the 76-gene signature of 611-CTF (see Fig. S11 in the supplemental material). *, patients that died from breast cancer; **, mean survival time (years). (D) Kaplan-Meier survival plots of the two patient groups classified in panel C.

identified as targets of HER2 and 611-CTF in MCF7 cells (Fig. 4A) divided them into 357 and 267 generally up- and down-regulated genes, respectively (see Fig. S10A in the supplemental material). To investigate the expression patterns of these genes in human breast cancer, we combined two publicly available gene array data sets (24, 30). The resulting data set contained 395 transcriptomic profiles of primary breast tumors with corresponding clinical information on the patients (Table 3). Unsupervised clustering of the tumor profiles on the basis of the expression levels of the 357 upregulated genes (in MCF7) resulted in two distinct groups (see Fig. S10B in the supplemental material). The smaller of the two groups contained a high proportion of patients with HER2-positive tumors and patients (HER2-positive and -negative) that died from breast cancer (see Fig. S10C in the supplemental material). This result is in agreement with the known ability of HER2 to regulate the expression of genes important for tumor progression (43).

To determine the importance of genes preferentially regu-

TABLE 3. Patient survival in the combined 395-profile data set

Patients	*n*	No. dead from cancer (%)	Mean survival time (yr)
All	395	84 (21)	10.6
HER2 positive	44	16 (36)	8.2
HER2 negative	351	68 (19)	10.8
Grade 3	112	33 (29)	9.4
Not grade 3	283	51 (18)	11.0

lated by 611-CTF, we repeated the unsupervised clustering of the 395 profiles on the basis of the 76 genes upregulated more than threefold by 611-CTF and less than twofold by HER2 (see Table SI in the supplemental material). Again the profiles fell into two groups, of which the smaller one had a higher incidence of patients that died from breast cancer (Fig. 4C and D). The 76-gene signature contains many genes that are causally involved in metastasis, like those for MMP1, ANGPTL4, MET, and IL-11, as well as genes that contribute to various aspects of malignant development, for example, those for CD44, BCL2A1, ADAM9, PLAUR, EPHA1, and components of the EGFR pathway such as EGFR and TGFalpha (see Fig. S11 in the supplemental material). These results demonstrated that the genes regulated by 611-CTF play an essential role in breast cancer.

Mechanism of activation of 611-CTF. Previous reports have shown that deletions leading to an imbalance of cysteine residues in the extracellular domain of HER2 result in constitutive receptor activation due to the formation of disulfide-bonded dimers (37). Since 611-CTF contains an odd number of extracellular cysteine residues (Fig. 1A), we investigated whether it is activated through a similar mechanism. Analysis of cell lysates in the absence of a reducing agent unveiled the existence of species with the expected electrophoretic migration of 611-CTF dimers (Fig. 5A, upper panel). Furthermore, coexpressed FLAG- and hemagglutinin-tagged 611-CTFs efficiently coimmunoprecipitated, supporting the supposition that the high-molecular-weight complexes represent 611-CTF homodimers (see Fig. S12A in the supplemental material). The high-molecular-weight complexes were phosphorylated, indicating that they are active (Fig. 5A, bottom panel). Preincubation of cells with lapatinib, a tyrosine kinase inhibitor currently in clinical trials which targets both HER2 and EGFR, prevented the phosphorylation of 611-CTF dimers but not their generation (Fig. 5A). Thus, dimerization stabilized by disulfide bonds and subsequent transphosphorylation provided a feasible explanation for the hyperactivity of 611-CTF.

To corroborate this conclusion, we transiently transfected MCF7 cells with 611-CTF constructs with one or several of these cysteines mutated (Fig. 5B). Mutation of one cysteine reduced the generation of the high-molecular-weight 611-CTF complexes (Fig. 5C). Mutation of three and five cysteines further reduced and almost prevented, respectively, the generation of the complexes, further supporting the fact that they are maintained by disulfide bonds. Analysis of P-Erk1/2 and P-Akt levels in cells expressing the different constructs verified that the cysteines are required for the full activity of 611-CTF (Fig. 5D). Since the transfection efficiency of MCF7 cells was low (~20%), we used the highly transfectable HEK293T cell line to confirm that the formation of disulfide-bridged complexes is the mechanism of hyperactivation of 611-CTFs (see Fig. S12B in the supplemental material).

Generation of animal models to characterize the effect of CTF expression in vivo. Mouse models have been instrumental in showing the oncogenic potential and relevance of HER2 in tumor progression (38). To characterize its oncogenic potential, we established TG mice expressing 611-CTF under the control of the mouse mammary tumor virus long terminal repeat, which is preferentially active in the mammary gland. Although the cellular models indicated that soluble intracellular CTFs are inactive, to further explore the consequences of expression of these fragments, we also generated TG animals expressing 687-CTF. As a control, we used the classical and well-characterized model expressing wild-type HER2 (i.e., rat neu).

At an age of 7 weeks, the levels of 611-CTF expressed in the heterozygous TG 611 lines F3 and F2 were approximately equal to and one-third of, respectively, the levels of endogenous HER2, while the level in F1 was below the detection threshold (Fig. 6A). The levels of 687-CTF in the homozygous lines developed varied from approximately double to half the levels of HER2 in the TG 687 lines F2 and F1, respectively (Fig. 6A).

Mammary glands of the TG animals exhibited no macroscopic abnormalities at 7 weeks of age. However, as previously reported (14), morphological examination of carmine-stained whole mounts revealed hyperplasic abnormalities in the mammary ductal trees of TG HER2 mice (Fig. 6B). Similar abnormalities, albeit less pronounced, were present in all three lines of TG 611 mice (Fig. 6B; also data not shown). In contrast, the glands of TG 687 mice were indistinguishable from those of wild-type mice.

611-CTF expression leads to the development of aggressive mammary tumors. Despite the more-pronounced hyperplasia in TG HER2 mice, the three lines of TG 611 animals developed more aggressive tumors, in terms of number of tumors per animal (Fig. 7A and B), tumor onset (Fig. 7C and Table 4), and tumor growth (Fig. 7D). No tumors or abnormalities were observed in TG 687 animals even after a follow-up of more than one year (Fig. 7C).

Histological analysis of the tumors showed the same typical invasive solid nodular carcinomas induced by HER2 (27) in the TG 611 mice (see Fig. S13A in the supplemental material). The only histological difference between the tumors initiated by HER2 and 611-CTF was a higher number of mitotic images in the ones from TG 611 mice (see Fig. S13A in the supplemental material; also data not shown).

As previously shown, TG HER2 mice developed lung metastasis (14). Three to six weeks after detection of breast tumors by palpation, immunohistochemical analyses of sacrificed animals showed that approximately one-fourth of TG HER2 mice (two of nine) had nodules in the lungs (data not shown). Histological analysis of these lung metastases confirmed the expression of HER2, and staining against cytokeratin 18 verified that the cells originated from the primary tumor (see Fig. S13B in the supplemental material). In comparison to that for the TG HER2 animals, the frequency of detectable metastases in mice expressing 611-CTF was more than double (five of nine) (data not shown). This shows that the tumors initiated by this CTF have a more-pronounced tendency to invade the lungs.

Overexpression of HER2 alone does not seem sufficient to generate mammary tumors in mice. The TG HER2 mice only develop tumors after genetic activation of the transgene (35). This consists of in-frame deletions, insertions, or mutations that affect the number of cysteine residues in the extracellular domain. The imbalance of cysteines results in the constitutive dimerization through the formation of intermolecular disulfide bonds (36). In agreement with this, we identified a variety of genetic alterations in the transgene from tumors developed in TG HER2 animals (see Fig. S14 in the supplemental material).

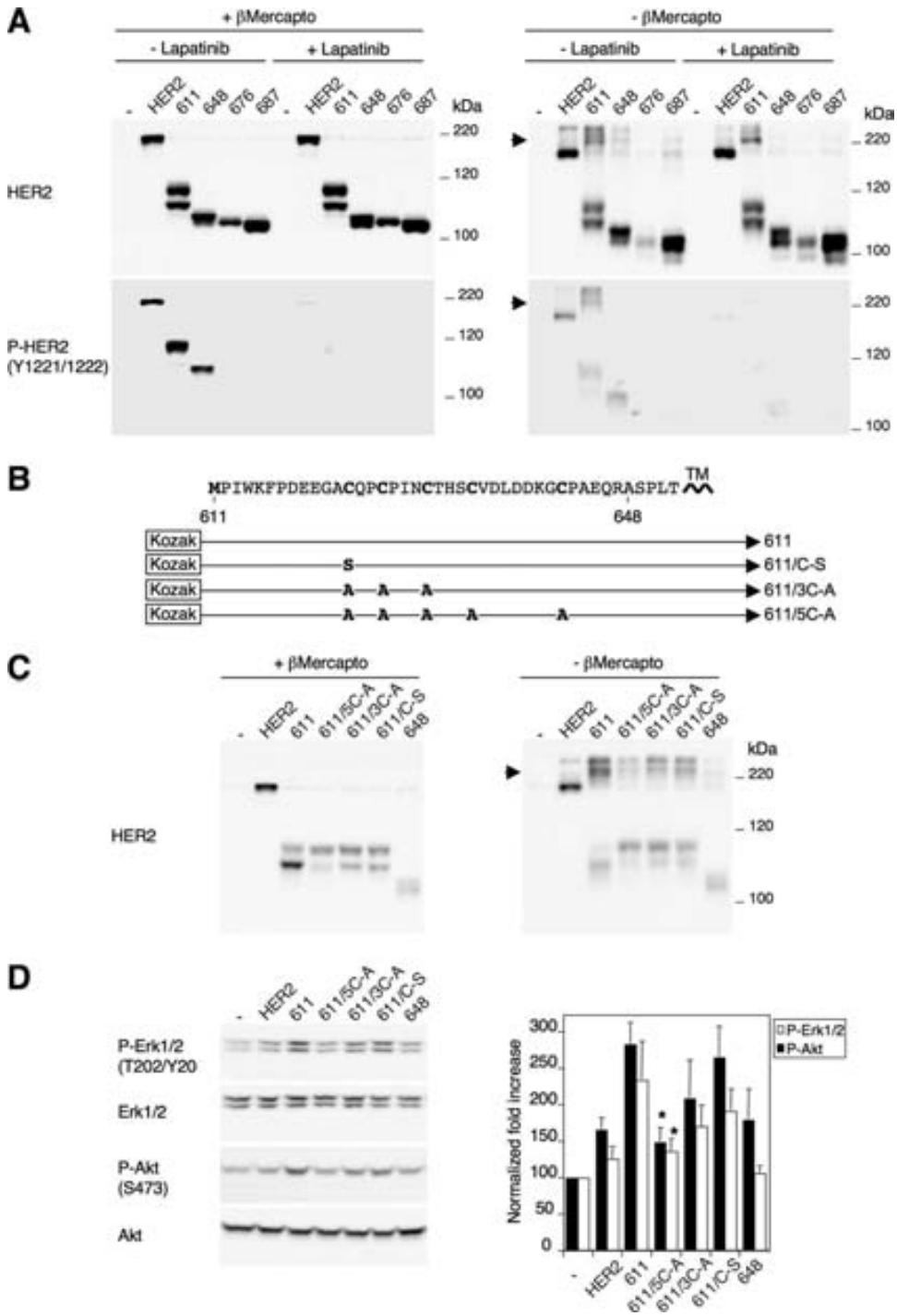

FIG. 5. Active 611-CTF complexes are maintained by disulfide bonds. (A) The MCF7 clones stably transfected with vector (-), HER2, or 611-, 648-, 676-, or 687-CTF, as in Fig. 1C, were washed with media without doxycycline, cultured for 24 h in the presence or absence of 1 mM lapatinib, lysed, fractionated by SDS-PAGE in the presence or absence of beta-mercaptoethanol, and analyzed by Western blotting with the indicated antibodies. Arrow, dimers. (B) Schematic showing the primary sequence of the extracellular juxtamembrane region of HER2 with the transmembrane domain (TM), the position of amino acids 611 and 648, and the five juxtamembrane cysteines marked. The schematics below the sequence show the different cysteine substitutions inserted in the cDNA of 611-CTF. (C) MCF7 cells were transiently transfected with the empty vector (-), the vector containing the cDNA of HER2, or wild-type 648- or 611-CTF or CTF-611 with one (C-S), three (3C-A), or five (5C-A) cysteines substituted. After 48 h, the cells were lysed and analyzed as in panel A. (D) The same lysates as in panel C with beta-mercaptoethanol were analyzed by Western blotting with the indicated antibodies. The specific signals of three independent experiments were quantified as in Fig. 3B. Statistical analysis of the normalized ratios using Student's *t* test showed statistically significant differences for P-Erk1/2 and P-Akt (S473) between cells expressing 611/5C-A and wild-type 611-CTF (*, $P < 0.01$).

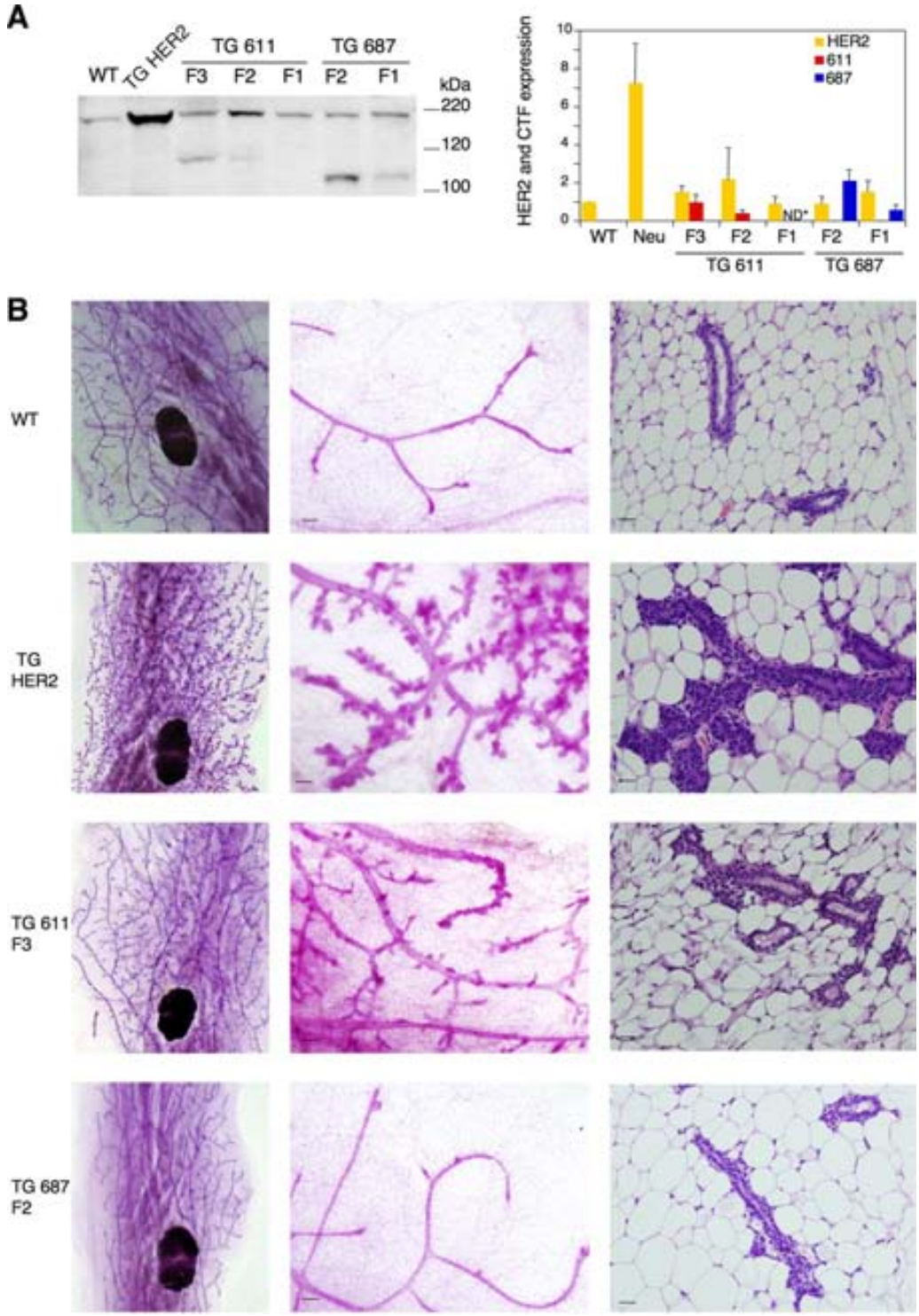

FIG. 6. Expression of 611-CTF in mouse mammary glands results in mild abnormal alveolar development. (A) Total protein lysates from mammary glands of 7-week-old TG mice were analyzed by Western blotting with an antibody against the cytoplasmic domain of HER2 (left). The average expression, normalized to HER2 in wild-type (WT) mice, in four independent Western blot analyses is presented as bars ± standard deviations (right). (B) Carmine-stained whole mounts (left), ×25 magnifications of the same whole mounts (middle), and hematoxylin and eosin-stained sections of mammary glands (right; magnification, ×400) from 7-week-old animals.

All 13 independent alterations identified affected the number of cysteines, confirming that this is the preferred mechanism of oncogenic activation in mice.

In contrast, and consistent with the constitutive activity of 611-CTF, we did not find any genetic alteration in the transgene encoding 611-CTF in 23 independent tumors samples (data not shown). Collectively, these results clearly demonstrate the hyperactivity and oncogenic potential of 611-CTF in vivo and suggest

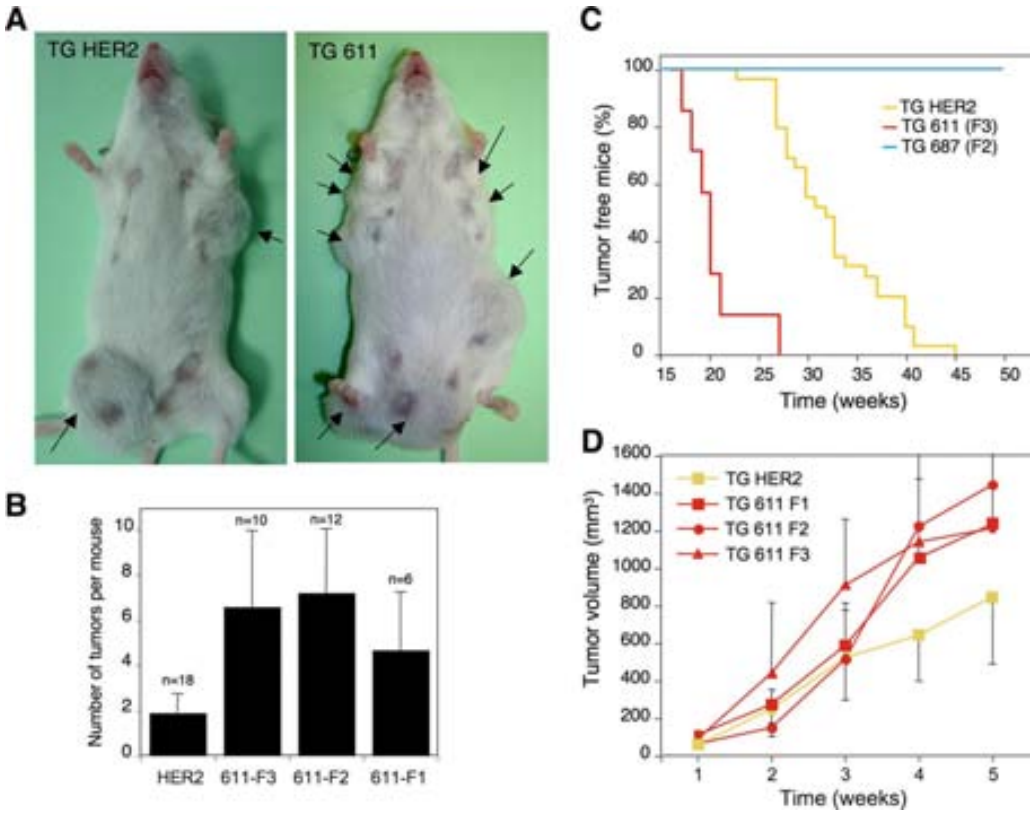

FIG. 7. TG 611-CTF mice develop mammary adenocarcinomas more aggressive than those in HER2-expressing mice. (A) Representative TG HER2 (35-week-old) and 611-CTF (25-week-old) mice. (B) Numbers of tumors that had developed in 40-week-old mice. Animals with tumors in every gland were counted as 10. The averages are presented as bars ± standard deviations. (C) Tumor-free survival curves of TG HER2 (n = 32), 611-CTF (n = 7), and 687-CTF (n = 26) mice. (D) Individual tumors from the indicated TG animals were measured at different time points. Each point represents the average ± standard deviation of ten individual tumors.

that expression of this CTF could contribute to mammary tumor progression in humans.

DISCUSSION

Extracellular domain shedding modifies the activity of hundreds of unrelated transmembrane proteins, including cell adhesion molecules, transmembrane growth factors, and growth factor receptors (2). Probably because of the generality of this type of endoproteolysis, it has been widely assumed that HER2 CTFs occurring in breast cancer patients arise exclusively through this mechanism. In accordance with this assumption, and despite the fact that they constitute a group of proteins ranging from ~90 to 120 kDa, HER2 CTFs are frequently referred to as P95 (6, 23, 33), the predicted molecular weight of the transmembrane product of HER2 ectodomain shedding. In a previous publication (1), we showed the existence of an additional mechanism of CTF generation, the alternative initiation of translation. Our present analysis of human mammary tumors showed that the combined products of both mechanisms can explain most of the naturally occurring HER2 isoforms, which include two transmembrane and several soluble CTFs (Fig. 1 and 2).

TABLE 4. Tumor onset in TG mice expressing HER2 or 611-CTF in the mammary glands[a]

Mice	Average onset (wk)	n
HER2 (Neu)	30.3 ± 7.5	22
611-F1	26.3 ± 4.6	6
611-F2	22.2 ± 4.8	12
611-F3	23.7 ± 5.5	3

[a] The appearance of mammary tumors was monitored by palpation weekly.

The transmembrane domain of HER2 facilitates incorporation of CTFs into the secretory pathway. To analyze their functions, we generated stable transfectants expressing each individual CTF. This approach was straightforward for the soluble CTFs, because their expression from cDNA constructs is not expected to affect their subcellular localization. For the transmembrane CTFs, this strategy was feasible because CTFs lacking a signal peptide but containing the transmembrane domain efficiently incorporated into the secretory pathway (Fig. 1; also see Fig. S1 and S2 in the supplemental material). As a typical type I transmembrane protein, HER2 starts with an N-terminal signal peptide that inserts the nascent peptide into the lumen of the endoplasmic reticulum (ER). However, when located near the N terminus, as in 611- and 648-CTFs, the transmembrane domain was also able to recruit the necessary signal proteins to ensure insertion into the ER. Insertion in the membrane of type Ib integral proteins or single-pass

type III membrane proteins, such as the neuregulins and cytochrome P450, is also directed by the transmembrane domain (3). However, to our knowledge HER2 is the first reported case in which this function has been attributed to the transmembrane domain of a type I protein that, in the full-length version, also contains a signal peptide.

611-CTF controls genes that predict poor prognosis in breast cancer. We have previously shown that the expression of CTFs correlates with poor prognosis and increased likelihood of developing metastasis (26, 32). However in these studies, patients were classified as CTF positive or negative without taking into consideration the type of CTFs expressed. The functional characterization presented here indicates that, while the expression of soluble CTFs is likely irrelevant, the transmembrane CTFs, especially 611-CTF, could play a causal role in the particularly poor clinical outcome of certain HER2-positive patients. In agreement with this suggestion, our transcriptomic analysis showed that the group of genes preferentially upregulated by 611-CTF predicted poor prognosis (Fig. 4; also see Fig. S11 in the supplemental material). In fact, several of the genes regulated by 611-CTF have been shown to participate in tumor spreading. Interesting examples include genes that play a causal role in metastasis, such as those for ANGPTL4 (29) and IL-11 (17). Furthermore, we validated target genes involved in metastasis, such as those for MET, EPHA2, and MMP1 (4, 11, 13), at the protein level (Fig. 4; also see Fig. S8 and S9 in the supplemental material).

Mechanism of activation of HER2 and CTFs. The invariable presence of a mutated transgene in tumors from TG HER2 mice suggests that, although it likely contributes, the mere overexpression of the receptor is not sufficient to drive malignant transformation in this animal model. Although the mutations are diverse, they all cause an imbalance in the number of cysteine residues (35) (see Fig. S14 in the supplemental material). This molecular abnormality results in constitutive activation of the receptor through the formation of covalent homodimers (36). Thus, intermolecular disulfide bonding appears to be the favored mechanism of oncogenic activation of HER2 in vivo. In agreement with this conclusion, we did not find any mutations in the transgenes of tumors induced by 611-CTF expression. Because of its intrinsic ability to form disulfide-bonded dimers (Fig. 5), this HER2 isoform does not require mutations in order to generate aggressive tumors in mice (Fig. 6 and 7).

In contrast to the situation in TG mice, HER2 is not frequently mutated in samples from human mammary tumors (34). Thus, it has been concluded that overexpression may be enough to activate HER2 in human cancers (16). Our results point to an additional possibility. Cells expressing even very low levels of 611-CTF in humans may have an advantage similar to that of cells expressing the mutant forms of HER2 in mice. This hypothesis may explain, at least in part, why HER2 mutations are rare in human tumors.

611-CTF in human tumors. It could be argued that if 611-CTF plays an important role in HER2-induced tumorigenesis, expression of this isoform, rather than mutations in the transgene, should occur in the HER2 TG mice. However, although the regulation of alternative initiation of translation in mammalian genes is poorly understood (18), it is clear that it does require *cis*-acting sequences that might be absent in the cDNA constructs used in the animal model. Nevertheless, a better understanding of the mechanism(s) responsible for the translation of 611-CTF is warranted in order to more precisely define its role in cancer. Furthermore, it cannot be ruled out that in the highly complex and heterogeneous tumor setting, in addition to alternative initiation of translation, other mechanisms may contribute to the generation of 611-CTF. It is not unlikely that incomplete gene duplication, aberrant mRNA splicing, and/or initiation of transcription lead to synthesis of 5′-truncated HER2 mRNA transcripts. Should these transcripts lack a region affecting the sequence between methionine codons 1 and 347 (the upstream methionine codon nearest to methionine 611), they may result in synthesis of 611-CTF.

Interestingly, several studies have reported the existence of an alternatively spliced form of HER2, known as ΔHER2, that lacks an exon encoding 16 amino acids of the extracellular juxtamembrane region (19). This deletion also causes an imbalance in the number of cysteines and the generation of dimers maintained by intermolecular disulfide bonds (37). Since ΔHER2 was detected in most breast cancer samples analyzed and accounted for 4 to 9% of total HER2 transcripts, this HER2 isoform likely contributes to tumor progression too.

Even though its activity was much lower than that of 611-CTF, 648-CTF (P95) was also capable of signaling (Fig. 3). Since this fragment of HER2 completely lacks the extracellular domain, its mechanism of activation remains unknown. In this respect, it was recently suggested that an undefined CTF of HER2 can form active complexes with HER3 (42). However, the generation of TG mice expressing the P95 isoform is needed in order to establish its pathophysiological importance.

Our finding that 611-CTF is a hyperactive form of HER2 with a clear link to metastasis-promoting genes suggests that in future studies, classification of patients according to the presence of this fragment could lead to improved clinical correlations. The development of tools to specifically and robustly detect the presence of this fragment would be instrumental in accomplishing this goal.

ACKNOWLEDGMENTS

We thank Pieter Eichhorn for critical reading of the manuscript and José Jimenez for the tumor samples.

This research was supported by grants from the Instituto de Salud Carlos III (Intrasalud PI081154), the network of cooperative cancer research (RTICC), the Breast Cancer Research Foundation, and La Marató de TV3 to J.A. K.P. and J.L.P.-P. were supported by the Juan de la Cierva postdoctoral program. J.G.-C. and P.-D.A. were supported by postdoctoral and predoctoral fellowships from the Spanish Ministry of Education, respectively.

REFERENCES

1. **Anido, J., M. Scaltriti, J. J. Bech Serra, B. S. Josefat, F. Rojo Todo, J. Baselga, and J. Arribas.** 2006. Biosynthesis of tumorigenic HER2 C-terminal fragments by alternative initiation of translation. EMBO J. **25:**3234–3244.
2. **Arribas, J., and A. Borroto.** 2002. Protein ectodomain shedding. Chem. Rev. **102:**4627–4638.
3. **Black, S. D.** 1992. Membrane topology of the mammalian P450 cytochromes. FASEB J. **6:**680–685.
4. **Brantley-Sieders, D. M., G. Zhuang, D. Hicks, W. B. Fang, Y. Hwang, J. M. Cates, K. Coffman, D. Jackson, E. Bruckheimer, R. S. Muraoka-Cook, and J. Chen.** 2008. The receptor tyrosine kinase EphA2 promotes mammary adenocarcinoma tumorigenesis and metastatic progression in mice by amplifying ErbB2 signaling. J. Clin. Investig. **118:**64–78.
5. **Burgess, A. W., H.-S. Cho, C. Eigenbrot, K. M. Ferguson, T. P. J. Garrett, D. J. Leahy, M. A. Lemmon, M. X. Sliwkowski, C. W. Ward, and S. Yokoyama.** 2003. An open-and-shut case? Recent insights into the activation of EGF/ErbB receptors. Mol. Cell **12:**541–552.

6. **Christianson, T. A., J. K. Doherty, Y. J. Lin, E. E. Ramsey, R. Holmes, E. J. Keenan, and G. M. Clinton.** 1998. NH2-terminally truncated HER-2/neu protein: relationship with shedding of the extracellular domain and with prognostic factors in breast cancer. Cancer Res. **58:**5123–5129.
7. **Citri, A., and Y. Yarden.** 2006. EGF-ERBB signalling: towards the systems level. Nat. Rev. Mol. Cell Biol. **7:**505–516.
8. **Codony-Servat, J., J. Albanell, J. C. Lopez-Talavera, J. Arribas, and J. Baselga.** 1999. Cleavage of the HER2 ectodomain is a pervanadate-activable process that is inhibited by the tissue inhibitor of metalloproteases-1 in breast cancer cells. Cancer Res. **59:**1196–1201.
9. **Ding, X., L. Y. Yang, G. W. Huang, W. Wang, and W. Q. Lu.** 2004. ADAM17 mRNA expression and pathological features of hepatocellular carcinoma. World J. Gastroenterol. **10:**2735–2739.
10. **Garrett, T. P., N. M. McKern, M. Lou, T. C. Elleman, T. E. Adams, G. O. Lovrecz, M. Kofler, R. N. Jorissen, E. C. Nice, A. W. Burgess, and C. W. Ward.** 2003. The crystal structure of a truncated ErbB2 ectodomain reveals an active conformation, poised to interact with other ErbB receptors. Mol. Cell **11:**495–505.
11. **Gentile, A., and P. M. Comoglio.** 2004. Invasive growth: a genetic program. Int. J. Dev. Biol. **48:**451–456.
12. **Giri, D. K., M. Ali-Seyed, L. Y. Li, D. F. Lee, P. Ling, G. Bartholomeusz, S. C. Wang, and M. C. Hung.** 2005. Endosomal transport of ErbB-2: mechanism for nuclear entry of the cell surface receptor. Mol. Cell. Biol. **25:**11005–11018.
13. **Gupta, G. P., D. X. Nguyen, A. C. Chiang, P. D. Bos, J. Y. Kim, C. Nadal, R. R. Gomis, K. Manova-Todorova, and J. Massague.** 2007. Mediators of vascular remodelling co-opted for sequential steps in lung metastasis. Nature **446:**765–770.
14. **Guy, C. T., M. A. Webster, M. Schaller, T. J. Parsons, R. D. Cardiff, and W. J. Muller.** 1992. Expression of the neu protooncogene in the mammary epithelium of transgenic mice induces metastatic disease. Proc. Natl. Acad. Sci. USA **89:**10578–10582.
15. **Hsu, S. C., and M. C. Hung.** 2007. Characterization of a novel tripartite nuclear localization sequence in the EGFR family. J. Biol. Chem. **282:**10432–10440.
16. **Hynes, N. E., and H. A. Lane.** 2005. ERBB receptors and cancer: the complexity of targeted inhibitors. Nat. Rev. Cancer **5:**341–354.
17. **Kang, Y., P. M. Siegel, W. Shu, M. Drobnjak, S. M. Kakonen, C. Cordon-Cardo, T. A. Guise, and J. Massague.** 2003. A multigenic program mediating breast cancer metastasis to bone. Cancer Cell **3:**537–549.
18. **Kochetov, A. V.** 2008. Alternative translation start sites and hidden coding potential of eukaryotic mRNAs. Bioessays **30:**683–691.
19. **Kwong, K. Y., and M. C. Hung.** 1998. A novel splice variant of HER2 with increased transformation activity. Mol. Carcinog. **23:**62–68.
20. **Lee, H. J., K. M. Jung, Y. Z. Huang, L. B. Bennett, J. S. Lee, L. Mei, and T. W. Kim.** 2002. Presenilin-dependent gamma-secretase-like intramembrane cleavage of ErbB4. J. Biol. Chem. **277:**6318–6323.
21. **Lin, Y. Z., and G. M. Clinton.** 1991. A soluble protein related to the HER-2 proto-oncogene product is released from human breast carcinoma cells. Oncogene **6:**639–643.
22. **Linggi, B., and G. Carpenter.** 2006. ErbB-4 s80 intracellular domain abrogates ETO2-dependent transcriptional repression. J. Biol. Chem. **281:**25373–25380.
23. **Liu, P. C., X. Liu, Y. Li, M. Covington, R. Wynn, R. Huber, M. Hillman, G. Yang, D. Ellis, C. Marando, K. Katiyar, J. Bradley, K. Abremski, M. Stow, M. Rupar, J. Zhuo, Y. L. Li, Q. Lin, D. Burns, M. Xu, C. Zhang, D. Q. Qian, C. He, V. Sharief, L. Weng, C. Agrios, E. Shi, B. Metcalf, R. Newton, S. Friedman, W. Yao, P. Scherle, G. Hollis, and T. C. Burn.** 2006. Identification of ADAM10 as a major source of HER2 ectodomain sheddase activity in HER2 overexpressing breast cancer cells. Cancer Biol. Ther. **5:**657–664.
24. **Miller, L. D., J. Smeds, J. George, V. B. Vega, L. Vergara, A. Ploner, Y. Pawitan, P. Hall, S. Klaar, E. T. Liu, and J. Bergh.** 2005. An expression signature for p53 status in human breast cancer predicts mutation status, transcriptional effects, and patient survival. Proc. Natl. Acad. Sci. USA **102:**13550–13555.
25. **Molina, M. A., J. Codony-Servat, J. Albanell, F. Rojo, J. Arribas, and J. Baselga.** 2001. Trastuzumab (herceptin), a humanized anti-Her2 receptor monoclonal antibody, inhibits basal and activated Her2 ectodomain cleavage in breast cancer cells. Cancer Res. **61:**4744–4749.
26. **Molina, M. A., R. Saez, E. E. Ramsey, M. J. Garcia-Barchino, F. Rojo, A. J. Evans, J. Albanell, E. J. Keenan, A. Lluch, J. Garcia-Conde, J. Baselga, and G. M. Clinton.** 2002. NH(2)-terminal truncated HER-2 protein but not full-length receptor is associated with nodal metastasis in human breast cancer. Clin. Cancer Res. **8:**347–353.
27. **Muller, W. J., E. Sinn, P. K. Pattengale, R. Wallace, and P. Leder.** 1988. Single-step induction of mammary adenocarcinoma in transgenic mice bearing the activated c-neu oncogene. Cell **54:**105–115.
28. **Ni, C. Y., M. P. Murphy, T. E. Golde, and G. Carpenter.** 2001. Gamma-secretase cleavage and nuclear localization of ErbB-4 receptor tyrosine kinase. Science **294:**2179–2181.
29. **Padua, D., X. H. Zhang, Q. Wang, C. Nadal, W. L. Gerald, R. R. Gomis, and J. Massague.** 2008. TGFbeta primes breast tumors for lung metastasis seeding through angiopoietin-like 4. Cell **133:**66–77.
30. **Pawitan, Y., J. Bjohle, L. Amler, A. L. Borg, S. Egyhazi, P. Hall, X. Han, L. Holmberg, F. Huang, S. Klaar, E. T. Liu, L. Miller, H. Nordgren, A. Ploner, K. Sandelin, P. M. Shaw, J. Smeds, L. Skoog, S. Wedren, and J. Bergh.** 2005. Gene expression profiling spares early breast cancer patients from adjuvant therapy: derived and validated in two population-based cohorts. Breast Cancer Res. **7:**R953–R964.
31. **Pupa, S. M., S. Menard, D. Morelli, B. Pozzi, G. De Palo, and M. I. Colnaghi.** 1993. The extracellular domain of the c-erbB-2 oncoprotein is released from tumor cells by proteolytic cleavage. Oncogene **8:**2917–2923.
32. **Saez, R., M. A. Molina, E. E. Ramsey, F. Rojo, E. J. Keenan, J. Albanell, A. Lluch, J. Garcia-Conde, J. Baselga, and G. M. Clinton.** 2006. p95HER-2 predicts worse outcome in patients with HER-2-positive breast cancer. Clin. Cancer Res. **12:**424–431.
33. **Scaltriti, M., F. Rojo, A. Ocana, J. Anido, M. Guzman, J. Cortes, S. Di Cosimo, X. Matias-Guiu, S. Ramon y Cajal, J. Arribas, and J. Baselga.** 2007. Expression of p95HER2, a truncated form of the HER2 receptor, and response to anti-HER2 therapies in breast cancer. J. Natl. Cancer Inst. **99:**628–638.
34. **Shigematsu, H., T. Takahashi, M. Nomura, K. Majmudar, M. Suzuki, H. Lee, I. I. Wistuba, K. M. Fong, S. Toyooka, N. Shimizu, T. Fujisawa, J. D. Minna, and A. F. Gazdar.** 2005. Somatic mutations of the HER2 kinase domain in lung adenocarcinomas. Cancer Res. **65:**1642–1646.
35. **Siegel, P. M., D. L. Dankort, W. R. Hardy, and W. J. Muller.** 1994. Novel activating mutations in the neu proto-oncogene involved in induction of mammary tumors. Mol. Cell. Biol. **14:**7068–7077.
36. **Siegel, P. M., and W. J. Muller.** 1996. Mutations affecting conserved cysteine residues within the extracellular domain of Neu promote receptor dimerization and activation. Proc. Natl. Acad. Sci. USA **93:**8878–8883.
37. **Siegel, P. M., E. D. Ryan, R. D. Cardiff, and W. J. Muller.** 1999. Elevated expression of activated forms of Neu/ErbB-2 and ErbB-3 are involved in the induction of mammary tumors in transgenic mice: implications for human breast cancer. EMBO J. **18:**2149–2164.
38. **Ursini-Siegel, J., B. Schade, R. D. Cardiff, and W. J. Muller.** 2007. Insights from transgenic mouse models of ERBB2-induced breast cancer. Nat. Rev. Cancer **7:**389–397.
39. **Vidal, G. A., A. Naresh, L. Marrero, and F. E. Jones.** 2005. Presenilin-dependent gamma-secretase processing regulates multiple ERBB4/HER4 activities. J. Biol. Chem. **280:**19777–19783.
40. **Wang, S. C., H. C. Lien, W. Xia, I. F. Chen, H. W. Lo, Z. Wang, M. Ali-Seyed, D. F. Lee, G. Bartholomeusz, F. Ou-Yang, D. K. Giri, and M. C. Hung.** 2004. Binding at and transactivation of the COX-2 promoter by nuclear tyrosine kinase receptor ErbB-2. Cancer Cell **6:**251–261.
41. **Williams, C. C., J. G. Allison, G. A. Vidal, M. E. Burow, B. S. Beckman, L. Marrero, and F. E. Jones.** 2004. The ERBB4/HER4 receptor tyrosine kinase regulates gene expression by functioning as a STAT5A nuclear chaperone. J. Cell Biol. **167:**469–478.
42. **Xia, W., L. H. Liu, P. Ho, and N. L. Spector.** 2004. Truncated ErbB2 receptor (p95ErbB2) is regulated by heregulin through heterodimer formation with ErbB3 yet remains sensitive to the dual EGFR/ErbB2 kinase inhibitor GW572016. Oncogene **23:**646–653.
43. **Yarden, Y., and M. X. Sliwkowski.** 2001. Untangling the ErbB signalling network. Nat. Rev. Mol. Cell Biol. **2:**127–137.
44. **Yuan, C. X., A. L. Lasut, R. Wynn, N. T. Neff, G. F. Hollis, M. L. Ramaker, M. J. Rupar, P. Liu, and R. Meade.** 2003. Purification of Her-2 extracellular domain and identification of its cleavage site. Protein Expr. Purif. **29:**217–222.
45. **Zabrecky, J. R., T. Lam, S. J. McKenzie, and W. Carney.** 1991. The extracellular domain of p185/neu is released from the surface of human breast carcinoma cells, SK-BR-3. J. Biol. Chem. **266:**1716–1720.